



NTNU – Trondheim
Norwegian University of
Science and Technology

Decision Making Methodology for the Selection of Gas-liquid Separators

Carlos Eduardo Sanchez Perez

Natural Gas Technology

Submission date: June 2012

Supervisor: Carlos Alberto Dorao, EPT

Co-supervisor: Luis Castillo, EPT

Norwegian University of Science and Technology
Department of Energy and Process Engineering

EPT-M-2012- 106

MASTER THESISCarlos Eduardo Sanchez Perez
Stud.techn.
Spring 2012***Decision making methodology for the selection of gas-liquid separators***
Beslutningsprosesser metodikk for valg av gass-væske separatorer

Gas liquid separators are critical component found in several industries, in particular in the oil and gas industry. The separators can be used for adjusting the specification of the final product or for protecting costly equipments such as heat exchangers or compressors.

A gas liquid separator consists of a vessel with several internals with the main goal of dividing the multiphase stream into a liquid and gas stream. The efficiency of the separator is related to ability of removing micro- size droplets from the stream.

During the last decade several designs of gas liquid separator can be found in the open market ranging from bulky equipment to very compact concepts. Selecting a gas-liquid separator is becoming a complex task demanding some previous experience in the area.

In this work, a decision making methodology will be developed for selecting gas-liquid separators. This tool will focus on studying the relevance of critical parameters such as cost, size, weight, and maturity of the product in the final decision.

The following tasks are to be considered:

1. Review the sizing of the some selected gas-liquid separators.
2. Construct an economical and technological model for each separator concept.
3. Evaluate with the tool different case scenarios and the impact in the selection of the technology

.. " ..

Within 14 days of receiving the written text on the master thesis, the candidate shall submit a research plan for his project to the department.

When the thesis is evaluated, emphasis is put on processing of the results, and that they are presented in tabular and/or graphic form in a clear manner, and that they are analyzed carefully.

The thesis should be formulated as a research report with summary both in English and Norwegian, conclusion, literature references, table of contents etc. During the preparation of the text, the candidate should make an effort to produce a well-structured and easily readable report. In order to ease the evaluation of the thesis, it is important that the cross-references are correct. In the making of the report, strong emphasis should be placed on both a thorough discussion of the results and an orderly presentation.

Page 1 of 2

The candidate is requested to initiate and keep close contact with his/her academic supervisor(s) throughout the working period. The candidate must follow the rules and regulations of NTNU as well as passive directions given by the Department of Energy and Process Engineering.

Risk assessment of the candidate's work shall be carried out according to the department's procedures. The risk assessment must be documented and included as part of the final report. Events related to the candidate's work adversely affecting the health, safety or security, must be documented and included as part of the final report.

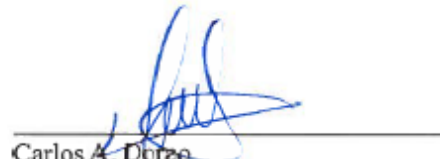
Pursuant to "Regulations concerning the supplementary provisions to the technology study program/Master of Science" at NTNU §20, the Department reserves the permission to utilize all the results and data for teaching and research purposes as well as in future publications.

The final report is to be submitted digitally in DAIM. An executive summary of the thesis including title, student's name, supervisor's name, year, department name, and NTNU's logo and name, shall be submitted to the department as a separate pdf file. Based on an agreement with the supervisor, the final report and other material and documents may be given to the supervisor in digital format.

Department of Energy and Process Engineering, 30. January 2012



Olav Bolland
Department Head



Carlos A. Dorao
Academic Supervisor

Research Advisors: Luis A. Castillo

Abstract

Gas liquid separation is a critical operation in many industries, including the gas and oil industry. In fact, costly equipment like heat exchangers and compressors rely on the good performance of gas scrubbers. In the particular case of Norway, most of these operations are offshore where the plot area is critical. On the other hand, the separation of liquid droplets from the gas stream is generally performed in bulky and heavy pressure vessels. More compact technologies are emerging though. However, it is becoming difficult to select the appropriate separator and it is required engineering experience. Therefore, the objective of this project is to develop mathematical models for selected technologies to facilitate the selection. The technologies selected were the traditional knitted mesh separator and the recent multi-cyclone scrubber. The models provide the basic dimensions, weight, purchase and installed costs for both scrubbers. The results of both models were compared and extrapolated to hypothetical situations to establish when a compact technology becomes competitive. For this comparison, gas load factor and costs per flow rate were used. In fact the vessel compactness is related to the former. Therefore, it is intended to have values much higher than 0.107 m/s corresponding to traditional separators at atmospheric pressure. In fact, a factor slightly higher than 0.14 m/s would make very competitive multi-cyclones; which can be achieved at pressures higher than 70-80 bar. Furthermore, technologies with factors up 0.5 to 1 m/s might be much more attractive. Nevertheless, there would be restrictions in achieving the maximum gas load factor expected.

Preface

This thesis is submitted as partial requirement of the International Master Degree in Natural Gas Technology, at the Norwegian University of Science and Technology (NTNU). This project was carried out between January and June 2012 at the Department of Energy and Process Engineering. It was supervised by the associate professor Carlos A. Dorao and co-supervised by the PhD candidate Luis Castillo.

Acknowledgements

First of all, I would like to thank my teaching supervisor, Carlos, for having given to me the opportunity of working with him. He gave me very important pieces of advice during all phases of the thesis. Firstly, he provided the main guidelines and scope of the present work. I am also very grateful to him for his direct supervision in different tasks. Moreover, this experience has been very beneficial to me since I have increased significantly my knowledge about the technical and economical evaluation of chemical equipment. Furthermore, my computing skills have been enhanced in the same way.

I am also very grateful to Luis for his direct guidance during the first and last stages of the project.

Andrea Shmueli also played an important role on this thesis since she gave me support and pieces of advices, especially in tasks related to computing programming.

Finally, I would like to express my eternal gratitude to my parents and siblings who have made me possible to stay and study in Norway during the last two years.

Trondheim, June 2012.

Carlos Eduardo Sanchez Perez

TABLE OF CONTENTS

<i>Abstract</i>	iv
<i>Preface</i>	v
<i>Acknowledgements</i>	v
<i>List of figures</i>	vii
<i>List of tables</i>	ix
<i>List of symbols</i>	x
1. INTRODUCTION	1
2. GAS SCRUBBERS: TYPES AND MAIN FEATURES	4
3. SIZING OF GAS SCRUBBERS.....	9
3.1 Features of the gas-liquid stream and physical-chemical properties	10
3.2 Sizing of knitted-mesh separators.....	14
3.3 Sizing of multi-cyclone separators.....	21
4. ECONOMICAL EVALUATION.....	32
4.1 Purchase cost estimate	33
4.2 Estimate of capital investment.....	41
5. METHODOLOGY	46
6. RESULTS.....	51
6.1 Dimensions and weight of gas scrubbers	53
6.2 Costs and economical evaluation.....	56
6.3 Other parameters and considerations	63
7. DISCUSSION OF RESULTS.....	67
8. CONCLUSIONS AND RECOMMENDATIONS	72
9. REFERENCES.....	74

LIST OF FIGURES

Figure 2.1 Particle size range from different sources and appropriate demister pads	5
Figure 2.2 Vertical knitted-mesh separation unit and demister pads.	6
Figure 2.3 The coalescence principle on vane separators and flexichevron vane-type for high capacity	7
Figure 2.4 Typical gas-liquid multi-cyclone design and two multi-cyclone gas scrubbers in a metering station in Western Canada	8
Figure 3.1 Typical crude oil viscosities at different temperatures.....	12
Figure 3.2 Estimation of the height of a vertical mist eliminator	16
Figure 3.3 Stairmand Dimensions for high-efficiency gas-solid cyclone . Sketch of a gas/liquid cyclone, incorporating some Stairmand dimensions	22
Figure 3.4 Typical dust cyclone dimensions, showing the corresponding notation	24
Figure 4.1 Sketch of price per size of chemical equipment, according to economies of scale.....	34
Figure 4.2 Comparison of annual cost indexes	37
Figure 4.3 Proportion of direct and indirect costs of vertical vessels. At the right, the field materials costs are discriminated	44
Figure 5.1 Decision-making framework for knitted-mesh and multi-cyclone scrubbers.....	46
Figure 5.2 Sketch of the staggered layout in heat exchanger of shell-and-tube and cyclone bundle in a gas-liquid scrubber	47
Figure 6.1 Variation of the internal scrubber diameter with diameter nominal for knitted-mesh and multicyclone scrubbers at 80 bar	53
Figure 6.2 Effect of the gas load factor (K_s) on the scrubber internal diameter at 20 and 80 bar respectively	53
Figure 6.3 Weight of knitted mesh and multi-cyclone scrubbers, including nozzles and internals.....	54
Figure 6.4 Mean ratio between weight per separator length of knitted-mesh and multi-cyclone scrubbers at different pressures	54
Figure 6.5 Effect of the gas load factor in reducing scrubber weight.....	54
Figure 6.6 Weight reduction of multi-cyclones compared to knitted-mesh scrubbers.....	55
Figure 6.7 Effect of the gas load factor in the reduction of weight of gas scrubbers at 80 bars.....	55
Figure 6.8 Variation of the gas load factor (K_s) with regard to pressure for knitted-mesh and multi-cyclone scrubbers with cyclone inlet velocity of 20 m/s.....	55
Figure 6.9 Ratios between vessel, purchase and bare module costs of knitted-mesh and multi-cyclone scrubbers at different pressures	57
Figure 6.10 Comparison between purchase costs of knitted-mesh and multi-cyclones at 20 and 80 bars respectively.....	57
Figure 6.11 Effect of the gas load factor increase in the reduction of vessel and purchase costs respectively for hypothetical scrubbers at 20 bar.....	58
Figure 6.12 Ratio between cost of the vessel and total purchase cost for knitted mesh separators at 40, 80 and 120 bar respectively	58
Figure 6.13 Mean ratio between vessel and total purchase (fob) costs for knitted-mesh and multi-cyclone scrubbers.....	59
Figure 6.14 Ratio between demisting pads costs for multi-cyclone and knitted-mesh scrubbers at different pressures	59

Figure 6.15 Variation of the ratio between bare module cost and purchase cost with regard to pressure for traditional scrubbers.....	59
Figure 6.16 Purchase cost of the vessel per weight for knitted mesh separators at 40, 80 bar respectively	60
Figure 6.17 Purchase cost of the vessel per volumetric flow rate for knitted mesh separators at 40 and 80 bars respectively.....	60
Figure 6.18 Bare module cost per flow rate (actual m ³ per hour) for knitted-mesh and multi-cyclone scrubbers at 40, 50, 70 and 80 bar respectively	61
Figure 6.19 Purchase cost per flow rate (actual m ³ per hour) for knitted-mesh and multi-cyclone scrubbers at 40, 50, 70 and 80 bar respectively	61
Figure 6.20 Comparison between the ratios of purchase cost per weight of separator and purchase cost per flow rate for knitted-mesh and multi-cyclone scrubbers at 20 and 120 bar respectively	62
Figure 6.21 Effect of the gas load factor on the ratio of purchase cost per flow rate at 20 bar	62
Figure 6.22 Average pressure drop across the cyclonic pad for multi-cyclone separators with cyclone inlet velocity of 20 m/s.....	63
Figure 6.23 Trade-off between a multi-cyclone initial investment and pressure drop with DN 450 at 20 and 70 bar respectively	63
Figure 6.24 Variation of the cut-point droplet diameter (x_{50}) with cyclone inlet velocity.....	65
Figure 6.25 Effect of pressure on reentrainment for percentage of liquid on the gas stream of 0.02, 0.1, 0.2 and 0.5 respectively.....	65
Figure 6.26 Validation of the vessel weight for knitted-mesh scrubbers against pressure vessels fabricated by KW International at 80 bar.....	66

LIST OF TABLES

Table 1.1 Gas load factors for selected gas scrubbers.....	3
Table 2.1 Summary of relative performance characteristics for demisters	6
Table 3.1 Typical molar compositions of natural gas from Åsgard field and Kårstø after being treated	10
Table 3.2 Composition of processed natural gas in different fields	11
Table 3.3 Some typical surface tensions.....	12
Table 3.4 Recommended velocities of natural gas for selection of pipe size at low and moderate pressure.....	13
Table 3.5 External diameters for different nominal pipe sizes	13
Table 3.6 Effect of pressure on K_S factor.....	15
Table 3.7 Maximum recommended pressure for carbon steel flanges at 840 F	17
Table 3.8 Joint efficiency.....	18
Table 3.9 Thickness increments to round-up the nearest metal plate.....	18
Table 3.10 Minimum thicknesses for process vessels	19
Table 3.11 Weight of mist eliminators.....	20
Table 3.12 Weight of pressure vessel nozzles.....	20
Table 3.13 Standard Size Distribution for droplets.....	21
Table 4.1 Main categories of capital cost estimates for chemical plants	32
Table 4.2 Typical parameters of the Six-tenths Rule for selected chemical equipment	35
Table 4.3 Typical materials of construction and capital cost factors for pressure vessels and distillation columns	35
Table 4.4 Typical equipment pressure capital cost factors.....	36
Table 4.5 Typical equipment temperature capital cost factors (Smith 2005)	36
Table 4.6 Cost Indexes	37
Table 4.7 Comparison among purchase cost equations of pressure vessel	38
Table 4.8 Values of the parameters of purchase cost equations of vertical pressure vessel.....	39
Table 4.9 Values of the parameters of the Turton et al. (1998) equation.....	39
Table 4.10 Purchase cost equations for gas-solid cyclones	40
Table 4.11 Pressure factors for pressure vessels.....	40
Table 4.12 Estimate of the bare module cost factor for selected equipment.....	43
Table 4.13 Bare module factors of selected equipment.....	44
Table 4.14 Typical investment site factors.....	45
Table 6.1 General data and conditions used in the result presented.....	51
Table 6.2 Properties of the natural gas composition selected at different pressures.....	52
Table 6.3 Dimensions and costs for selected knitted-mesh scrubbers.....	56
Table 6.4 Dimensions and costs for selected multi-cyclones (D_c equal to 6'' or 0.1524 m).....	56
Table 6.5 Comparison among different cyclonic configurations at P=20 bar, DN 450 and cyclone diameter of 6''	64
Table 6.6 Comparison among different cyclonic configurations at P=70 bar, DN 450 mm and cyclone diameter of 6''	64

LIST OF SYMBOLS

A	Area
A	Coefficient of a polynomial in cost equations
A_R	Total surface area of a cyclone
b	Width or diameter at the cyclone inlet
B_1, B_2	Coefficients used to the bare module costs
C	Corrosion allowance
C	Cost
c_o	Mass fraction of liquid on the gas stream
cp	Mass heat capacity
d	Diameter of the vessel inlet pipe
D	Diameter of scrubber vessel
d_{HI}	Liquid hydraulic diameter
D_C	Diameter of each cyclone
D_g	Diameter corresponding to the gas area (Estimated by using 'ε')
E	Joint efficiency
e	Wall roughness
f	Friction factor
F	Cost factor
F	Cumulative undersize factor related to droplet distribution
F_g	Factor of adjustment related to the liquid holdup in a vessel
f_s	Factor of adjustment to estimate nominal pressure
g	Gravitational acceleration
H	Height of cyclone
h	Liquid column in the scrubber vessel
I	Cost index
k	Distribution function exponent for empirical correlations to c_{oL}
K_S	Gas load or Souders-Brown factor
k_s	Absolute wall roughness
L	Length
l_{pad}	Height of the wire mesh demisting pad
m	Exponent used on the Rule of Six-tenth equation
m	Mass
MW	Molecular weight
N	Number of stages
n	Efficiency
n_C	Number of cyclones in a multi-cyclone unit
n_{sep}	Cyclone efficiency without considering reentrainment
N_μ	Reentrainment number
P	Pressure
Q	Volumetric flow rate of gas
q_l	Volumetric flow rate of liquid
R	Radius
R	Constant of ideal gases
Re	Reynolds number
Re_{l*}	Reynolds number corresponding to the liquid film
S	Stress allowance
S	Length of the vortex finder in a cyclone
sg	Specific gravity

<i>size</i>	Size parameter in equipment: dimension, weight, etc
<i>t</i>	Thickness
<i>T</i>	Temperature
<i>t_R</i>	Time of residence of liquid
<i>U'_{t50}</i>	Particle velocity relative to gas
<i>V</i>	Volume
<i>v</i>	Velocity
<i><v></i>	Mean velocity
<i>v_{max}</i>	Design velocity according to the gas load factor used
<i>W</i>	Weight
<i>W_{comp}</i>	Work of hypothetical recompression
<i>We</i>	Webber number
<i>W_{turbine}</i>	Power required for hypothetical recompression
<i>x</i>	Droplet size (Usually expressed in μm)
<i><x></i>	Mean droplet size
<i>x_{fact}</i>	Empirical correction factor

Greek letters

<i>α</i>	Restriction coefficient in cyclones
<i>β</i>	Angle of the gas helix in a cyclone
<i>δ</i>	Liquid film thickness
<i>Δ</i>	Difference operator
<i>ΔP</i>	Pressure drop
<i>ε</i>	Gas void fraction
<i>μ</i>	Viscosity
<i>ξ</i>	Ratio between b and R _c (Cyclone radius)
<i>ρ</i>	Density
<i>σ</i>	Surface tension
<i>τ</i>	Shear stress

Abbreviations

<i>API</i>	American Petroleum Institute
<i>BM</i>	Bare module cost
<i>CEPCI</i>	Chemical Engineering Plant Cost Index
<i>CS</i>	Carbon steel
<i>f.o.b</i>	Free on board
<i>GOR</i>	Gas oil ratio
<i>M&S</i>	Marshall & Swift cost index
<i>SS</i>	Stainless steel
<i>TFI</i>	Total fixed investment
<i>IS</i>	Investment at site

Subscripts

<i>50</i>	Referred to cut size (Efficiency 50%)
<i>acc</i>	acceleration
<i>b</i>	Related to vessel weight per length
<i>body</i>	In the cyclone body
<i>C</i>	Related to cyclones
<i>c</i>	Vortex cone
<i>cycle</i>	Related to the Brayton gas turbine cycle
<i>d</i>	Design
<i>d</i>	Dust/Liquid outlet
<i>tot</i>	Total
<i>SS</i>	Seam to seam
<i>e</i>	Empty vessel
<i>E</i>	Actual
<i>g</i>	Gas
<i>g</i>	global
<i>g,i</i>	Gas in contact to the gas-liquid interface
<i>i</i>	Internal
<i>i</i>	Index
<i>I</i>	Internals (weight of demisting pads)
<i>in</i>	Related to the cyclone inlet
<i>inlet</i>	Inlet pipe of the scrubber
<i>Inlet-max</i>	Maximum allowable at the inlet pipe
<i>l</i>	Liquid
<i>l</i>	Ladders and platforms (Weight estimation)
<i>l,w</i>	Liquid in contact to the wall
<i>M</i>	Metal
<i>M</i>	Material
<i>m</i>	Geometric mean
<i>max</i>	Maximum
<i>med</i>	Median
<i>mix</i>	Mixture (Two phase flow: gas and liquid)
<i>multicyclone</i>	Related to scrubbers with several cyclones in parallel
<i>N</i>	Nozzles
<i>out</i>	External
<i>P</i>	Depends on pressure
<i>p</i>	Purchase
<i>p</i>	Referred to polytropic efficiency
<i>pad</i>	Related to the knitted-mesh or wire-mesh pad
<i>q</i>	Quantity
<i>R</i>	Cyclone body
<i>r</i>	Includes wall roughness
<i>Reent.</i>	Reentrainment
<i>Sa</i>	Souder mean
<i>sm</i>	Smooth pipes or surfaces
<i>std</i>	Standard
<i>T</i>	Depends on temperature
<i>v</i>	vessel

w	wall
x	Vortex finder or gas exit tube
$year_1$	Related to base period in cost indexes
$year_2$	Related to actual period in cost indexes
z	Axial direction
θ	Tangential direction
θ_{CS}	Tangential velocity component in the surface

Superscripts

$^{\circ}$	Angular or temperature degree
\bullet	Flow rate (Used especially for mass)
0	At atmospheric conditions and carbon-steel based material

1. INTRODUCTION

Natural gas industry has become very competitive during the last decade. In fact, due to the declining oil availability and its negative effect on the environment are making natural gas in one of its possible substitutes. In spite of both are fossil fuels, oil contributes at much higher level on the global warming effect. In addition, natural gas has taken an important place on the generation of electricity and eventually might overtake coal in this regard. Nowadays, natural gas is the third source of energy worldwide and ExxonMobile predicts that it will be the second by 2025 (Tillerson 2012). Furthermore, Russia and Norway are the most important suppliers of this fuel in Europe; and this represents a very important source of income for both countries.

This very profitable industry requires of very costly equipment and processes though. Gas-liquid separation is one of these important operations, and together with heat exchangers and compressors are crucial in obtaining the hydrocarbon dew point specifications (Fredheim 2010). These specifications among others must be fulfilled to transport and commercialise the gas. Gas liquid separations are actually performed in a process vessel with several components. The design and selection of this equipment is vital to avoid bottlenecks and decrease the capacity of an entire facility. Depending on the liquid capacity, we can have different categories of gas-liquid separators. For instance, if the liquid flow rate is very high we can have a slug-catcher which is commonly used in gas gathering pipelines (Steward and Arnold 2008). On the other hand, we have separators employed to get rid of small quantities of liquid from the gas stream. They are so-called gas scrubbers and their liquid handling capacity is below than 3 to 5% in volume (Fredheim 2010). Generally, the liquid is in form of droplets for the last case.

This small portion of liquid is generally harmful, especially for rotating equipment and heat exchangers. For example, *compressors might be damage, destroyed, or rendered ineffective by free liquid* (Steward and Arnold 2008, p. 83). If heat exchangers operate at very low temperature, liquids could freeze down and cause inefficiency or damage in the equipment. Moreover, dehydration equipment would lose efficiency or even being damage or destroyed by the presence of liquid hydrocarbons (Steward and Arnold 2008). For these reasons, it is required selecting the appropriate equipment to avoid these potential dangers.

Traditional technology, employed as gas scrubbers, implies a combination of reduction of gas velocity and impingement of droplets to a demisting pad. In this way, droplets coalesce and drain to flow out at the bottom of the vessel. The most used of these impingement technologies is the knitted mesh which is a very dense wire network. This kind of demisting devise is allocated close to the top of a pressure vessel, where is allowed gravity separation in previous sections. These scrubbers have been proven successfully for several years and provide gas-liquid separation with very high efficiency (higher than 98-99%). On the other hand, these mist eliminators are very bulky and heavy; especially when the gas handling

and/or pressure are high. Therefore, it is challenging and costly to use this equipment where the plot area is restricted like in offshore operations.

Different kinds of cutting-edge technology are emerging and they tend to be much more compact than the traditional equipment. One of these technologies is the cyclonic scrubbers; where the droplets are separated by accelerating the gas stream thus droplets impact to the vessel walls. Nevertheless, the selection of a separator is becoming a difficult task because it is required engineering experience to choose the proper scrubber. This is motivated to the number of factors that are required for decision making in this case. Therefore, a methodology to facilitate this selection might be beneficial.

In fact, the main objective of this thesis is develop models of decision making for selecting gas scrubbers for decision making based on technical and economical parameters. Then, a big question arises in how develop these models and where can be found the bases of them. Therefore, an alternative is to generate mathematical models for one or two of these technologies and extrapolate to others. For instance, the knitted-mesh scrubbers could be the starting point since they have long tradition and there may be enough data to construct the model. In addition, the gas-liquid cyclones can be used for a second model because they have similarities with dust-cyclones and data from the latter might be used to the former. Furthermore, both gas scrubbers are more or less the same capabilities to separate droplets from the gas stream. For example the droplet size range and efficiency. The information related might be found on diverse source of literature such as books, catalogues, technical magazines and websites.

Another issue is selecting the appropriate parameters that can be generated from these models, and would be useful in the decision-making process. A solution may imply the estimation of dimensions, weight and cost of the separator to establish a pattern of comparison. Furthermore, some of these parameters could be combined to estimate additional variables which allow the selection in a more absolute manner. For example, gas load factor, cost per weight and an alternative variable. Nowadays, the gas load factor or Souders-Brown factor is used on sizing knitted-mesh scrubbers and it has been extrapolated to other technologies. This factor is usually provided by vendors since it is estimated based on experience. The equation (1.1) shows the equation of Souders-Brown where the load factor and gas and liquid densities are used to estimate design gas velocity in the vessel. Additionally, table (1.1) presents load factors for some demisting technologies.

$$v_{\max} = K_s \sqrt{\frac{\rho_l - \rho_g}{\rho_g}} \quad (1.1)$$

Table 1.1 Gas load factors for selected gas scrubbers ('Sulzer' 2010; Campbell 2004; 'NORSOK' 2001)

Demister	Ks range (m/s)
Knitted-mesh	0.08-0.107
Typical vanes	0.13-0.17
Cutting-edge vanes	Up 0.3-0.35
Cyclones	0.15, 0.25 ¹

This thesis is structured as follows:

Chapter 2, Gas scrubbers: types and main features. In this part is presented an overview of different gas scrubber characteristics and similarities and differences among the most common mist eliminators.

Chapter 3, Sizing of gas scrubbers: In this section are provided equations, data, ratios and additional information used to estimate dimensions, weight, among other parameters of the selected technologies of knitted mesh and cyclonic scrubbers.

Chapter 4, Economical evaluation: In this chapter provides the procedure followed to estimate the cost of equipment, focused on gas liquid separators. In this part, it is also described the different costs associated to the installation of equipment.

Chapter 5, Methodology: In this section is shown how the information contained in the three previous chapters is used to develop the models proposed.

Chapter 6, Results: Presented the most relevant information obtained in form of graphs and tables.

Chapter 7, Discussion of results

Chapter 8, Conclusions and recommendations

¹ NORSOK P-100 recommends 0.15 but other authors are less conservative and estimate a Ks up 0.25 m/s

2. GAS SCRUBBERS: TYPES AND MAIN FEATURES

Gas scrubbers are two-phase gas liquid separators, where small fractions of liquid are recovered by using different mechanisms. The liquid is usually in form of droplets with any solid particles from the gas stream (Fabian et al. 1993). In the gas & oil industry, the liquid is originated from carryover onto gas outlets of production separators or condensation due to cooling or pressure drop (Stewart and Arnold 2008). On the other hand, the reaction of two vapours to produce a liquid originates very small droplets; e.g. sulphuric acid (Fabian et al. 1993).

There are different devices for demisting purposes, which involve different mechanisms of separation. Among them, we can find gravity setting, inertial impaction, flow-line interception, diffusion deposition, electrostatic attraction and particle agglomeration (Perry et al. 1997). All these mechanisms are somehow based on the natural balance between gravitational and drag forces. This is achieved in different ways: overcoming drag force by reducing velocity, introducing additional forces and increasing gravitational force by boosting droplet size. Under the first category we can find gravity separators while centrifugal separators, electrostatic precipitators and venturi scrubbers belong to the second. In the same way, impingement separators correspond to the third category (Fabian et al. 1993).

The simplest equipment used for gas liquid separation is gravity settlers or knock-out drums. However, this kind of equipment is just suitable for large droplets; typically on the order of 150-300 μm (Campbell 2004). On the other hand, impingement scrubbers add the action of direct impact and inertial forces. Therefore, the efficiency increases and these devices are capable to separate much smaller droplets. In state-of-the-art equipment, an additional force can be utilized in such way that particle collection is boosted in several hundredfold compared to gravity. Particularly, the centrifugal force in cyclones is on the order of 5 to 2500 times the gravitational force (Fabian et al. 1993).

Among all types of mist eliminators, the impingement separators are widely used by far; especially the called knitted mesh. Due to a good balance between efficiency, operating range, pressure drop and installed cost (Fabian et al. 1993a). The knitted mesh is in fact an intricate wire network which allows coalescence of liquid droplets. The other impingement demisters mostly used are the vane-type and fibre beds. The former has the same principle to knitted mesh, but the coalescing area is made by multiple channels. Regarding to fibre beds, it is composed for very small fibres which capture tiny droplets.

Before selecting the gas-liquid separator, it must be taken into account several factors. Among them, one can find: droplets size, allowable pressure drop, tolerance of the separator to plugging by solids (if they are present) and liquid and gas handling capacity. It is also considered: the availability of compatible materials with the process, possibility of

introducing the demisting device into an existing vessel, and costs of demisting units. The last item can be discriminated as costs of the mist eliminator itself and other required for vessels, piping, instrumentation and utilities (Fabian et al. 1993a). It is also gaining importance the plan area which is a critical factor on offshore platforms (Shell 2002).

The figure underneath shows typical droplet sizes according to their source and the appropriate demisting equipment into these ranges. In the same manner, table (2.1) provides a relative comparison among the main kinds of gas scrubbers mentioned above. Afterwards, it is presented a very brief description of the main gas scrubbers used in industry; emphasising their main characteristics, range of use and parameters of design.

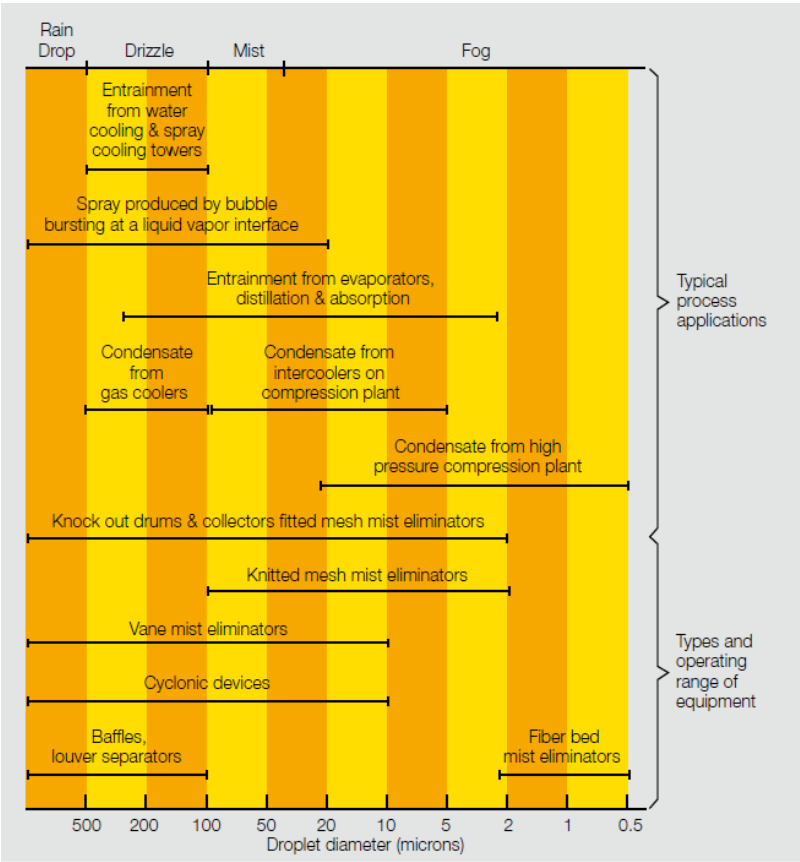


Figure 2.1 Particle size range from different sources and appropriate demister pads (Sulzer 2010)

Table 2.1 Summary of relative performance characteristics for demisters ('Koch-Glitsch' 2007; 'Sulzer' 2010; 'HAT International' 2009; 'Shell' 2002)

Parameter	Demister			
	Knitted mesh	Vane	Fibre beds	Multi-cyclone
Overall efficiency (%)	> 98	> 96	Up 99.9%	> 98
Cost (scale)	1	2-3	10	3-5
Gas capacity (scale)	5	6-15	1	15-20
Liquid capacity (scale)	5	10	1	10
Pressure drop (mbar)	less than 2.5	1-9	5-50	25-75*
Solid handling (scale)	3	10	1	8
The relative scale is 1 for the lowest, the others are scaled				
* The pressure drop is given at low and moderate pressure				

Knitted mesh eliminators

They are usually formed by a metallic knitted wire with high surface area and void fraction. In fact the wire diameter is often between 0.10 to 0.28 mm with a typical void fraction in the range of 95 to 99% (Fabian et al. 1993a). Each mist eliminator is tailor-made to fit to vessel dimensions ('Sulzer' 2010). They usually have vertical position, to handle easily high gas loads. An illustration of this kind of separators is offered by figure (2.2).

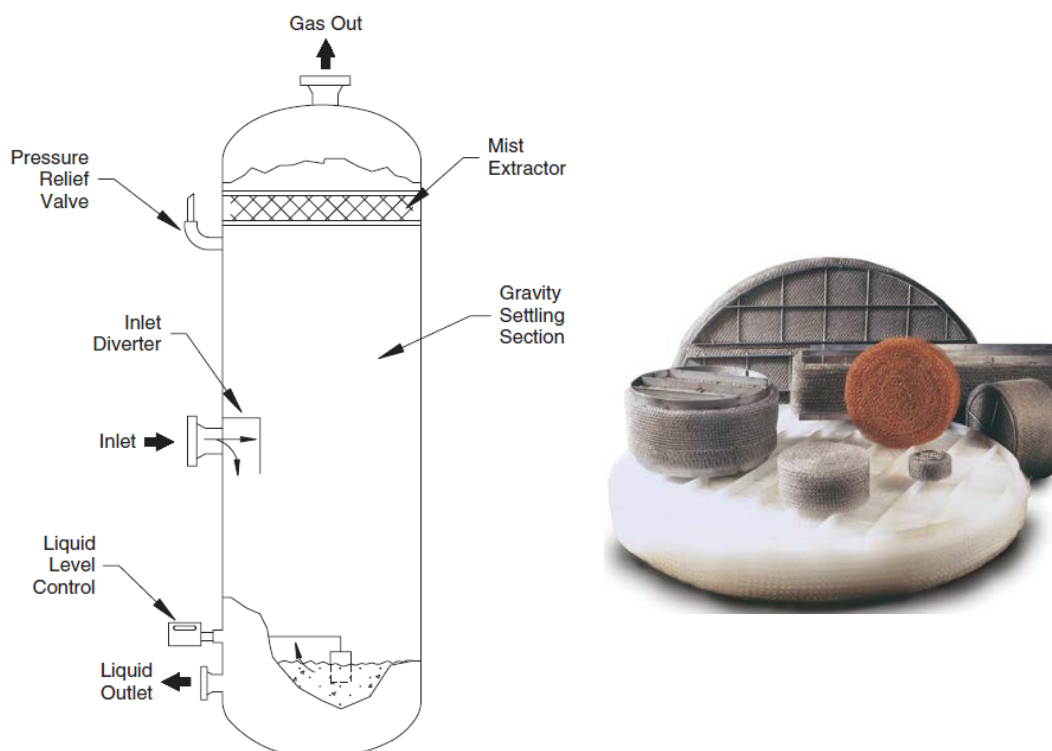


Figure 2.2 Vertical knitted-mesh separation unit and demister pads (at the right). (Steward and Arnold 2008; 'Koch-Glitsch' 2007)

They are widely used for demisting services where the gas feed has moderate liquid load in form of droplets. For instance, they are employed in production/test separator (for moderate GOR); before/after of glycol contactors and inlet scrubbers for gas export pipelines. Although they have high efficiency and low pressure drop, they are not appropriate for fouling services. For example wax, asphaltenes, sand and hydrates ('Shell' 2002)

Vane demisters

They consist in a series of baffles or plates where the gas must flow (Fabian et al. 1993). In fact the flow changes direction several times originating that droplets impinge on the vane surfaces, where a liquid film is formed and it drains afterwards ('Sulzer', 2010). The space between baffles is on the order of 5 to 75 mm, with a total depth in the flow direction of 150 to 300 mm (Fabian et al. 1993a). Figure (2.3) shows an illustration of vane demisters.

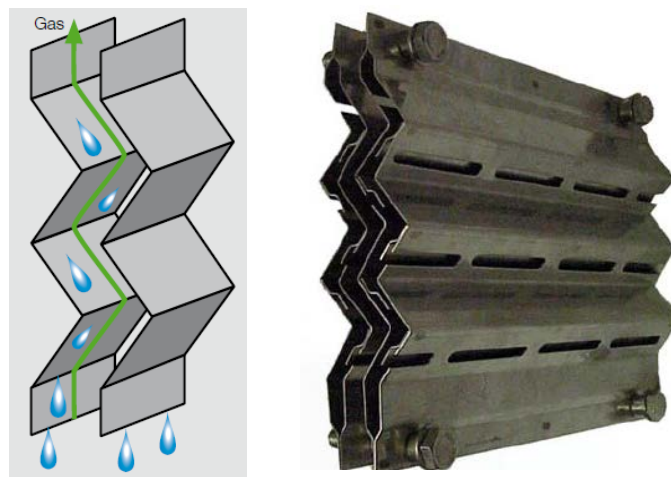


Figure 2.3 The coalescence principle on vane separators and flexichevron vane-type for high capacity (at the right) ('Sulzer' 2010; 'Koch-Glitsch' 2007)

This kind of separators is feasible when the mesh mats might become plugged, e.g. waxy crudes and sulphur recovery units ('Shell' 2002). Nevertheless, they are usually less efficiency than knitted mesh separators. Additionally, they are recommended when the pressure exceeds 70 bar ('Shell' 2002).

Fibre beds

This kind of equipment is extremely specialised and it just justified for separation of very small droplets (less than $2.0\ \mu\text{m}$). Liquid and gas flow horizontally and concurrently through very dense and small fibres. Their diameter is usually less than 0.02 mm. The surface area of the fibres is in the range of 3 to 150 times that of knitted mesh unit (Fabian et al 1993). Resulting in this way, very costly and provoking extremely high pressure drops.

Cyclonic separators

As mentioned before, the gas undertakes high velocities to allow the impingement of droplets to the cyclone walls. In the particular case of demisting operations, the cyclonic units are usually composed for several small cyclones; allowing to have a good performance. The diameter of each cyclone is usually less than 250 mm (Hoffmann and Stein 2008). In fact, most standard cyclones of this type have diameters of 2 and 4 inches (Approximately 50 and 100 mm respectively). The cyclones are fitted between two plates in a parallel fashion ('Shell 2002'). The bundle of cyclones is located inside of a vessel which is often more compact than that used for knitted mesh eliminators.

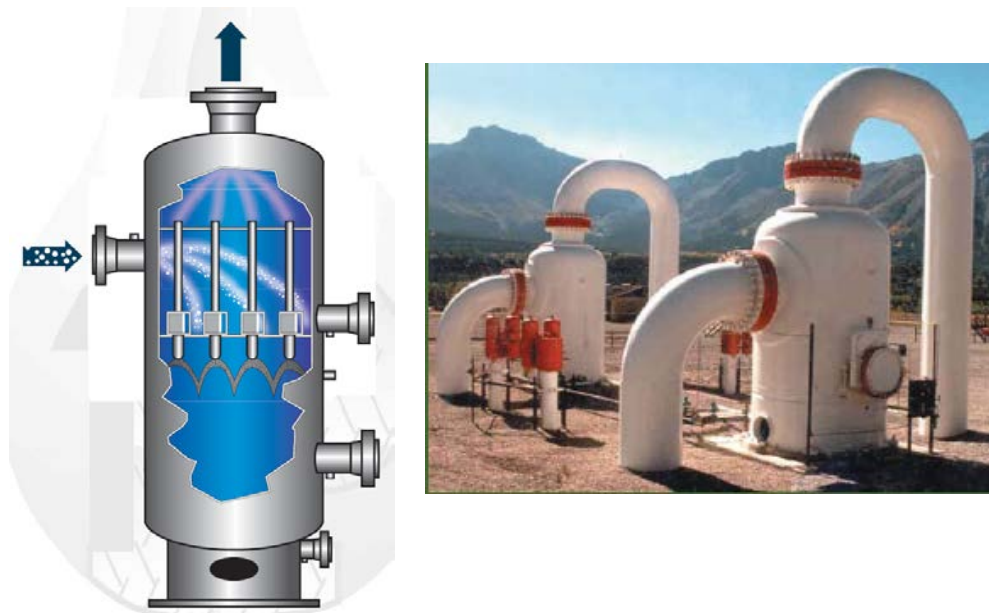


Figure 2.4 Typical gas-liquid multi-cyclone design and two multi-cyclone gas scrubbers in a metering station in Western Canada. (Peerless 2012)

Due to the compactness of this equipment, its use is attractive in places where the plot area is restricted like offshore platforms ('Shell' 2002). Nevertheless, the pressure drop is very high and the fluid dynamics is very complex in this devices; which requires more research related (Fabian et al. 1993). In addition to offshore platforms, the use of multi-cyclone scrubbers has been found suitable for very high pressure operations. It also allows higher liquid capacity than knitted mesh scrubbers, but not higher than 3% by volume ('Shell' 2002).

3. SIZING OF GAS SCRUBBERS

Different criteria are considered when gas scrubbers are designed. On one hand, the engineering experience has given to us some numbers, ratios, graphs and even equations to size chemical equipment. This contribution has been very useful since it is easy to apply and suitable under most working conditions. This kind of empirical knowledge is part of the so-called rules of thumb. A rule of thumb are defined "*a practical and approximate way of doing or measuring something*" ('Cambridge Dictionaries Online', 2011), those rules have been applied in several fields such as science, construction, cooking, etc. Branan (2005) and other authors have compiled rules of thumb for several kinds of chemical equipment. Nevertheless, most of this knowledge is not linked to theoretical bases as shown in the definition above. Furthermore, some of these rules are simple ratios which work well in a restricted range.

On the other hand, it has been obtained data based on pure theoretical bases. Nevertheless, that data is very scarce compared to that given by empirical knowledge. The main issue of develop pure theoretical models is their complexity. In many cases, there are several factors to take into consideration so the correlations obtained are extremely difficult to solve.

In the present work, most of the information is based on empirical knowledge but avoiding generalised use of ratios. In other words, it will be used equations instead of simple ratios to have a good range of reliance. The ratios can be use but only on their standard limits. To illustrate this, we can imagine a calculation of the weight of a separator just consider the diameter of the equipment. In this way, a standard proportion is given to estimate this directly. Consequently, the results might be reliable for just atmospheric conditions. Therefore, important parameters like pressure, content of liquid at the inlet stream, among others have been neglected.

In this chapter, it will be also shown empirical knowledge with theoretical fundamentals. For instance, the Souder-Brown equation used to determine the maximum velocity inside of the separator vessel. Furthermore, concepts such as re-entrainment, droplet size, friction factor will be presented in the estimation of cyclones efficiency.

On following pages, we are able to see a set of equations, tables and some ratios used in the sizing of knitted-mesh scrubbers and cyclones. Most of them are scattered in different literature sources. Therefore, it is intended to present an overview in how to size this kind of equipment. The sizing is mostly oriented to determine parameters such as diameter, length and weight used in the estimation of the purchase and installed cost of this kind of equipment. Nevertheless, the multi-cyclone design includes other parameters used in the efficiency and pressure drop calculation but they are useful in the economical evaluation as well.

3.1 Features of the gas-liquid stream and physical-chemical properties

Before starting sizing demisting equipment, it is required to have a general idea about the main characteristics of the gas-liquid stream to be treated. The gas is the dominating phase so it is vital to know intrinsic properties such as composition, pressure and average temperature. The most important parameter of the liquid is its density, which can be estimated by knowing the substance(s) that constitute it. On the other hand, the liquid could be a mixture of several compounds, especially for oil fractions. In the case of cyclones, this issue is worsened since are required additional properties in the calculations, specifically in the efficiency and pressure drop.

In the case of natural gas, we have some standard specifications after been treated for its commercialisation. However, the composition of gas relies on the location and age of the reservoir. For this reason, it is very important to have an average composition of the gas before the sizing or selection of a gas scrubber. The following tables present compositions of natural gas from different fields. The first corresponds to Åsgard field and reflects the composition at different stages. The second shows composition of processed gas at different locations.

Table 3.1 Typical molar compositions of natural gas from Åsgard field and Kårstø after being treated (Fredheim 2010)

Chemical compound	Formula	Well Stream	Rich gas	Sale gas
water	H ₂ O	3.00		
nitrogen	N ₂	0.50	0.58	0.54
carbon dioxide	CO ₂	3.00	3.71	1.89
methane	CH ₄	75.00	79.55	91.37
ethane	C ₂ H ₆	7.50	9.43	5.52
propane	C ₃ H ₈	4.00	4.49	0.6
isobutane	i-C ₄ H ₁₀	0.60	0.59	0.03
n-butane	n-C ₄ H ₁₀	1.00	1.07	0.04
isopentane	i-C ₅ H ₁₂	0.30	0.23	0.01
n-pentane	n-C ₅ H ₁₂	0.30	0.22	
Hexane +	C ₆ +	4.80	0.13	

Table 3.2 Composition of processed natural gas in different fields (Jakobsen, as cited in Vågenes 2011).

Chemical compound	Formula	Troll Norway	Sleipner Norway	Draugen Norway	Groningen Netherlands
methane	CH ₄	93.070	83.465	44.659	81.29
ethane	C ₂ H ₆	3.720	8.653	13.64	2.87
propane	C ₃ H ₈	0.582	3.004	22.825	0.38
isobutane	i-C ₄ H ₁₀	0.346	0.250	4.875	0,15
n-butane	n-C ₄ H ₁₀	0.083	0.327	9.466	0.04
Pentane +	C ₅ +	0.203	0.105	3.078	0.06
nitrogen	N ₂	1.657	0.745	0.738	14.32
carbon dioxide	CO ₂	0.319	3.429	0.720	0.89

After having a clear idea of the main characteristics of the gas phase, we are to estimate other properties. For knitted mesh scrubbers, we additionally need the gas density. In the case of cyclones, viscosity and specific heat capacity are required for the gas phase. Superficial tension and viscosity of the liquid are also required.

The properties of the gas phase can be easily estimated by using software packages for chemical engineering simulations. Among these software packages, we can find Pro II and Hysys. Selecting an appropriate thermodynamic model is vital to get reliable results, especially when the conditions are non-ideal like at high pressure and/or low temperature. When hydrocarbons and non-polar substances are present, the Peng-Robinson model is very accurate.

Regarding to the liquid density, it can be used the API gravity. This property allows characterise oil in different categories: light, medium, heavy and extra-heavy. The limit between one category from another changes according to the source. However, the most important is to have an estimate of the API gravity for the liquid fraction. The following equation allows convert °API into specific gravity. The liquid density is obtained by just multiplying the specific gravity by the density of water.

$$sg \text{ at } 60 \text{ } ^\circ\text{F} = 141.5 / (^\circ\text{API} + 131.5) \quad (3.1)$$

Other properties of liquid result more difficult to estimate, since its exact composition is unknown in many cases. This uncertainty might be detrimental, especially for multi-cyclone demisters where fluid properties such as surface tension play a crucial role on the separator performance (Fredheim 2010). Nevertheless, it can be taken some approximations, considering values for high hydrocarbons. The following table presents an approximate estimation of surface tension.

Table 3.3 Some typical surface tensions (Campbell 2004)

	σ (dyne/cm) at 38 °C
HP Oil/Condensate	10-20
LP Oil/Condensate	20-30
NGL	5-15
Water	70
TEG	45*
* Surface tension at 25 °C.	

Viscosity for oil fractions can be estimated by means of specific gravity, by using appropriate graphs. The figure (3.1) shows an estimation of viscosity for light, medium and heavy oils.

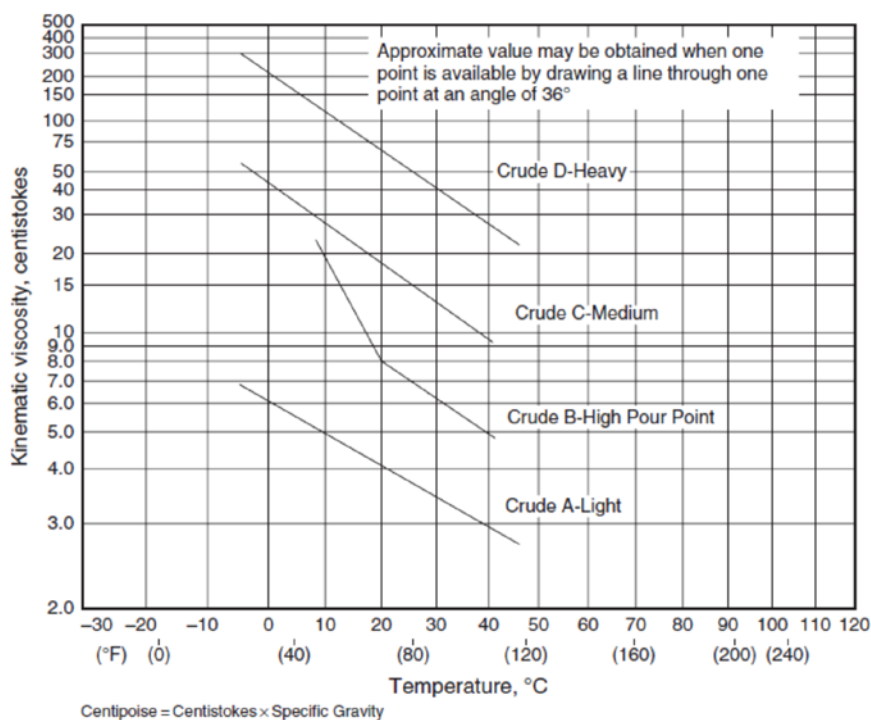


Figure 3.1 Typical crude oil viscosities at different temperatures (Stewart and Arnold 2008)

Other parameters such as gas volumetric flow, mixture velocity and liquid content in the gas are extremely important. Without them, it is not possible to estimate the dimensions of the separator. The velocity of the two-phase flow stream is usually linked with a maximum allowable at inlet nozzle. If the internal diameter of the nozzle and velocity are known, the volumetric flow rate is a straightforward calculation. The Table (3.4) shows maximum velocities for natural gas while table (3.5) presents external diameters for steel-based pipes respectively.

Table 3.4 Recommended velocities of natural gas for selection of pipe size at low and moderate pressure ('Mecon Limited', 2006)

<i>Diameter nominal</i> ²	<i>Maximum velocity (m/s)</i>
20-80	2
100-250	4-5
300-500	6-7
600-800	7-8
900-1200	9-12
1300-2000	13-20
>2000	23-28

NORSOK P-001 (2006) recommends use the equation below to avoid noise (the maximum velocity should not be higher than 60 m/s). However, the velocity given could origin an excessive pressure drop. This value usually fits with high diameter pipes. As a result, it is preferable to use the values reflected on the table.

$$v_{inlet-max} = 175\rho_g^{-0.43} \quad (3.2)$$

The velocity is expressed in m/s while the density in kg/m³. On the other hand, Campbell (2004) recommends lower velocities compared to those given by equation (3.2). He argues that nozzles size must minimise erosion/corrosion, pressure drop, entrainment, etc. The equations as follows give maximum velocities for the gas outlet, two phase flow inlet and liquid outlet. The last one corresponds to 1 m/s.

$$v_{inlet-max} = 60\rho_{mix}^{-0.5} \quad (3.3)$$

$$v_{outlet-max} = 75\rho_g^{-0.5} \quad (3.4)$$

Table 3.5 External diameters for different nominal pipe sizes ('Selmon co.' 2012)

Nominal Diameter (mm)	Outside Diameter (mm)	Nominal Diameter (mm)	Outside Diameter (mm)
20	26.7	350	355.6
25	33.4	400	406.4
40	48.3	450	457.2
50	60.3	500	508.0
80	88.9	600	609.6
100	114.3	650	660.4
125	141.3	700	711.2
150	168.3	750	762.0
200	219.1	800	812.8
250	273.1	850	863.6
300	323.9	900	914.4

² Diameter nominal or nominal diameter is abbreviated as DN. This abbreviation came from the French 'diamètre nominal'. Additionally, it is generally expressed in millimetres.

The internal diameter (d_i) is determined by subtracting the pipe thickness (t_{pipe}) from the outside diameter (d_{out}), in the following way:

$$d_i = d_{out} - 2t_{pipe} \quad (3.5)$$

The internal diameter is computed by using the following expression (Ellenberger 2010):

$$t_{pipe} = \frac{P_n d_{out}}{2S_{pipe} E_{pipe}} \quad (3.6)$$

Where P_n is the nominal pressure in psig, whose value are related to the working pressure according to different criteria. The procedure to estimate this pressure, it will be shown on the explanation of knitted-mesh sizing. S_{pipe} is the stress allowance, which is usually taken as 14400 psig, and E_{pipe} is the joint efficiency for the pipe which is usually taken as 1.

Regarding to the liquid proportion in the gas, this variable defines the height of the liquid column inside of separators. It can also define the efficiency of the demister and the friction factor of the mixture. Therefore, it is necessary to have an estimate of this parameter, especially to avoid flooding of the knitted mesh and high carry over in cyclones. Campbell (2004) claims that the maximum liquid loading on wire mesh pad is about 2.4 m³/h per m² of flow area. In the case of cyclones, the liquid capacity can double this value (Koch-Glitsch 2007) or could be up 3% by gas volume ('Shell' 2002).

3.2 Sizing of knitted-mesh separators

The design knitted-mesh is primary based on the estimation of the maximum velocity inside the chamber. This velocity is usually determined by the Souders-Brown equation, as mentioned before, the equation is shown as (1.1). It is crucial to introduce the right coefficient " K_s " into this equation. Campbell (2004) suggested that K_s is in the range of 0.08-0.107 and 0.122-0.152 m/s for vertical and horizontal separators respectively. In fact, most configurations are vertical since allows lower plot area and they are more adequate for handling high gas loads.

$$V_{max} = K_s \sqrt{\frac{\rho_l - \rho_g}{\rho_g}} \quad (1.1)$$

Some scholars, like Stewart and Arnold (2008), have proposed to determine the Souders-Brown coefficient by means of drag coefficient and Reynolds number. However, the calculation is tedious and it has resulted conservative. For this reason, most knitted-mesh

gas scrubbers are based on the maximum value of K_S shown above. On the other hand, this value should be corrected by means of pressure, as reflected on the following table.

Table 3.6 Effect of pressure on K_S factor (Fabian et al. 1993)

Pressure (bar)	Correction factor, % of the design value
1	100
5	94
10	90
20	85
40	80
80	75

Then, the internal diameter (D_i) of the vessel can be estimated by the equation (3.6). The diameter is often rounded off by increments of 6 inches, to adjust the vessel to standard designs in factory.

$$D_i = \sqrt{\frac{4Q}{\pi v_{\max} F_g}} \quad (3.8)$$

F_g is equal to 1 for vertical vessels. The volumetric flow rate is usually given but it can be correlated to the nominal diameter of the inlet vessel. Using the velocity of the table (3.4) for the respective diameter nominal and calculating the area of the pipe, it can be calculated the flow rate. Otherwise the flow rate can be used to determine the velocity at the inlet and the appropriate nominal diameter of the nozzle.

$$Q = v_{inlet} A_{pipe} = v_{inlet} \pi (d_i)^2 / 4 \quad (3.9)$$

Having estimated the diameter, it could be determine the vessel height. This variable is usually called seam-to-seam length and it is empirically related to the separator diameter. Many authors recommend determine this value by using a ratio between length and diameter in the range of 2-5. Others advise to correlate different sections of the vessel by means of the diameter or a fixed value. Figure (3.2) shows an example about estimating the separator length.

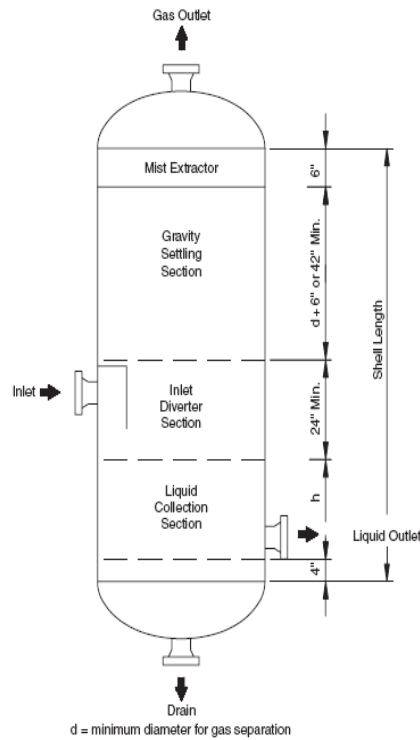


Figure 3.2 Estimation of the height of a vertical mist eliminator (Stewart and Arnold 2008)

From the graph above we can have, the following equation:

$$L_{SS} = \frac{(h + D_i + 1016)}{1000} \quad (\text{for } D_i \geq 194 \text{ mm}) \quad (3.10)$$

The diameter and the liquid height (h) are expressed in mm. The calculation of the liquid length will be explained in few lines. Alternatively, Towler and Sinnott (2008) have proposed equation (3.9) which allows have closer values regarding to slenderness ratio. The last definition is just another form to express the ratio between length and diameter.

$$L_{SS} = \frac{(h + 1.5D_i + 400)}{1000} \quad (3.11)$$

Towler and Sinnott (2008) also advises to adjust the length of the vessel if the slenderness ratio is lower than two. In this manner, the separator height should be at least twice its diameter. Other authors recommend even higher values, for example 2.5 or 3.

Campbell (2004) computes the liquid height, by using a similar expression as shown as follows:

$$h = 8.842 \cdot 10^{-4} \frac{q_I t_R}{D_i^2} \quad (3.12)$$

In equation (3.10), the 'h' value is given in m. q_l is the liquid volumetric flow rate in m^3/s but the residence time (t_R) is expressed in minutes. In respect of the latter, Campbell (2004) suggests 1-3 minutes for natural gas but Towler and Sinnott (2009) claims that it should be at least 10 minutes. The same authors advise to have at least 300 mm of liquid level thus level control is ensured.

After having estimated diameter and height of the separator, the second stage corresponds to the mechanical design of the vessel. At this step, a critical parameter is the design pressure. Guthrie (1969) suggests 50 % over the working pressure while other authors are less conservative. Seider et al. (2004) advises if the pressure is between 0-5 psig, the design pressure should be 10 psig. In the case, of pressures higher than 1000 psig, the design pressure is equal to 1.1 times the working pressure. The same authors give the following formula to compute the nominal pressure when operating pressures are from 10 to 1000 psig.

$$P_n = \exp \left[0.60608 + 0.91615 \ln P + 0.0015655 (\ln P)^2 \right] \quad (3.13)$$

Other possibility is used the pressure according to ANSI class flanges. Therefore, the nominal pressure corresponds to the immediately higher ANSI value than the working pressure. The ANSI pressure for flanges is shown as follows.

Table 3.7 Maximum recommended pressure for carbon steel flanges at 840 °F (Oruch et al. 2009)

ANSI class	150	300	400*	600	900	1500	2500
Pressure (bar)	20	50	68	100	150	250	420
* This flange class does not correspond to the ANSI class of nozzles							

The following step is the calculation of the vessel thickness. Most engineers follow the ASME divisions on the mechanical design. For pressure vessels, it is usually followed the ASME division 1 which gives us the following equation and conditions to compute the vessel thickness:

$$t_p = \frac{P_n D_i}{2SE - 1.2P_n} + C \quad (3.14)$$

$$S = \left(\frac{1}{3.5} \right) (\text{Tensile strength}) \quad (3.15)$$

The pressure is expressed in MPa, D_i and t_p in mm, E is the joint efficiency whose values are reflected on table (3.8). 'C' is the corrosion allowance which is usually 1.5 mm or 3 mm. The maximum stress allowance (S) is determined by eq. (3.16) as shown above, the tensile strength is 483 MPa for ASME division 1 (Campbell 2004).

Table 3.8 Joint efficiency (Campbell, 2004)

Double-Welded butt Joints		Single-Welded butt Joints (backing strip left in place)	
Fully radiographed	1.00	Fully radiographed	0.90
Spot radiographed	0.85	Spot radiographed	0.80
No radiograph	0.70	No radiograph	0.65

Other authors like Seider et al. (2004) and Mulet et al.(1981) consider other factors such as the wind effect or the possibility of an earthquake. Seider et al. (2004) modified and simplified the Mulet et al. (1981) in this respect, supplying the formula as follows which take into consideration the wind effect. In fact, the estimation considers a wind velocity up 140 miles/h (225 km/h) which also allows handle a potential earthquake.

$$t = t_p \left[0.75 + 0.22 \frac{(L_{ss}/D_i)^2}{P_n} \right] + C \quad (3.16)$$

The equation above only applies into the following interval of $10 > \frac{(L_{ss}/D_i)^2}{P_n} > 1.34$. Otherwise, if the value is lower than 1.34, t is equal to t_p from equation 3.14. The nominal pressure (P_n) in eq. (3.16) is expressed in psig.

Pressure vessels are generally made from metal plate, whose thicknesses are expressed in standard increments (Seider et al. 2004). Table (3.9) provides the standard increments to round-up the thickness calculated. Pressure vessels also have a minimum thickness regardless of the working pressure. Table (3.10) shows the minimum wall thicknesses according to the vessel diameter.

Table 3.9 Thickness increments to round-up the nearest metal plate

Increment (in)	Thickness range (in)	Source
1/16	3/16 – 1/2 inclusive	Seider et al. (2004)
1/8	5/8 – 2 inclusive	
1/4	2 1/4 – 3 inclusive	
1/4	> 3	Mulet et al. (1981)

Table 3.10 Minimum thicknesses for process vessels (Seider et al. 2010)

Internal diameter (m)	Minimum thickness (mm)
Up to 1 inclusive	5
1.0 – 2.0	7
2.0 – 2.5	9
2.5 – 3.0	10
3.0 – 3.5	12

Knowing diameter, length and thickness of the pressure vessel, it is possible to estimate its weight. This calculation implies determining the weight of the empty vessel and that corresponding for internals and nozzles. Campbell (2004) suggests a very simple equation to compute the weight of the vessel.

$$W_b = 0.032D_i t \quad (3.17)$$

$$W_v = W_b L + W_I + W_N \quad (3.18)$$

Equation (3.17) is based on 2:1 elliptical heads, which are generally used in this kind of equipment. W_b is the weight per vessel length, while W_I and W_N are the weight of internal and nozzles respectively. The last two terms are usually obtained from tables, which will be shown in few lines. Looking back to eq. (3.17), it gives good result for slenderness ratios between 3 and 5 but over this value could overestimate the weight up 20 % (Campbell 2004). On the other hand, Seider et al. (2004) provides a more complicated but more accurate expression.

$$W_e = \pi(D_i + t)(L_{SS} + 0.8D_i)t\rho_M \quad (3.19)$$

W_e is the weight of the empty vessel in pounds (lb) while ρ_M is the density of carbon steel taken as 490 lb/ft³ or 0.284 lb/in³. The term 0.8 D_i corresponds to the weight contribution for the two heads. By using eq. (3.19), the formula (3.18) is slightly modified.

$$W_v = W_e + W_I + W_N \quad (3.20)$$

The tables which contain weights of internals (knitted-mesh and vane pads) and nozzles are presented as follows.

Table 3.11 Weight of mist eliminators (Campbell, 2004)

Vessel diameter (mm)	Weight of internals (kg)	
	Vane	Mist mat
616	6	5
770	8	7
924	10	9
1078	13	10
1232	15	12
1386	18	15
1540	21	16
1694	25	19
1848	27	21
2002	31	23
2156	34	25
2310	38	28
2464	42	31
2618	47	34
2772	53	36
2926	57	39
3080	62	42
3234	65	45

Table 3.12 Weight of pressure vessel nozzles (in kg) (Campbell, 2004)

ANSI Class	Nominal Nozzle sizes (DN in mm)											
	50	75	100	150	200	250	300	350	400	450	500	600
150	9	7	11	20	29	43	61	75	97	150	194	267
300	12	11	18	32	50	66	100	129	168	277	321	513
600	15	18	27	54	79	129	165	233	315	424	564	823
900	28	20	34	70	118	170	249	351	437	625	767	1379

Alternatively, Gerunda (1981) suggested use a density of 9 lb/ft³ (145 kg/m³) and 4 in of demister pad height. The calculation of the weight by using this approximation is presented in eq (3.21).

$$W_i = \pi D_i^2 \rho_{pad} l_{pad} / 4 \quad (3.21)$$

Coulson et al. (2005) proposed to estimate the weight of nozzles as 8% of the weight of the empty vessel. Therefore, when there is a lack of data the Gerunda and Coulson et al assumptions result very useful.

3.3 Sizing of multi-cyclone separators

As mentioned before, the cyclone design requires extra parameter on its calculations. Moreover, the behaviour of the cyclones relies on upstream characteristics. Therefore, it is needed to have the following parameters:

Working pressure (P)

Working temperature (T), but we can use ambient temperature like 20 °C.

Both gas and liquid densities (ρ_g and ρ_l respectively) at working pressure and temperature

Viscosities of the gas and liquid (μ_g) and (μ_l)

Interfacial surface tension of the liquid (σ)

Superficial velocity of the mixture at inlet pipe (v_{in})

Additionally, it is also required to have the drop size distribution at the inlet. However, it is unknown in most cases. Fortunately, it was provided a general approximation which all droplet distributions are supposed identical.

Table 3.13 Standard Size Distribution for droplets (Hoffmann and Stein 2008)

$x/\langle x_{med} \rangle$	0	0.3	0.62	1	1.5	2.9
$F(x/\langle x_{med} \rangle)$	0	0.05	0.25	0.5	0.75	1.0

Where $\langle x_{med} \rangle$ is the median value of droplet size calculated by using the approximation provided by AIChE in 1978 (As cited in Hoffmann and Stein, 1978):

$$\langle x_{med} \rangle = 1.42 \langle x \rangle_{Sa} \quad (3.22)$$

x_{sa} is called the ‘‘Sauder mean’’ which is calculated in the following way:

$$\langle x \rangle_{Sa} = 1.91 D_t \frac{Re^{0.1}}{We^{0.6}} \left(\frac{\rho_g}{\rho_l} \right)^{0.6} \quad (3.23)$$

‘Re’ and ‘We’ are the Reynolds and Weber numbers respectively.

$$Re = \frac{\rho_g v_{inlet} d_i}{\mu_l} \quad (3.24)$$

$$We = \frac{\rho_g v_{inlet}^2 d_i}{\sigma} \quad (3.25)$$

Having estimated x_{med} , it is straightforward the determination of the droplet size (x) per each segment.

Alternatively, we can estimate the maximum drop size by using the formula proposed by (Campbell 2004)

$$x_{max} = 4.5d_i \left(\frac{\sigma}{\rho_g v_{in}^2 d_i} \right)^{0.6} \left(\frac{\rho_g}{\rho_l} \right)^{0.4} \quad (3.26)$$

After having considered the main properties of the prospective cyclonic separator, it is required to have some idea about the proportions of a standard cyclone. Each one of the length of the different parts of the cyclone are often related to its diameter, as shown in the following figure.

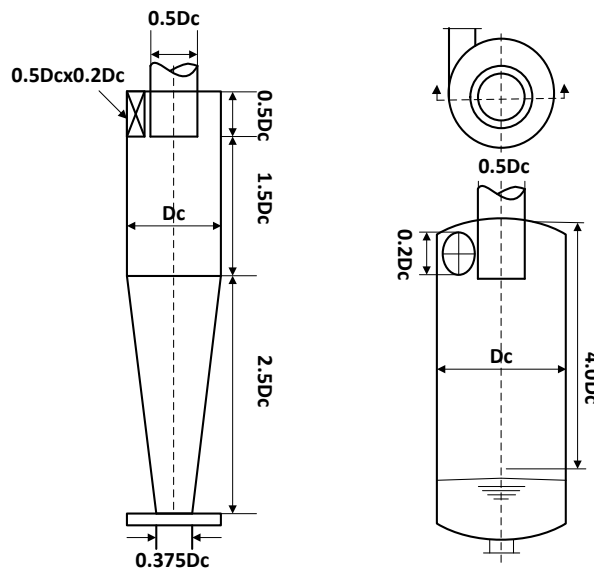


Figure 3.3 Stairmand Dimensions for high-efficiency gas-solid cyclone (at the left) (Towler and Sinnott 2008). Sketch of a gas/liquid cyclone, incorporating some Stairmand dimensions (at the right)

Usually, the design of gas-liquid cyclones are based on their ‘cousins’ used for gas-solid operations. However, there are differences which are being reflected in this chapter. For instance, the inlet is usually rectangular for gas-solid cyclones but it is often circular for those used in gas-liquid separators. In the specific case of demisters, multicyclones are used for boosting the separation efficiency.

The dimensions of each cyclone in the demister might be estimated by knowing beforehand the recommended velocity at the entrance. The literature advises a range between 10 and 20 m/s, which allows to have a good separation and mitigate the effect of liquid carry over. In fact, it was considered this range in velocity to diminish the potential liquid reentrainment. In addition, Hoffmann and Stein (2008) claim that the phenomenon is worsened at high pressure. Alternatively, ‘Sulzer’ (2007) suggests to use the Souder-Brown equation with Ks equal to 0.25m/s to determine the maximum allowable velocity in the cyclone chamber.

In the specific case of multicyclones, we have a set of small and standard cyclones in parallel. As a result, we know beforehand the diameter and other dimensions of the cyclone beforehand. For instance, we can use a standard cyclone of 0.4 m, as suggested Smith (2005). On the other hand, Hoffmann and Stein (2008) presented different standard geometries which

the diameter is in the range of 200-350 mm approximately. The same authors say that diameter of each cyclone should less than 250 mm in the case of gas-liquid multi-cyclones. Furthermore, Peerless (2012) has standard cyclones of two or four inches for this purpose.

Having known, the cyclone diameter and by using the Stairmand ratios, we can have the inlet pipe per each cyclone (b) and other dimensions.

$$b=0.2D_c \quad (3.27)$$

$$A_{in}=\pi b^2/4 \quad (3.28)$$

Then,

$$Q_c = A_{in}v_{in} \quad (3.29)$$

$$n_c = Q/Q_c \quad (3.30)$$

v_{in} and A_{in} are the velocity and area of the inlet respectively. Q is the total volumetric flow rate and Q_c the volumetric flow per cyclone. On the selection of the inlet velocity, several factors might take place. For instance, cyclonic separator size, pressure drop, efficiency and the possibility of liquid carry over. The pressure drop is directly proportional to the velocity while the opposite relation is observed for the separator size. Regarding to the separation efficiency, it is favoured by increasing the velocity but the probability of carry over or re-entrainment is favoured as well. Therefore, it should a balance between these factors to select the appropriate velocity. Most of the calculations are based on the Muschelknautz model (as cited in Hoffmann and Stein, 2008) for dust cyclones, although there are some modifications to adapt it to gas-liquid separation. Firstly, the symbols for the different dimensions in the cyclone correspond to the figure (3.4).

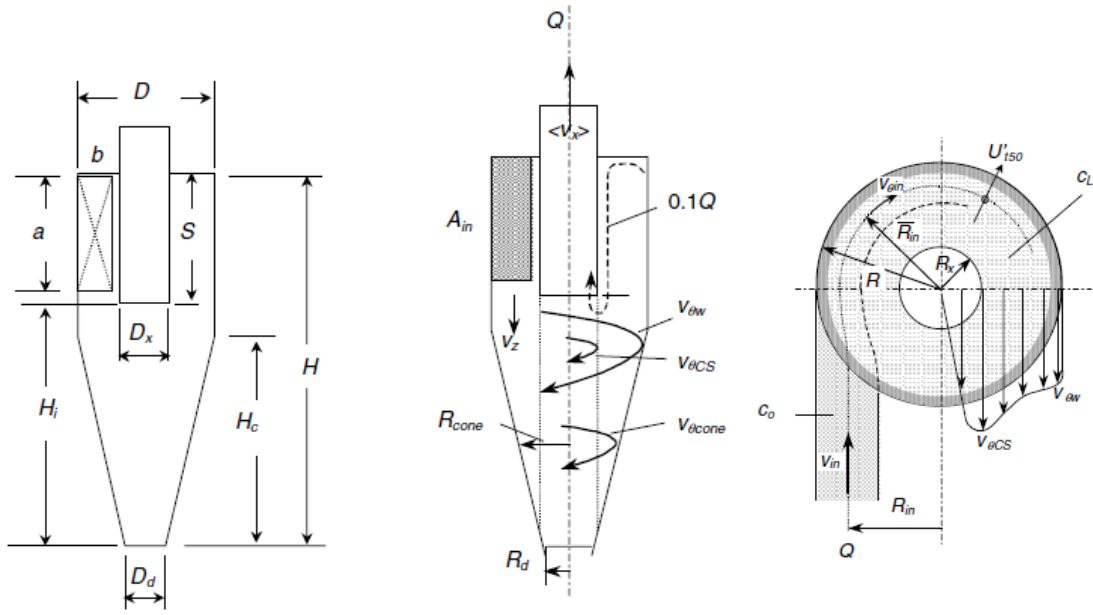


Figure 3.4 Typical dust cyclone dimensions, showing the corresponding notation (Hoffmann and Stein 2008)

Firstly, the restriction coefficient (α) is computed by using the following equation:

$$\alpha = \frac{1}{\xi} \left\{ 1 - \sqrt{1 + 4 \left[\left(\frac{\xi}{2} \right)^2 - \frac{\xi}{2} \right] \sqrt{1 - \frac{(1-\xi^2)(2\xi-\xi^2)}{1+c_0}}} \right\} \quad (3.31)$$

ξ is $b/(D_c/2) = b/R_c$ and c_0 is ratio between the mass of liquid and gas at the incoming flow. In the case of a circular inlet, the value of b can be taken for the inlet pipe diameter.

Then, we need a set of velocities inside the cyclone.

$$v_{\theta w} = v_{in} R_{in} / \alpha R_c \quad (3.32)$$

Where R_{in} is equal to $R_c - 1/2 b$.

$$R_m = \sqrt{R_x R_c} \quad (3.33)$$

And the axial wall velocity (v_{zw}) is determined by:

$$v_{zw} = \frac{0.9 Q_c}{\pi (R_c^2 - R_m^2)} \quad (3.34)$$

The cyclone body Reynolds number is expressed by:

$$Re_R = \frac{R_{in} R_m v_{zw} \rho_g}{H \mu_g \left(1 + \left(v_{zw} / v_{\theta m} \right)^2 \right)} \quad (3.35)$$

$$v_{\theta m} = \sqrt{v_{\theta w} v_{\theta CS}} \quad (3.36)$$

Where $v_{\theta CS}$ depends on Reynolds number as well. As first approximation, the term $(v_{zw}/v_{\theta m})^2$ is taken as zero. Then, it is calculated the real value in an iterative process by using the equations (13)-(21) as well. It usually does not take long for high Reynold numbers.

Now, we need to estimate the air friction factor. Firstly, we should consider the relative roughness (k_s/R_c). k_s is usually taken as 0.046 mm (0.0018 inches) and R_c the cyclone radius. However, the relative roughness should not lower than 6×10^{-4} which corresponds to smooth pipes (Hoffmann and Stein 2008). Then, we can estimate the friction factor by using the Reynolds number determined above. There are two equations for estimating it, corresponding to conical and cylindrical bodied cyclones respectively. For both equations, we have to add to terms. The first is related to the friction in smooth walls while the second considers the relative roughness.

$$f_{air} = f_{sm} + f_r \quad (3.37)$$

For conical bodies, we have:

$$f_{sm} = 0.323 R_e^{-0.623} \quad (3.38)$$

$$f_r = \left(\log \left(\frac{1.6}{k_s/R_c - 0.000599} \right)^{2.38} \right)^{-2} \left(1 + \frac{2.25 \cdot 10^5}{Re_R^2 (k_s/R_c - 0.000599)^{0.213}} \right)^{-1} \quad (3.39)$$

For cylindrical bodied, we have:

$$f_{sm} = 1.51 R_e^{-1} \quad (3.40)$$

$$f_r = \left(\log \left(\frac{1.6}{k_s/R_c - 0.000599} \right)^{2.38} \right)^{-2} \left(1 + \frac{2.25 \cdot 10^5}{Re_R^2 (k_s/R_c - 0.000599)^{0.213}} \right)^{-1} \quad (3.42)$$

In the case of gas-liquid cyclones, we usually have a cylindrical-bodied type. Both equations correspond to a fitting done by Hoffmann and Stein (2008) on the curves presented on the Muschelknautz and Trefz's work presented in 1991. The friction factor values provided on the graph are similar for both configurations, although for those conical they are slightly higher.

Having estimated the friction factor of air at the cyclone operating conditions, we are able to determine the value of the friction factor for the incoming two-phase flow (f_{mix}).

$$f_{mix} = f_{air}(1 + 0.4c_0^{0.1}) \quad (3.43)$$

Now we should estimate the tangential velocity of the inner vortex ($v_{\theta CS}$) to estimate the cut size or cut-point diameter. After that we are able to determine the efficiency.

$$v_{\theta CS} = v_{\theta W} \frac{(R_c/R_x)}{1 + \frac{f_{AR} v_{\theta W} \sqrt{R_c/R_x}}{2Q}} \quad (3.44)$$

A_R corresponds to the total internal area of the cyclone. It is computed following the same procedure to dust cyclones.

In the case of conical cyclones, the area is calculated as follows

$$\begin{aligned} A_R &= A_{roof} + A_{barrel} + A_{cone} + A_{vt} \\ &= \pi[R_c^2 - R_x^2 + 2R_c(H - H_c) + (R + R_d)\sqrt{H_c^2 + (R_c - R_d)^2} + 2R_x S] \quad (3.45) \end{aligned}$$

On the other hand, for cylindrical cyclones we have:

$$A_R = A_{roof} + A_{barrel} + A_{vt} = \pi(R_c^2 - R_x^2 + 2R_c H + 2R_x S) \quad (3.46)$$

Then, we are able to compute the cut-point diameter by using the Barth's formula.

$$x_{50} = x_{fact} \sqrt{\frac{18\mu_g(0.9Q_c)}{2\pi(\rho_l - \rho_g)v_{\theta CS}^2(H - S)}} \quad (3.47)$$

x_{fact} is a correction factor whose range is between 0.9 and 1.4 and it is used to correct the calculated value to the experimental data (Hoffmann and Stein, 2008). It can be used 1 if there is a lack of information related.

The Barth's equation is only valid when the droplets follow the Stokes law regime, which can be checked by determining the particle Reynolds number (Hoffmann and Stein 2008):

$$Re_p = \frac{\rho_g U'_{t50} x_{50}}{\mu} \quad (3.48)$$

$$U'_{t50} = v_{rCS} = \frac{Q}{2\pi R_x H_{CS}} \quad (3.49)$$

Usually, eq. (3.47) applies since the particle Reynolds number (Re_p) is rarely higher than 0.5. Otherwise, we can use eq. (3.50) to compute the cut-point diameter.

$$x_{50} = 5.18 \frac{\mu^{0.375} \rho_g^{0.25} U_{t50}^{0.875}}{\left\{ (\rho_l - \rho_g) v_{\theta cs}^2 / R_x \right\}^{0.625}} \quad (3.50)$$

The equation above is valid up Re_p equal to 1000.

Then, we should estimate the efficiency of the cyclone. Therefore, we use eq. (3.51) to have the efficiency for a particular droplet size, which is calculated from table (3.13). The value of 'm' is obtained from experiments, but we can use m equal to 3 if there is lack of information.

$$n_i = \frac{1}{1 + \left(\frac{x_{50}}{x_i}\right)^m} \quad (3.51)$$

The overall efficiency is the calculated by the addition of the efficiency contribution per each segment. This contribution is estimated by multiplying the efficiency computed by eq. (3.51) and ΔF from table (3.13). To illustrate this, we can take values from the second and third columns on the cited table. Thus the corresponding ΔF is 0.2 for the $x/\langle x_{med} \rangle$ interval of 0.3-0.62. Then, the overall efficiency formula is shown as follows:

$$n_{sep} = \sum_{i=1}^N n_i \cdot \Delta F_i \quad (3.52)$$

If the overall efficiency is lower than it is required, we can diminish the volumetric flow incoming to each cyclone or increase the inlet velocity. A good efficiency is in the range 90-99%, the upper value corresponds to the normal efficiency of knitted-mesh separators. Therefore, we can establish this value as a standard to analyse the cyclonic separator performance. Nonetheless, the Muschelknautz model tends to be conservative regarding to the efficiency calculation (Hoffmann and Stein 2008). As a result, the efficiency in practice is higher than that calculated by using this method.

Another important issue to be considered is 'Mass loading' or 'Saltation'. This effect implies that cyclones become in two-stage separator, where the exceeding proportion of liquid-loading will be centrifuged immediately after entering the separator. The remaining part will be separated at the inner vortex according to the droplet size; thus the typical 'Classification' takes place. The first phenomenon described ('Saltation') does not occur if the liquid mass fraction in the gas is lower than the mass-loading limit (c_{oL}). This parameter is determined by means of cut-point, droplet median size and the mass of liquid suspended (c_{ok}).

$$c_{oL} = 0.0078 \left(\frac{x_{50}}{\langle x \rangle} \right) (10c_{ok})^k \text{ valid for } 0.01 < c_{ok} < 0.5 \quad (3.53)$$

$$\text{Where: } k = 0.07 - 0.16 \ln c_{ok} \quad (3.54)$$

Unfortunately, the value of c_{ok} is unknown in most practical situations since it is difficult to measure or predict. For this reason, it is usually required substitute c_{ok} for c_o into eq. (3.53). Nonetheless, the result obtained in this manner is quite conservative. Therefore, it is

advisable to use 0.5 instead of c_o into eq. (3.53); if the latter value is higher than 0.5 (Hoffmann and Stein 2008).

When the phenomenon of ‘Saltation’ happens, the efficiency is modified. Consequently, eq. (3.52) should be adjusted to include the contribution of both ‘Saltation’ and ‘Classification’ phenomena. Then, the global efficiency becomes:

$$n_{sep} = \left(1 - \frac{c_{oL}}{c_o}\right) + \left(\frac{c_{oL}}{c_o}\right) \sum_{i=1}^N n_i \cdot \Delta F_i \quad (3.55)$$

Re-entrainment might also affect the global efficiency, although it is required much more research about. As a result, it is difficult to have an overall picture of the re-entrainment impact on the efficiency. Austrheim (2005) (As cited Hoffmann and Stein, 2008) argues that the cyclone efficiency is a function of the so-called re-entrainment number, which is the ratio between drag and surface tension forces respectively. The Austrheim’s work sounds attractive but the main problem is the estimation of the liquid film thickness in the cyclone.

Hoffmann and Stein (2008) proposed an implicit equation to estimate the film thickness. The equation was derived by making a force balance on the gas and liquid phases respectively. Then, we have:

$$\frac{4\tau_{l,w} \sin \beta}{(1-\varepsilon)D_c} - \frac{4\tau_{g,i} \sin \beta}{D_c \varepsilon^{0.5}(1-\varepsilon)} - (\rho_l - \rho_g)g = 0 \quad (3.56)$$

$\tau_{l,w}$ and $\tau_{g,i}$ are the shear stress for the liquid and gas phases respectively. In this case, it was assumed that the flow regime corresponds to annular flow. This flow pattern implies that the liquid film covers the pipe’s wall, so the gas flows through the pipe core. In this way, just liquid is in contact to the pipe wall. Therefore, the liquid shear stress is related to liquid-wall friction while the gas friction is an interfacial force. The corresponding friction factors are calculated by using the Swamee-Jain and Zhao-Liao equations for liquid and gas respectively.

By definition,

$$\tau_{l,w} \equiv \frac{1}{2} \rho_l \langle v_l \rangle^2 f_{l,w} \quad (3.57)$$

$$\tau_{g,i} \equiv \frac{1}{2} \rho_g \langle v_g \rangle^2 f_{g,i} \quad (3.58)$$

Where,

$$f_{l,w} = \frac{0.25}{\left[\log \left(e / 3.7 D_c + 5.74 / Re_l^{0.9} \right) \right]^2} \quad (3.59)$$

$$f_{g,i} = 0.046 Re_g^{-0.2} \quad (3.60)$$

' e ' is the absolute roughness (Usually taken as 0.000046 m), Re_g and Re_l are the Reynolds number for the liquid film and gas respectively, $\langle v_l \rangle$ and $\langle v_g \rangle$ are the mean velocities for liquid film and gas respectively. Regarding to eq. (3.56), ϵ is the void fraction of the gas which represents the area occupied by the gas compared to the total internal pipe area. The angle β was assumed taken into consideration that both gas and liquid goes down in the cyclone in a helical fashion. Then, the flow is assumed that always goes in the same inclination regarding to the horizontal. This angle is difficult to measure, so it can be approximately a value between 45 and 55°.

The Reynolds number for the liquid and gas fraction are expressed by the following equations:

$$Re_l = \frac{\rho_l \langle v_l \rangle d_{HL}}{\mu_l} \quad (3.61)$$

$$Re_g \equiv \frac{\rho_g \langle v_g \rangle D_g}{\mu_g} \quad (3.62)$$

d_{HL} is the liquid hydraulic diameter which is equal to $(1 - \epsilon)D_c$ for this particular case. D_g is the diameter corresponding to the gas area, which could be expressed as $\epsilon^{1/2}D_c$. Substituting the velocities by means of mass gas flows, \dot{m}_g and \dot{m}_l for gas and liquid respectively, we have:

$$\langle v_l \rangle = \frac{\dot{m}_l}{\rho_l A_l} = \frac{\dot{m}_l}{\rho_l A(1-\epsilon)} = \frac{4\dot{m}_l}{\rho_l \pi D_c^2 (1-\epsilon)} \quad (3.63)$$

$$\langle v_g \rangle = \frac{\dot{m}_g}{\rho_g A_g} = \frac{\dot{m}_g}{\rho_g \epsilon A} = \frac{4\dot{m}_g}{\rho_g \epsilon \pi D_c^2} \quad (3.64)$$

The Reynolds numbers and shear stresses are expressed:

$$Re_l = \frac{4\dot{m}_l}{\pi D_c \mu_l} \quad (3.65)$$

$$Re_g = \frac{4\dot{m}_g}{\pi \mu_g \epsilon^{1/2} D_c} \quad (3.66)$$

$$\tau_{l,w} = \frac{8\dot{m}_l^2}{\pi^2 D^4 \rho_l (1-\epsilon)^2} f_{l,w} \quad (3.67)$$

$$\tau_{g,i} = \frac{8\dot{m}_g^2}{\pi^2 D^4 \rho_g \epsilon^2} f_{g,i} \quad (3.68)$$

Then, substituting into equation (3.56) we get an implicit equation to determine the gas void fraction.

$$\frac{32 \sin \beta}{\pi^2 D_c^5 (1-\epsilon)} \left[\frac{\dot{m}_l^2}{\rho_l (1-\epsilon)^2} f_{l,w} - \frac{\dot{m}_g^2}{\rho_g \epsilon^{5/2}} f_{g,i} \right] - (\rho_l - \rho_g)g = 0 \quad (3.69)$$

Having calculated the void fraction, the liquid film thickness (δ) could be determined by using the following expression:

$$\delta = \frac{D_c(1-\sqrt{\varepsilon})}{2} \quad (3.70)$$

Austrheim (2005) (As cited Hoffmann and Stein, 2008) adjusted the re-entrainment non-dimensional number proposed by Ishii and Grolmes (1975) (As cited Hoffmann and Stein, 2008). Then, we can estimate the efficiency of the cyclone related to re-entrainment.

$$N_{Reent.} = \frac{(\mu_l \langle v_g \rangle / \sigma)(\rho_g / \rho_l)^{0.8}}{N_\mu^{0.4} Re_{l*}^{\frac{1}{3}}} \quad (3.71)$$

N_μ is a non-dimensional number so-called 'viscous number', which is calculated according to eq. (3.72). Re_{l*} is the Reynolds number corresponding to the liquid film by calculated by means of liquid film thickness (δ).

$$N_\mu = \frac{\mu_l}{\sqrt{\rho_l \sigma} \sqrt{\frac{\sigma}{g \Delta \rho}}} \quad (3.72)$$

$$Re_{l*} = \frac{\rho_l \langle v_l \rangle \delta}{\mu_l} \quad (3.73)$$

Using the Austrheim's data for re-entrainment efficiency at different pressures and working fluids, we can obtain a linear equation as shown as follows:

$$n_{Reent.} = -0.1429 N_{Reent.} + 1.0357 \quad \text{valid for } 0.25 \leq N_{Reent.} \leq 2.25 \quad (3.74)$$

If $N_{Reent.} < 0.25$, the efficiency is equal to 1.

Considering re-entrainment and the expected separation performance in the separator, we can adjust the formula to determine the overall efficiency of the cyclone.

$$n_g = n_{Reentr.} \cdot n_{sep} \cdot 100 \quad (3.75)$$

As mentioned before if the calculated efficiency is lower than expected, it should be diminish the size of the cyclones. In this way, we are increasing the number of cyclones as well.

Finally, pressure drop is the last of the main factors that should be addressed in the design of gas-liquid cyclones. Although its value tends to be much less than that registered in filter beds, it could be high in some conditions, especially at high pressures.

Basically, we have three components of the pressure drop. Firstly, the fluid registered losses due to wall friction, which is called pressure drop in the cyclone body. Afterwards, we have pressure loss in the vortex core, whose notation corresponds to the figure 2. As a result, this pressure drop is called ' ΔP_x '. The velocity v_x is computed by dividing the volumetric flow rate at the cyclone by the vortex core area ' A_x '. The last pressure term corresponds to losses

due to possible acceleration of the stream, which happens for changing in velocities in the two-phase inlet flow. For example, if we have a change in diameter at the inlet pipe. In this way, v_2 and v_1 correspond to velocities after and before to the diameter reduction.

$$\Delta P_{body} = \frac{f_{mix} A_R (v_{\theta CS} v_{\theta w})^{1.5}}{1.8Q} \quad (3.76)$$

$$\Delta P_x = \frac{1}{2} \rho_g v_x^2 \left[2 + \left(\frac{v_{\theta CS}}{v_x} \right)^2 + 3 \left(\frac{v_{\theta CS}}{v_x} \right)^{\frac{4}{3}} \right] \quad (3.77)$$

$$\Delta P_{acc} = (1 + c_o) \frac{\rho_g (v_2^2 - v_1^2)}{2} \quad (3.78)$$

There is lack of information about how to compute the dimension of the common chamber which contains the cyclones, in the case of a multi-cyclone. However, it has found some parameters and correlations in the literature. For example, 'Shell' (2002) suggested applied equation (3.79) where each cyclone has 2 inches (0.0508 m) of diameter and for a vessel with gas outlet at the top. In addition, recommends estimate the liquid column with 0.8 m of minimum length. Regarding to the multi-cyclone bundle, they argue that all cyclones should be at the same level and vertical staggering is not allowed to safe space. They also supplied a minimum pitch among the cyclones of 80 mm.

$$LSS_{multicyclone} = h + 0.2D_i + d_{out} + 0.9 \quad (3.79)$$

4. ECONOMICAL EVALUATION

The estimation of cost of equipment and other costs related to capital investment play a crucial role in selecting design alternatives (Seider et al. 2004). As a result, this chapter presents the procedure of determining purchase cost of gas knitted mesh and cyclonic gas scrubbers. Afterwards, it is introduced the estimation of the capital investment for the equipment mentioned above. In this section, different costs associated to capital cost are briefly described such as installation, freight, contingencies, investment site factors and working capital.

These estimations have a grade of uncertainty, which means that a minimum error is expected. The preliminary estimations are based on prices of previous equipment which have been fitted in different equations or factors. The grade of uncertainty diminishes as long as more data are available. In other words, if there are more details about equipment features, vendor quotes, labour and installation costs, among others, the error will decrease. Nevertheless, when accuracy increases the cost of the estimation goes up as well. The following table contents the categories of capital cost estimates.

Table 4.1 Main categories of capital cost estimates for chemical plants (Viguri 2011; Peters et al. 2003)

Estimate	Bases	Expected Error (%)	Rate to get results	Used to
Order of magnitude (Ratio estimate)	Similar or previous cost data. Production rate and PFD.	40-50	Very fast	Profitability Analysis
Study (factored estimate)	Knowledge of major items of equipment. Mass & energy balance and equipment sizing	25-40	Fast	Preliminary design
Preliminary	Enough data for budget estimation. Mass & energy balance, equipment sizing, construction materials and P&ID. Individual factors of the Guthrie's method*.	15-25	Medium	Budget approval
Definite	Full data before completion of drawings and specifications	10-15	Slow	Construction control
Detailed	Complete engineering drawings, specifications and site surveys.	5-10	Very slow	Turnkey contract

* The Guthrie's factors are related to different costs at different stages of the project including: installation, labour, freight, contingencies and so on.

4.1 Purchase cost estimate

Capital cost is generally estimated by means of purchase cost, which alternatively is called f.o.b (free on board) cost. The latter just represents the price of equipment at the factory. Therefore, other associated costs like transport, installation, royalties and so on are not included.

The simplest way to determine a purchase cost is multiplying a size by the cost per this particular size. For example, the f.o.b price of a pressure vessel could be obtained multiplying the vessel weight by a factor so-called '\$/lb figure'. This factor is provided by vendors (Branan 2002). However, most purchase data are presented as graphs and equations in function of one or more equipment size factors (Seider et al. 2004). These factors are usually diameter, length and weight. The f.o.b cost equations have become most popular since they can be incorporated in software related.

These equations are based on economies of scale, which implies lower cost per unit as production rate increases. The Economist (2008) illustrated this concept comparing the production of magazines at two different scales. Hence it might cost \$ 3,000 to produce 100 copies but only \$ 4,000 for 1000 copies, thus the cost per unit decreases from \$30 to \$ 4. In both cases the major costs of publishing a magazine are the same, editorial and design. Seider et al. (2004) also claim that producing a larger of piece equipment can be made in a single-train plant with no or some adjustments.

On the other hand, both authors commented that economies of scale have a dark side, called diseconomies of scale. Increasing the production or size of the product also involves a gradual growth of complexity. When the complexity overcomes the profit, the concept of diseconomies of scale takes place thus the cost per unit goes up. For instance, the economy of scale is lost when the maximum size of equipment to be fabricated or transported is reached (Seider et al. 2004). It is due to more manufacturing units are required and/or transport capacity must be enhanced. The following graph gives an overall idea about the behaviour of economy of scales.

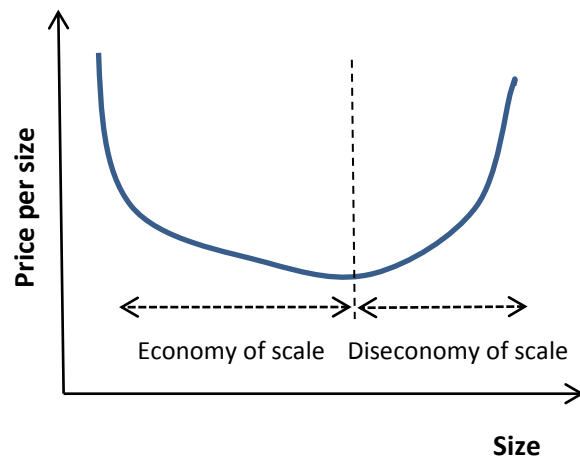


Figure 4.1 Sketch of price per size of chemical equipment, according to economies of scale

Applying the definition of economy of scales in chemical equipment, it was obtained equation (4.1). This expression is actually so-called 'The Six-tenths Rule'. In this case, the classical variable of capacity has been substituted by equipment size which has provided reasonable results in this context. The exponent 'm' usually varies from 0.48 to 0.87 and the average value is about 0.6 (Seider et al. 2004).

$$C_E = C_{base} \left(\frac{Size_E}{Size_{base}} \right)^m \quad (4.1)$$

C_E and $Size_E$ are referred to actual conditions. Regarding to the base price and size, they correspond to standard equipment whose price was provided by a vendor in a particular period of time. Most of these costs are based on carbon steel and atmospheric pressure. The following table gives us an overview of the parameters used in equation for different equipment.

Table 4.2 Typical parameters of the Six-tenths Rule for selected chemical equipment (Smith 2005)

Equipment	Material	Capacity measure	Base cost (\$)	Size range	Exponent (m)
Agitated reactor	CS	Volume (m ³)	1.15x10 ⁴	1-50	0.45
Pressure vessel	SS	Mass (t)	9.84x10 ⁴	6-100	0.82
Distillation column (Empty shell)	CS	Mass (t)	6.56x10 ⁴	8-300	0.89
Cyclone	CS	Diameter (m)	1.64x10 ³	0.4-3.0	1.2
Shell-and-tube heat exchanger	CS	Heat transfer area (m ²)	3.28x10 ⁴	80-4000	0.68
Centrifugal pump (Large, including motor)	CS	Power (kW)	9.84x10 ³	4-700	0.55
Compressor (Including motor)	CS	Power (kW)	9.84x10 ⁴	250-10000	0.46
Storage tank (Large atmospheric)	CS	Volume (m ³)	1.15x10 ⁴	5-200	0.53
Cooling tower (Forced draft)		Water flow rate (m ³ h ⁻¹)	4.43x10 ³	10-40	0.63

CS is carbon steel and SS is high-grade steel, for example 316. All costs are referred to January 2000.

As mentioned before, most of these costs are based on low-moderate pressure, carbon steel and ambient temperature. Consequently, the value provided by equation (4.1) has to be adjusted according to actual conditions. Smith (2005), among other authors, has provided different factors to be incorporated into equation (4.1). Tables 4.3 to 4.5 supply these factors.

Table 4.3 Typical materials of construction and capital cost factors for pressure vessels and distillation columns (Smith 2005)

Material	Correction factor F _M
Carbon steel	1.0
Stainless steel (low grades)	2.1
Stainless steel (high grades)	3.2
Monel	3.6
Inconel	3.9
Nickel	5.4
Titanium	7.7

Table 4.4 Typical equipment pressure capital cost factors (Smith 2005)

Design pressure (bar)	Correction factor F_p
0.01	2.0
0.1	1.3
0.5 – 7.0	1.0
50	1.5
100	1.9

Table 4.5 Typical equipment temperature capital cost factors (Smith 2005)

Design temperature (°C)	Correction factor F_T
0 - 100	1.0
300	1.6
500	2.1

As a result, equation (4.1) is modified as follows:

$$C_{fob} = C_{base} \left(\frac{Size_E}{Size_{base}} \right)^m F_M F_P F_T \quad (4.2)$$

C_{fob} is the purchase cost of the equipment. Seider et al. (2010) has alternatively provided an equation to determine the pressure factor.

$$F_p = 0.9803 + 0.018(P_n \cdot 0.147) + 0.0017(P_n \cdot 0.147)^2 \quad (4.3)$$

Inflation must be taken into consideration as well since costs tend to change rapidly. In fact, quotes from vendors are usually applicable for one or two months (Seider et al. 2004). The most common approximation to solve this issue is obtained by multiplying the base cost by a ratio of cost indexes. Equation (4.3) gives the idea of this simple calculation. These indexes are usually found in specialised magazines, e.g. Chemical Engineering. The chemical engineering plant cost index (CEPCI) is the most used by far. The Marshall & Swift (MS) Equipment Cost Index is also used. There are other cost indexes but they are not widely used. Table (4.6) presents these indexes from 1975 to the quarter of 2011 while graph (4.2) shows the tendency for those throughout the period.

$$C_{year2} = C_{year1} \left(\frac{I_{year2}}{I_{year1}} \right) \quad (4.3)$$

Table 4.6 Cost Indexes (Seider et al. 2004; “Chemical Engineering” 2012)

Year	CECPI	M&S	Year	CECPI	M&S
1975	182	452	1994	368	1000
1976	192	479	1995	381	1037
1977	204	514	1996	382	1051
1978	219	552	1997	387	1068
1979	239	607	1998	390	1075
1980	261	675	1999	391	1083
1981	297	745	2000	394	1103
1982	314	774	2001	395	1110
1983	317	786	2002	396	1121
1984	323	806	2003	404	1124
1985	325	813	2004	444	1179
1986	318	817	2005	488	1245
1987	324	830	2006	500	1302
1988	343	870	2007	525	1373
1989	355	914	2008	575	1449
1990	361	952	2009	522	1469
1991	361	952	2010	551	1457
1992	358	960	2011	591	1537
1993	359	975	2012		

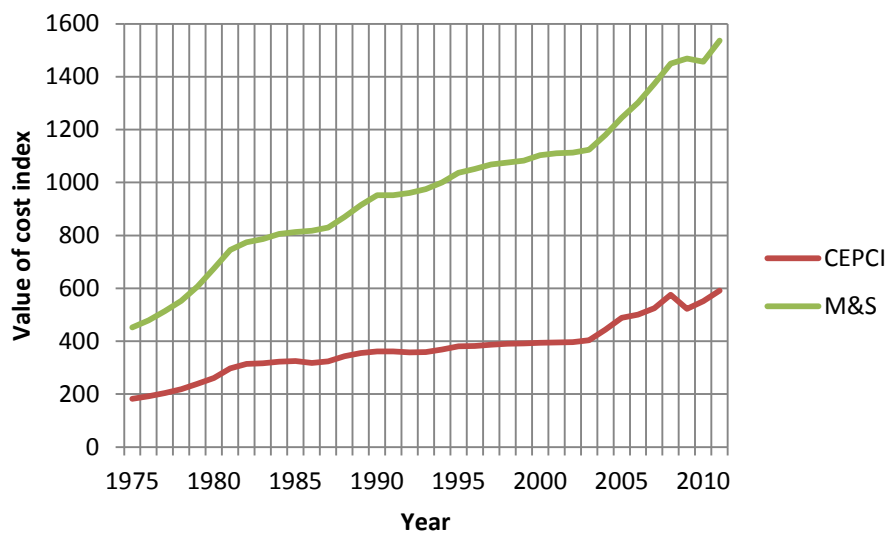


Figure 4.2 Comparison of annual cost indexes

Looking back to the six-tenths rule, its might result inaccurate especially when the equipment size is far from the base value. Consequently, this equation has been improved taking the natural logarithm in both sides and adding extra terms as a polynomial (Seider et al. 2004). Equation (4.4) is the result of this mathematical operation, where ‘S’ is the size parameter of the equipment. This equation is the general form of the mostly used equation

in estimating purchase costs. The parameters equations have been obtained by fitting real prices in industry during a specific period.

$$C_{fob} = \exp\{A_0 + A_1[\ln(S)] + A_2[\ln(S)]^2 + \dots\} \quad (4.4)$$

The tables as follows show the main equations which have been used in estimations of purchase costs for pressure vessels, cyclones and demister pad. On table (4.7), we can see the general form for equations employed in pressure vessels. The parameters of these equations are contained on table (4.8) and (4.9) respectively. While table (4.10) presents the main equations used in cyclones.

Table 4.7 Comparison among purchase cost equations of pressure vessel

Name/ Reference	Data Year	Parameters	Equation(s)
Seider et al. (2010)	2006	C_v : Vessel cost	$\ln C_v = a + b * \ln W_t + c * (\ln W_t)^2$ (4.5)
Mulet et al. (1981)	1978	C_i : Cost of platform and ladders.	$C_i = eD_i^\alpha L_{SS}^\beta$ (4.6)
Couper (2010)	2007		$C_p = f_M * C_v + C_i$ (4.7)
Turton et al. (1998)	1996	C_p^0 : Purchase base cost at low pressure K_i : Constants which depends on D_i	$\log C_p^0 = K_1 + K_2 \log(L_{SS}) + K_3 (\log(L_{SS}))^2$ (4.8)
Guthrie (1969)	1968		$C_p^0 = eD_i^\phi L_{SS}^\gamma$ (4.9)
Sinnot & Towler (2009)	2007	C_{std} : Price for standard equipment	$C_p = C_{std} + h * W_{tot}^m$ (4.10)
All prices are given in US\$			

Table 4.8 Values of the parameters of purchase cost equations of vertical pressure vessel

Parameter	Name/Reference				
	Seider et al. (2010)	Mulet et al. (1981)	Couper et al. (2010)	Guthrie (1969)	Sinnot & Towler (2009)
<i>a</i>	7.0132	8.6000	9.1000	--	--
<i>b</i>	0.18255	-0.21651	-0,2889	--	--
<i>c</i>	0.02297	0.04576	0.04576	--	--
<i>e</i>	361.8	1017	246	101.9	--
<i>h</i>	--	--	--	--	29
<i>C_{std}</i> (\$)	--	--	--	--	10000
α	0.73960	0.73960	0.73960	--	--
β	0.70684	0.70684	0.70680	--	--
φ	--	--	--	1.066	--
<i>Y</i>	--	--	--	0.820	--
<i>m</i>	--	--	--	--	0.85
Units	U.S (lb,ft)	SI (kg, m)	U.S (lb,ft)	U.S (ft)	SI(kg)
Weight range	4200-10 ⁶	2210-1.03*10 ⁵	5000-2.26*10 ⁵	--	160-2.5*10 ⁵
Diameter range	3-21	1.83-3.66	6-10	1-10	--
Length range	12-40	3.05-6.10	12-20	4-100	--

For the first three equations, the range for diameter and length corresponds to the cost of ladders and platforms.

Table 4.9 Values of the parameters of the Turton et al. (1998) equation

<i>D_i</i> (m)	<i>K₁</i>	<i>K₂</i>	<i>K₃</i>	<i>L_{SS}</i> range (m)
0.3	3.3392	0.5538	0.2851	1.2-16
0.5	3.4796	0.5893	0.2053	1.5-20
1.0	3.6237	0.5262	0.2146	2.5-30
1.5	3.7559	0.6361	0.1069	3.0-41
2.0	3.9484	0.4623	0.1717	4.0-45
2.5	4.0547	0.4620	0.1558	5.0-50
3.0	4.1110	0.6094	0.0490	6.0-50
4.0	4.3919	0.2859	0.1842	7.0-50

Table 4.10 Purchase cost equations for gas-solid cyclones

Name/Reference	Data Year	Parameter	Equation	Range
Couper et al(2010)	2003	Q_c (K scfm)	$C_p = 790Q_c^{0.91}$ (4.11)	2-40 K scfm
Seider et al (2010)	2006	Q_c (actual cfm)	$\ln(C_p) = 9.227 - 0.7892\ln Q_c + 0.08487(\ln Q_c)^2$ (4.12)	200-10 ⁵ cfm
Smith (2005)	2000	D_c (m)	$C_p^0 = 1640(D_c/0.4)^{1.2}$ (4.13)	0.4-3 m
Turton et al. (2009)	2001	Volume of cyclone (m ³)	$\log(C_p^0/V_c) = 3.6298 - 0.4991\log V_c + 0.0411(\log V_c)^2$ (4.14)	0.06-200 m ³

Looking back to table (4.8), it is observed that the estimation of costs of platforms and ladders is restricted in some cases. In this way, Coulson et al. (2005) proposed to estimate that 5% of the empty vessel price corresponds to the cost of platform and ladders.

Some of the equation above show the variable ' C_p^0 ' which is a purchase base cost. This value is based on low-pressure and carbon steel, as shown in equation (4.15). Consequently, it should be adjusted by using the appropriate pressure and material factors. The latter usually is found on tables, as shown previously. The former is determined by tables or equations which vary from author and equipment. In the case of lack of information, the pressure factor can be determined by table (4.4) or equation (4.3). Guthrie (1969) provided these factors for different pressures, shown in table (4.11). He advised to increase the working pressure by 50% to read the correct value. On the other hand, Turton et al. (1998) supplied equations for different equipment. Specifically, equation (4.16) corresponds to vertical pressure vessels.

$$C_p = C_p^0 F_M F_P F_T \quad (4.15)$$

Table 4.11 Pressure factors for pressure vessels (Guthrie, 1969)

P (psig)	Up to 50	100	200	300	400	500	600	700	800	900	1000
F_P	1.00	1.05	1.15	1.20	1.35	1.45	1.60	1.80	1.90	2.30	2.5

$$F_P = 0.5146 + 0.6838\log P + 0.2970(\log P)^2 + 0.0235(\log P)^6 + 0.0020(\log P)^8 \quad (4.16)$$

Equation (4.15) is valid for 3.7<P<400 barg. If the pressure is in the range of -0.5<P<3.7 barg, the pressure factor is equal to 1.

The cost of accessories in pressure vessels like knitted mesh and vane pads are determined separately. Turton et al. (2009) has supplied an equation for demister pad, based on data from 2001. Equations (4.17) and (4.18) present the purchase cost of this accessory, including

firstly a base purchase cost while the installation cost is introduced in the second. Equation (4.17) is valid from 0.7 to 10.5 m² of demisting area.

$$\log C_{p-pad}^0 = 3.253 + 0.4838 \log A_{pad} + 0.3434 (\log A_{pad})^2 \quad (4.17)$$

$$C_{BM-pad} = C_{p-pad}^0 N F_q F_{BM} \quad (4.18)$$

The subscript “BM” is referred to the bare module cost, which includes the purchase price, installation cost and other expenses. The foundations behind this are discussed in the following subchapter. N is the number of stages and F_q is the quantity factor related to the number of stages. It is usually 3 when the number of stages is less than four. The bare module cost factor (F_{BM}) is 1.2 when is used stainless steel in demister pads.

4.2 Estimate of capital investment

As mentioned before, the purchase cost is just a part of the equipment cost. Additionally, it should be taken into consideration other expenses such as installation, instrumentation and controls, piping, direct labour, among others. Indirect costs like freight, insurance, engineering and contractor’s fee are also taken into account. Peters et al. (2003) offered a detailed description of different kind of these expenses. In the present work, it is just introduced the expenses related to equipment; particularly to gas scrubbers.

Most of description of the costs shown underneath corresponds to the Peters et al. (2003) work. There are also comparisons between the Guthrie works in 1969 and 1974. Actually, the latter author compiled lots of these costs and correlated them to purchase cost. After that, he introduced the concept of bare module cost which takes into account direct and indirect costs for equipment. Most of these factors are still used with some or no modifications.

Purchased- equipment delivery

Equipment is usually quoted as f.o.b (free on board) which means that the customer pays the freight. Peters et al. (2003) estimate that delivery allowance of 10% of the purchase cost is recommended. In the same way, Guthrie (1969) gave 8% of the purchase cost. Nevertheless, there are many factors which influence on freight costs such as weight and equipment dimensions, distance from the fabricator and methods of transport.

Installation

It covers costs for labour, supports, foundations, platform, construction and other expenses related to the erection of purchased equipment. It is generally included as installation costs piping and equipment insulation. Depending on the complexity of the equipment, these

costs vary from 20 to 60% of the f.o.b cost. However, Guthrie (1969) reflected that installation costs for vertical vessels might be slightly higher than 100% of the f.o.b cost.

Instrumentation and controls

It includes instrument costs and labour and installation cost for auxiliary equipment. It might vary from 8 to 50 % of the purchase cost.

Piping

It involves labour, valves, pipes, supports and other items used in the complete erection of all piping devices used directly in the erection process. The estimation of the costs related is key since it can be as high as 80% of the delivered purchased cost.

Electrical systems

They are mainly power wiring, lightning, transformation and service, and instrument and control wiring (Peters et al. 2003). The costs related are ranged between 15 and 30 % of the f.o.b cost.

Engineering and supervision

The costs associated involve engineering design; including drawing, licensed software use, calculations and so on. They also include accounting, travelling, communications and home office expenses, among others. This is an indirect cost which is estimated as 30% of delivered-equipment cost.

Construction expenses

It is another indirect cost related to field expenses and construction. It includes construction tools, temporary construction and operation, travelling and payment of personnel from manufacturing home office, construction payroll, among others. These expenses are occasionally incorporated under equipment installation, or more often under engineering and supervision costs. Construction expenses are about 8 to 10 % of the fixed capital investment.

Legal expenses

As the name suggests, they are related to legal costs. They are approximately 1-3% of the fixed capital investment.

Contingencies and contractor's fee

A portion of the capital investment is destined to cover expenses originate for unexpected events. They could be storms, floods, accidents in transportation, price changes, strikes, errors in estimation, among others (Peters et al. 2003). The portion of capital investment

used to this purpose is usually referred to as contingencies, which are added to the bare module cost. The latter includes all direct and indirect expenses described above and the purchase cost. The bare module cost is in the range of 80 to 90% of the fixed capital investment while contractor's fee and contingencies represent the remaining part (Guthrie 1969). They are usually estimated as 15% and 3% for contingencies and contractor's fee respectively (Seider et al. 2004).

Basically, most of the costs used to determine the capital investment for chemical equipment have been mentioned above. It is often added an extra 15% of the fixed capital investment as working capital. In this way, the estimate of total capital investment is complete but this is out of the scope of the thesis.

Table (4.12) illustrates how to determine the multiplying factors called as bare module factors or Guthrie factors. There are four main fields in the total equipment cost: purchase, field materials, direct field labour and indirect cost. Most of the direct and indirect costs are included, excepting contingencies and contractor's fee. The pie charts of figure (4.3) reflect the proportion among these values. Afterwards, table (4.13) shows bare module factors for selected equipment from two sources.

Table 4.12 Estimate of the bare module cost factor for selected equipment (Guthrie 1969)

Module	Equipment			
	Shell and tube heat exchanger	Air cooler	Process vessel (Vertical)	Process vessel (Horizontal)
Equipment f.o.b	100	100	100	100
Piping	46.1	18.2	60.6	42.0
Concrete	5.1	1.9	10.0	6.3
Steel	3.1	--	8.0	--
Instruments	10.2	4.8	11.5	6.3
Electrical	2.0	12.0	5.0	5.2
Insulation	4.9	--	8.0	5.2
Paint	0.5	0.6	1.3	0.5
Fields materials	71.9	37.5	104.4	65.5
Material erection	55.8	31.5	84.5	53.3
Equipment setting	8.5	6.4	15.5	10.5
Direct field labour	64.3	37.9	100	63.8
Freight, insurance and taxes	8.0	8.0	8.0	8.0
Other indirect costs	94.4	70.2	121.6	91.7
Total indirect costs	102.4	78.2	129.6	91.7
Relative bare module cost	338.6	253.6	434.0	329.0
Bare module cost factor (F_{BM})	3.39	2.54	4.34	3.29

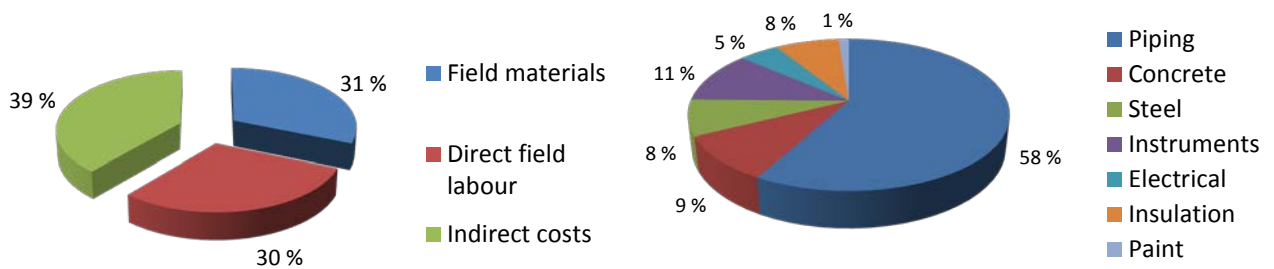


Figure 4.3 Proportion of direct and indirect costs of vertical vessels. At the right, the field materials costs are discriminated

Table 4.13 Bare module factors of selected equipment

Equipment	Source	
	Seider et al. (2004) ^a	Couper et al. (2010) ^b
Cyclones	--	1.4
Distillation column	--	3.0
Furnaces and direct heaters	2.19	1.3
Pressure vessels (Horizontal)	3.05	2.8
Pressure vessels (Vertical)	4.16	
Reactors, multi-tubular	--	2.2
Shell-and-tube heat exchangers	3.17	2.2

^a The values were taken from Guthrie (1974) where the multiplying factor corresponds to equipment at low pressure and carbon steel based. ^b The values correspond to Cran (1981) where the effect of pressure is included.

Although the values of table (4.13) are based on the same principle, there are significant differences between those from both columns. This is motivated that Guthrie factors are valid for near atmospheric conditions and carbon-steel-based materials. Otherwise the equipment cost is overestimated because costs which are not related to pressure and material are counted twice. Foundations, supporting structure and ladders, electrical systems, paint, among other direct costs remain the same (Seider et al. 2004). In the same way, indirect costs are not usually affected by changing pressure or increasing the quality of the material. On the other hand, piping cost is strongly depending on actual pressure and material used. For example, if the pressure is higher the thickness of attached pipes increases. Furthermore, the material of equipment and attached piping has to be the same (Seider et al. 2004).

There are different criteria to avoid overestimation of the capital cost by using the Guthrie factors. Firstly, it would be used the bare module factors provided by Couper et al. (2010) as first approximation. On the other hand, Seider et al. (2004) has provided equation (4.19) where pressure and material factors are taken into account. In this case, the purchase cost of the equipment corresponds to near atmospheric conditions and carbon steel material. Turton et al. (1998) employed the base purchase cost following the same criteria but they do

not use the Guthrie factors. In fact, the factors called B_1 and B_2 are used instead as shown in equation (4.20).

$$C_{BM} = C_p^0 [F_{BM} + (F_d F_p F_M - 1)] \quad (4.19)$$

$$C_{BM} = C_p^0 [B_1 + B_2 F_p F_M] \quad (4.20)$$

F_d is the design factor which is equal to 1 for process vessels. Regarding to B_1 and B_2 , they are supplied by Turton et al. (2003) for different equipment. Particularly for vertical pressure vessels, they are 2.5 and 1.72 respectively. The corresponding pressure factor (F_p) of equation (4.20) is computed by using equation (4.16).

Finally, the location factor has to be taken into consideration. Most costs are based in plants in the U.S Gulf Coast area. As a result, the costs should adjusted according the actual plant location, although there is scarce information related. Seider et al. (2004) has provided some investment site factors, F_{IS} , which are correlated to the fixed capital investment (C_{TFI}). Table (4.14) shows these factors while equation (4.21) illustrates how to use them. However, the factor for Western Europe is very general since the conditions from one region to another change. Specifically, Norway is much more expensive than the neighbouring countries thus this factor gives us a rough approximation.

$$C_{TFI_{adjusted}} = F_{IS}(\text{Currency rate})C_{TFI} \quad (4.21)$$

Table 4.14 Typical investment site factors (Seider et al. 2004)

Location	F_{IS}
U.S Gulf Coast	1.00
U.S Southwest	0.95
U.S Northeast	1.10
U.S Midwest	1.15
U.S West Coast	1.25
Western Europe	1.20
Mexico	0.95
Japan	1.15
Pacific Rim	1.00
India	0.85

5. METHODOLOGY

Most of the equations shown before were included in two Matlab scripts for sizing and economical evaluation of both technologies selected. The knitted-mesh model requires the following parameters: pressure, gas and liquid density, percentage of liquid on the gas stream and diameter nominal (DN). The last parameter is nominal size of the inlet pipe and the abbreviation DN came from the French 'diàmetre nominal' and it is generally expressed in millimetres. This parameter is correlated to the volumetric flow by using the maximum velocities from table (3.4). The density of gas and other properties were estimated by using Hysys. Regarding to the economical evaluation, it was used equations to estimate the purchase costs of vessels and demisting pads for cyclonic and knitted-mesh separators. Afterwards, it was determined costs related to installation, transport and so on for the selected technologies. All these costs are included in the so-called bare module cost. A very schematic sketch of the models developed in presented in figure (5.1).

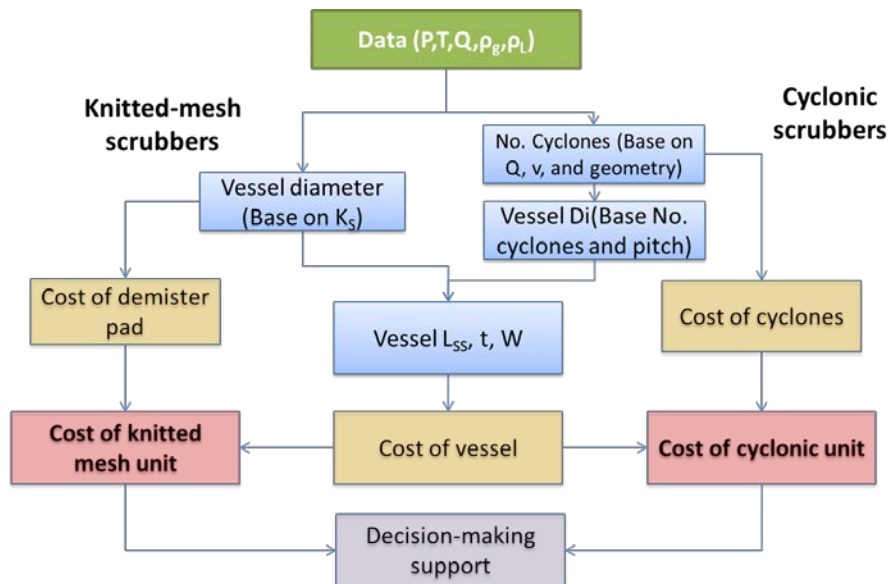


Figure 5.1 Decision-making framework for knitted-mesh and multi-cyclone scrubbers

Regarding to the gas properties, they were estimated by using Hysys and the thermodynamical model of Peng-Robinson. The gas composition was taking for sale natural gas from Åsgard field after being treated in Kårstø. The figures related are shown in chapter of results. Regarding to the liquid, it was estimated a mixture of hydrocarbons from a light oil fraction with a gravity API of 45. The latter as well known is related to the specific gravity. For the calculation of cyclones, it was estimated more properties to introduce in the model. For example: the viscosity and heat calorific capacity of the gas and the surface tension and viscosity of the liquid. The additional properties for the gas stream were computed by using Hysys as well. On the other hand, those for the liquid phase were estimated by using tables and graphs for oil fractions and hydrocarbons.

In respect with sizing of both scrubbers, the methodology was similar. Firstly, it was calculated the internal diameter of the scrubber vessel. Secondly, it was estimated its length and thickness. Then, it was computed its weight based on diameter, length and thickness by using equation (3.19). Nevertheless, there are considerable differences to obtain the diameter of the vessel. For the traditional knitted-mesh scrubber, it was used the Souder-Browns equation to estimate the maximum velocity by using the gas load factor. On the other hand, the gas stream on multi-cyclones is split into a number of cyclones (with cylindrical form). According to the geometry and inlet velocity of each cyclone, there is a standard volumetric flow rate for each one. Having this standard parameter, it is straightforward to compute the number of cyclones. Then, internal diameter of the vessel is estimated by the number the cyclones; considering its geometry, thickness and separation among each other. The thickness is calculated by using equation (3.6), while the pitch among the cyclones is assigned as 1.2 times its external diameter or 80 mm. The layout of the cyclones in the bundle was assumed as a staggered distribution in heat exchangers of shell and tube, but in a horizontal fashion. A sketch of the staggered distribution is shown on figure (5.2) and an illustration of the cyclone bundle.

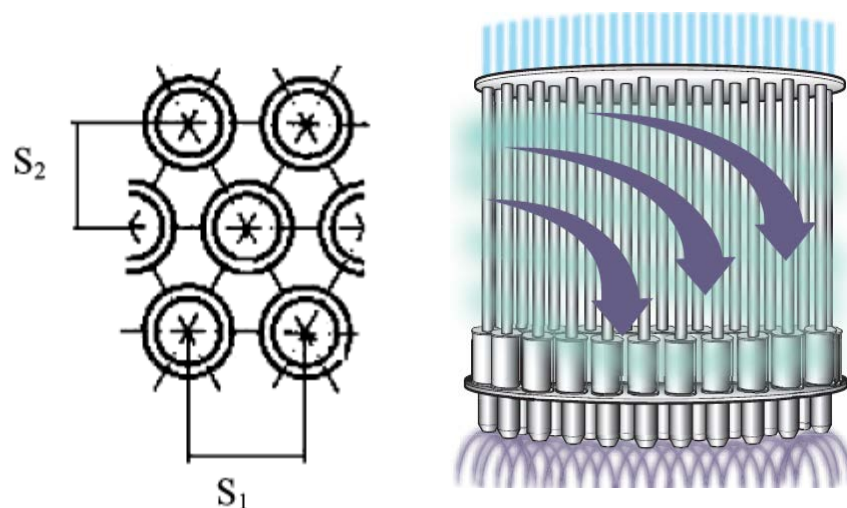


Figure 5.2 Sketch of the staggered layout in heat exchanger of shell-and-tube and cyclone bundle in a gas-liquid scrubber. S_1 and S_2 are the longitudinal and transversal pitch and they are equal to 1.2 and 1.5 respectively (Karno and Ajib 2006; Peerless 2012)

The length was estimated following some expressions obtained by data compiled from experience in industry. For instance, equation (3.11) gives an estimate using internal diameter and height of the liquid column. The minimum value of the latter was estimated in 300 mm as suggested the literature review. It was assigned a minimum slenderness ratio Of 2.5. Regarding to multi-cyclone scrubbers, the length of the chamber were estimated based on equation (3.79) but incorporating the length of the cyclones in the bundle. In this way, it is possible to include standard cyclones with different diameters as shown on equation (5.1).

$$L_{SS_{multicyclone}} = h + 0.2D + H + d_{out} + 0.9 \quad (5.1)$$

The vessel thickness was estimated by following the same criteria exposed for pressure vessels for both demisting units. The nominal pressure used for this purpose was calculated by following the Seider et al. equation as reflected equation (3.13). However, it was introduced an additional security factor (f_s) as shown equations (5.2) and (5.3). In this way, the criteria of Seider et al. and Guthrie (1969) are linked and it is ensured the safety of operations at high pressure (The factor is in this case equal to 1.4). The vessel thickness also takes into consideration of a potential earthquake and the effect of wind. The equations related are (3.14) to (3.16). The vessel thickness allows determine the vessel weight as shown before. However, the calculation of the weight of the vessel should take into consideration the weight of nozzles and internals. This data related is contained on tables 3.10 and 3.11. The criteria of Gerunda (1981) and Coulson (2005) also applies where there is lack of information.

If $10 \text{ psig} \leq P \leq 1000 \text{ psig}$

$$P_n = \exp\left[0.60608 + 0.91615 \ln P + 0.0015655 (\ln P)^2\right] f_s \quad (5.2)$$

If $P > 1000 \text{ psig}$

$$P_n = P \cdot 1.1 \cdot f_s \quad (5.3)$$

After having sizing the gas scrubbers, it is calculating their cost by using equations as reflected in chapter (4). For the vessels, it was plotted the estimated purchase costs per weight of separator versus nominal diameter. The purchase costs of the vessels were obtained from the equations reflected on table (4.7) and their parameters can be found on tables (4.8) and (4.9). They were updated to prices of December of 2011, by using the chemical engineering indexes found on table (4.6). Then, it was compared the tendency of the curves to verify somehow the versatility of the models and equation selected. The cost of the knitted-demisting pad is based on equations (4.17) and (4.18). While the cost of the cyclonic pad were estimated by multiplying the number of cyclones by the price per unit. The price per unit was estimated by using the equation from Turton et al (2009) reference, shown on table (4.10). However, this equation is out range for small cyclones (diameter less than 250 mm). For this reason, it was used the Rule of Six-Tenth reflected on equation (4.1) but using as base value that calculated from the equation Turton et al. (2009) and an exponent of 0.6.

The bare module cost was estimated by using the equation (4.20). However, this equation was modified, as shown in equation (5.4), to avoid calculation of purchase costs at two conditions. In this manner, the purchase cost based on weight of the separator and for a determined material can be used straightforwardly.

$$C_{BM} = C_{fob} \left[\frac{B_1}{F_p F_M} + B_2 \right] \quad (5.4)$$

Regarding to the centrifugal demisters, it was performed a trade-off between bare module cost and pressure drop since it is expected that the latter would be very high. This evaluation was used to estimate an appropriate velocity where the bare module cost and pressure drop are balanced. The latter required being monetised to compare to the installed cost of the equipment. For instance, it can be expressed my means of electricity cost for recompression. To illustrate this, we can assume that the recompression system is based on the Brayton cycle where we have the compression section itself, a combustor and a gas turbine. In this way, we need to estimate the power required in the compressor(s) by using and standard polytropic efficiency of 92.5%. Then, we can compute electricity required by using a cycle efficiency of 36% as suggested Bolland (2010). Afterwards, we can determine the hypothetical recompression cost by selecting a period like 10 years (lifespan) and price per kWh of 29.7 øre for industry ('Statistics Norway' 2012). The bare module cost of equipment was adjusted, in this particular case, by using the investment site location factors to Western Europe. The following equations are used in these calculations:

$$W_{comp} = Q\rho_g c p_g (T_2 - T_1) \quad (5.5)$$

T_1 and T_2 are the temperatures after and before of the compressor respectively. The ratios between both temperatures is shown as follows

$$\left(\frac{T_2}{T_1}\right) = \left(\frac{P_2}{P_1}\right)^{R/(Cp_g MW_g n_p)} = \left(\frac{P_1 + \Delta P}{P_1}\right)^{R/(Cp_g MW_g n_p)} \quad (5.6)$$

R is the gas constant, Cp_g is the specific heat capacity of the gas, MW_g is the molecular weight and n_p is the polytropic efficiency, P_1 and P_2 are the pressure after and before of the compressor and ΔP is the pressure drop. Substituting eq. (5.6) into (5.5) we can have the power required for recompression. P_1 in this case is the working pressure of the separator. We need to take into consideration that the temperatures must be absolute in eq. (5.6).

The electricity required is estimated as follows:

$$W_{turbine} = W_{comp}/n_{cycle} \quad (5.5)$$

The electricity required (in kWh) is determined by multiplying the turbine ($W_{turbine}$) power by the number of hours of the selected period. Then, it can be estimated the price of recompression by multiplying this figure by the electricity price and divide it by the current NOK/\$ rate.

Finally, it was incorporated equations from (3.31) to (3.78) to estimate the efficiency and pressure drop of the cyclone. For the former it was also introduced the general droplet distribution provided on table (3.12) and equations (3.22)-(3.26) to determine the mean droplet size. For the pressure drop, it was used the equation of friction factor for conical bodies instead of the corresponding for cylinders. It was motivated to the underestimation observed where the latter equation was used compared to the curves presented by Muschelknautz and Trefz in 1991 (as cited Hoffmann and Stein 2008).

6. RESULTS

Table 6.1 General data and conditions used in the result presented

Parameter		Value
Temperature (°C)		20
Gas composition (% mole)		
Name	Formula	
Nitrogen	N ₂	0.54
Carbon dioxide	CO ₂	1.89
Methane	CH ₄	91.37
Ethane	C ₂ H ₆	5.52
Propane	C ₃ H ₈	0.6
Isobutane	i-C ₄ H ₁₀	0.03
n-butane	n-C ₄ H ₁₀	0.04
Isopentane	i-C ₅ H ₁₂	0.01
Thermodynamical model used		Peng-Robinson
Reference material on calculations		Carbon steel
Reference currency on calculations		US\$
Reference region on calculations		U.S Gulf Coast
Main liquid properties		
Density (kg/m ³)		800
° API		45
Viscosity (cP)		3.2
Surface tension (dy/cm)		22
Content in the gas (% vol.)		0.02
Maximum liquid flow rate (m ³ /h) per m ² flow area		2.04
Allowable liquid flow rate (m ³ /h) per m ² flow area in knitted-mesh		2.40
Other parameters of multi-cyclone scrubbers		
Minimum velocity (m/s)		10
Maximum velocity (m/s)		20
Velocity used to compare to knitted mesh separators (m/s)		20
Overall efficiency (%)		>99

Table 6.2 Properties of the natural gas composition selected at different pressures

P (bar)	Viscosity*10² (cP)	Mass density (kg/m³)	Heat capacity kJ/(kg°C)
10	1.128	7.423	2.615
15	1.139	11.28	2.201
20	1.150	15.25	2.239
25	1.161	19.32	2.278
30	1.174	23.49	2.319
35	1.188	27.77	2.362
40	1.202	32.15	2.407
45	1.217	36.64	2.454
50	1.234	41.24	2.502
55	1.251	45.93	2.552
60	1.269	50.73	2.603
65	1.289	55.62	2.656
70	1.309	60.59	2.709
75	1.331	65.55	2.763
80	1.353	70.79	2.818
85	1.377	75.99	2.872
90	1.402	81.25	2.925
95	1.428	86.55	2.978
100	1.455	91.89	3.029
105	1.484	97.25	3.079
110	1.513	102.6	3.126
115	1.543	108.0	3.171
120	1.575	113.3	3.213
125	1.607	118.7	3.252
130	1.641	124.0	3.287
135	1.675	129.2	3.320
140	1.710	134.4	3.349

6.1 Dimensions and weight of gas scrubbers

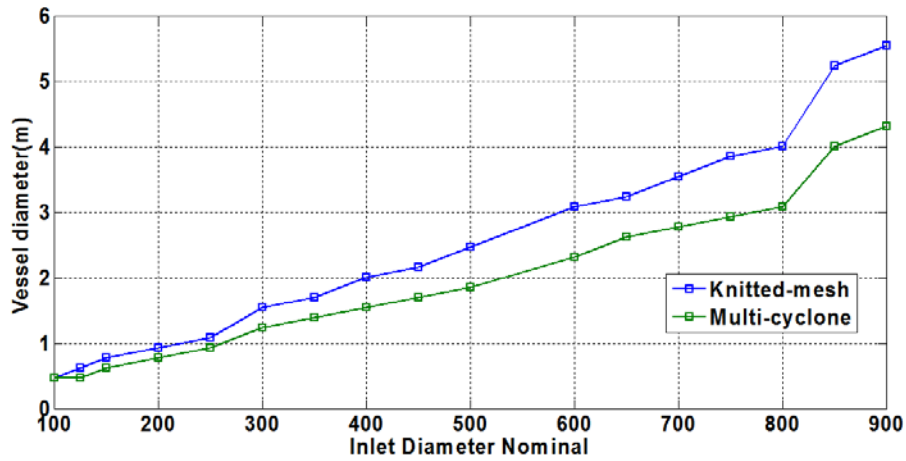


Figure 6.1 Variation of the internal scrubber diameter with diameter nominal for knitted-mesh and multicyclone scrubbers at 80 bar

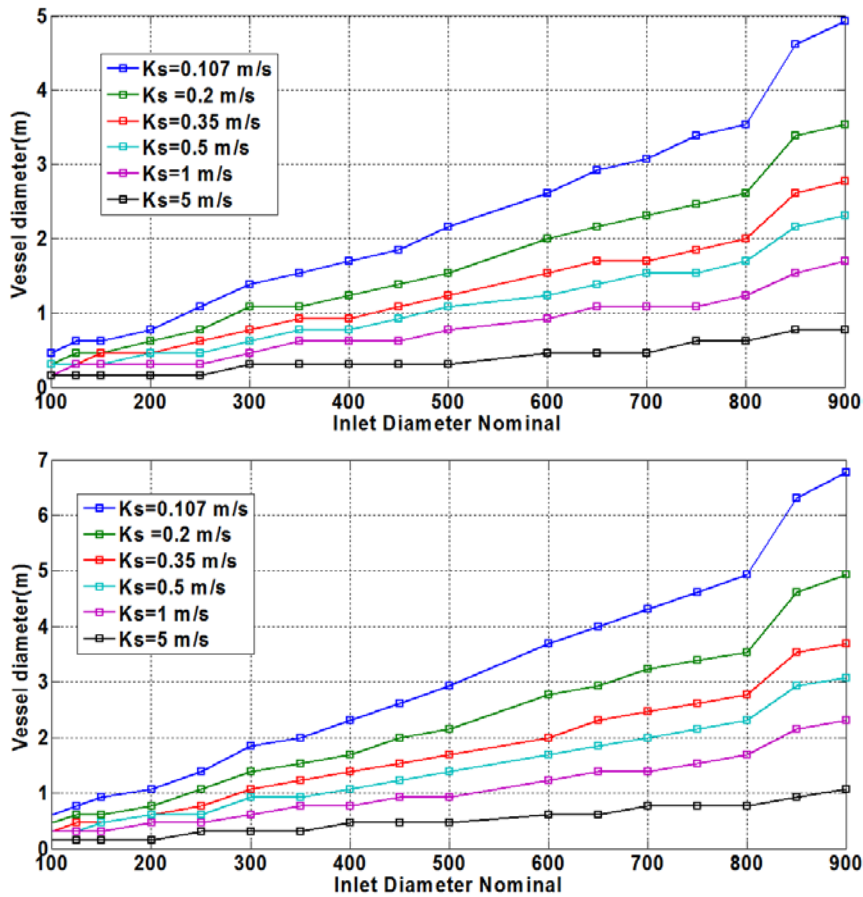


Figure 6.2 Effect of the gas load factor (K_s) on the scrubber internal diameter at 20 and 80 bar respectively

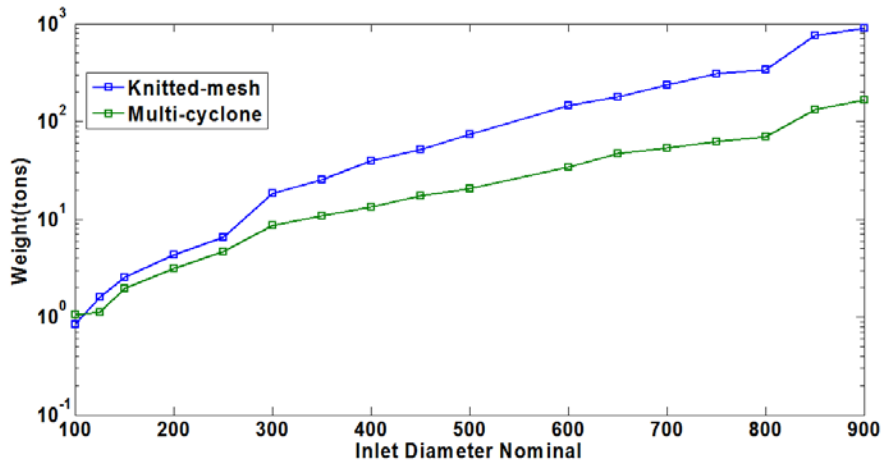


Figure 6.3 Weight of knitted mesh and multi-cyclone scrubbers, including nozzles and internals

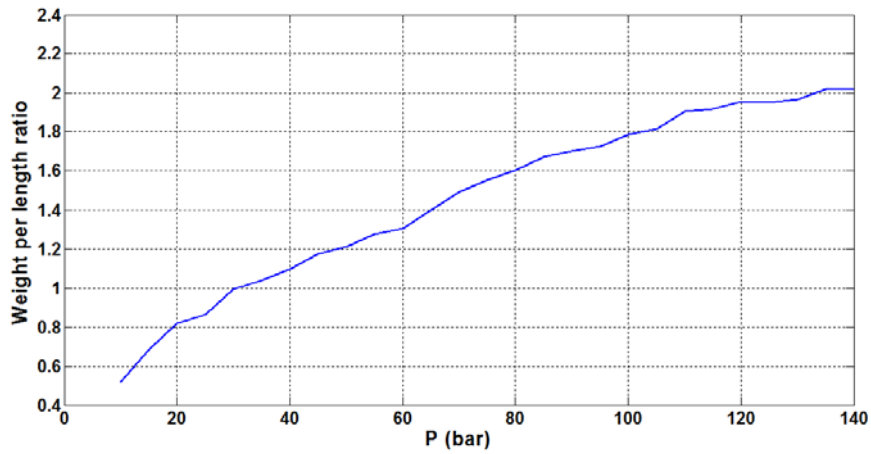


Figure 6.4 Mean ratio between weight per separator length of knitted-mesh and multi-cyclone scrubbers at different pressures

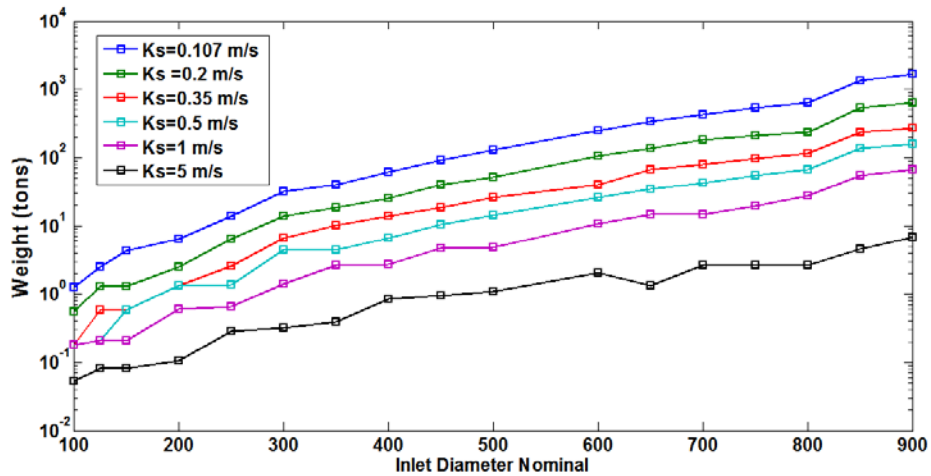


Figure 6.5 Effect of the gas load factor in reducing scrubber weight (In this case the ratio length diameter is equal to 2 for all cases)

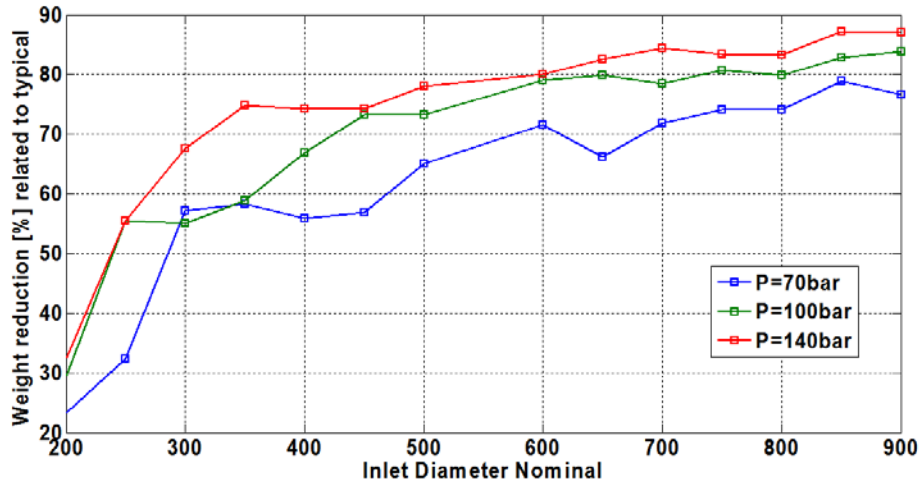


Figure 6.6 Weight reduction of multi-cyclones compared to knitted-mesh scrubbers

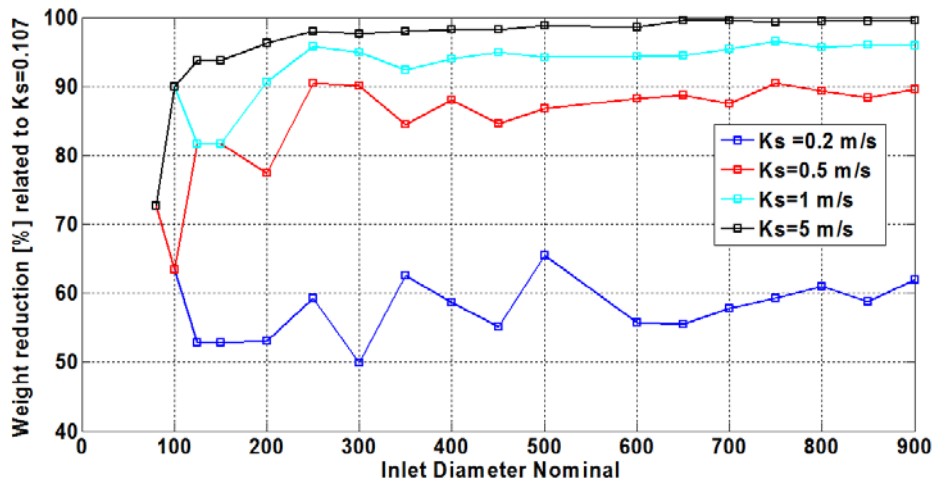


Figure 6.7 Effect of the gas load factor in the reduction of weight of gas scrubbers at 80 bar

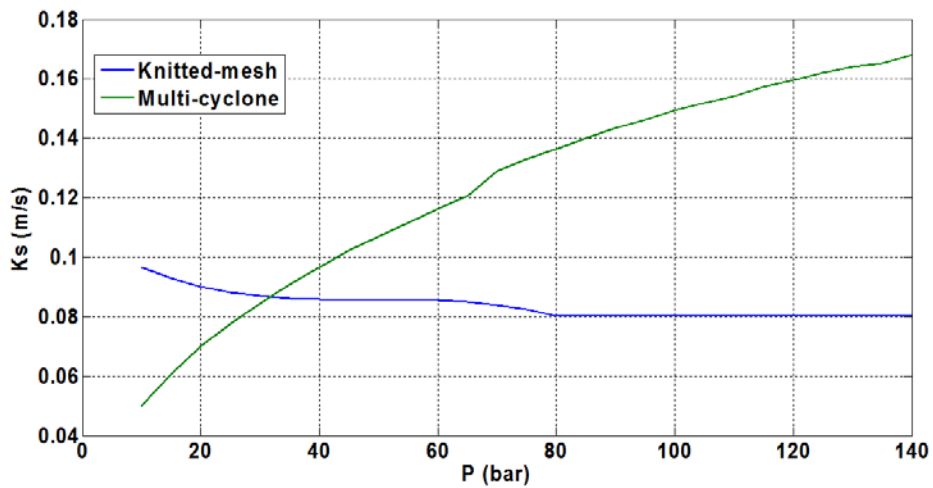


Figure 6.8 Variation of the gas load factor (K_s) with regard to pressure for knitted-mesh and multi-cyclone scrubbers with cyclone inlet velocity of 20 m/s

6.2 Costs and economical evaluation

Table 6.3 Dimensions and costs for selected knitted-mesh scrubbers

Parameter	DN 300			DN 450		
	40	80	120	40	80	120
Pressure (bar)						
Internal diameter (m)	1.23	1.54	1.69	1.85	2.16	2.31
Length (m)	3.08	3.85	4.23	4.62	5.39	5.78
Thickness (mm)	47.6	88.9	152.0	69.8	127.0	203.0
Total weight (t)	6.2	18.4	39.2	20.5	51.4	96.9
Purchase vessel cost (M\$)	71.7	140.7	233.3	151.1	282.0	443.4
Demister pad cost (M\$), including installation	10.2	13.4	15.3	17.4	22.5	25.4
Total purchase cost (M\$)	81.9	154.1	248.6	168.5	304.4	468.8
Bare module cost (M\$)	187.3	330.6	504.3	385.5	653.1	950.8

Parameter	DN 600			DN 700		
	40	80	120	40	80	120
Pressure (bar)						
Internal diameter (m)	2.46	3.08	3.23	2.93	3.54	3.7
Length (m)	6.16	7.70	8.09	7.32	8.86	9.24
Thickness (mm)	95.3	178.0	286.0	114.0	203.0	324.0
Total weight (t)	49.5	146.4	266.7	89.6	237.6	424.0
Purchase vessel cost (M\$)	274.6	558.6	879.3	391.4	808.2	1270.0
Demister pad cost (M\$), including installation	28.6	45.1	50.2	40.4	61.7	63.5
Total purchase cost (M\$)	303.3	603.7	929.5	431.8	870.0	1334
Bare module cost (M\$)	693.7	1295	1885	987.5	1866	2705

Table 6.4 Dimensions and costs for selected multi-cyclones (D_c equal to $6''$)

Parameter	DN 300			DN 450		
	40	80	120	40	80	120
Pressure (bar)						
Internal diameter (m)	1.23	1.23	1.23	1.69	1.69	1.69
Length (m)	2.88	2.88	2.88	3.11	3.11	3.11
Thickness (mm)	47.6	76.2	114.0	69.8	102.0	152.0
Total weight (t)	6.0	9.5	14.2	13.0	18.9	28.2
Purchase vessel cost (M\$)	70.2	92.7	119.1	112.9	143.4	186.5
Demister pad cost (M\$), including installation	30.7	28.0	24.4	60.6	55.1	47.9
Total purchase cost (M\$)	100.9	120.8	143.5	173.5	198.6	234.5
Bare module cost (M\$)	230.8	259.1	291.0	396.8	426.0	475.5

Parameter	DN 600			DN 700		
	40	80	120	40	80	120
Pressure (bar)						
Internal diameter (m)	2.31	2.31	2.31	2.77	2.77	2.62
Length (m)	3.38	3.38	3.38	3.58	3.58	3.54
Thickness (mm)	88.9	133.0	203.0	108.0	159.0	235.0
Total weight (t)	24.8	37.0	55.9	39.7	58.2	80.5
Purchase vessel cost (M\$)	171.2	224.4	299.1	235.7	307.6	387.5
Demister pad cost (M\$), including installation	122.0	112.1	96.7	166.3	151.9	131.1
Total purchase cost (M\$)	293.2	336.5	395.8	402.1	459.4	518.6
Bare module cost (M\$)	670.7	721.9	802.8	919.6	985.6	1052.0

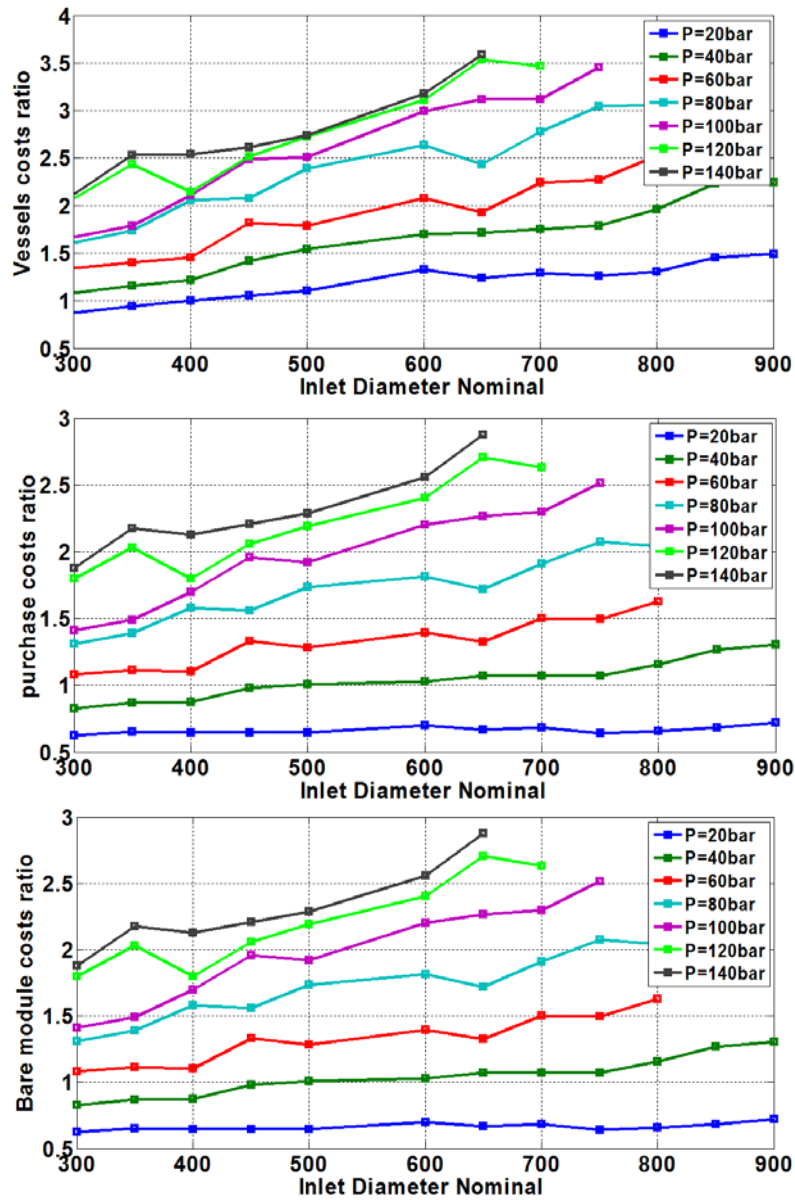


Figure 6.9 Ratios between vessel, purchase and bare module costs of knitted-mesh and multi-cyclone scrubbers at different pressures

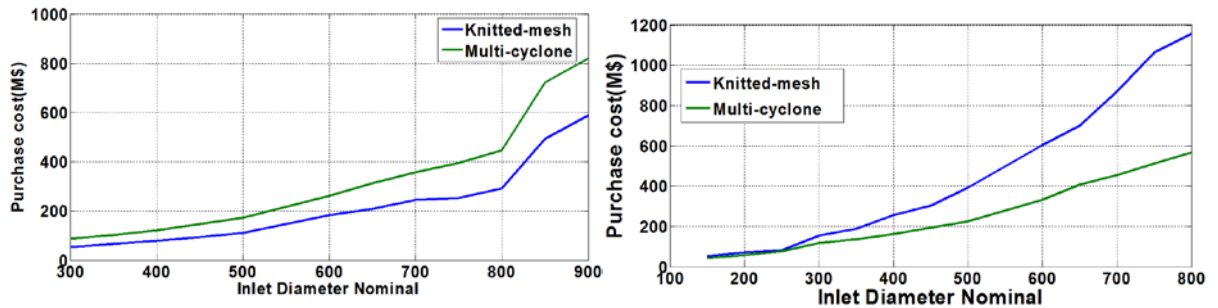


Figure 6.10 Comparison between purchase costs of knitted-mesh and multi-cyclones at 20 and 80 bar respectively

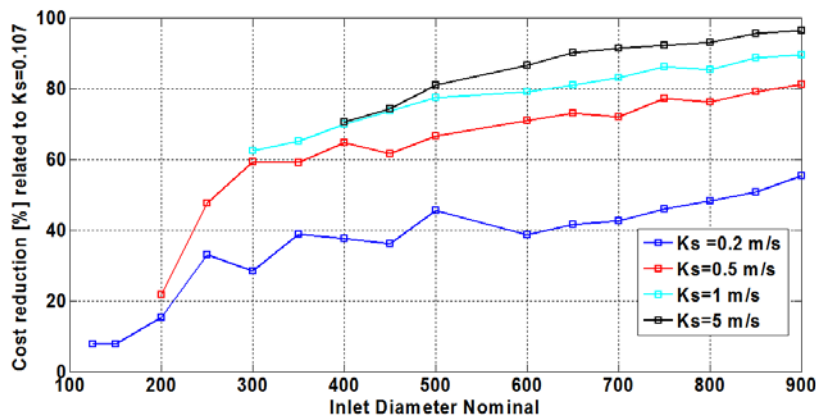
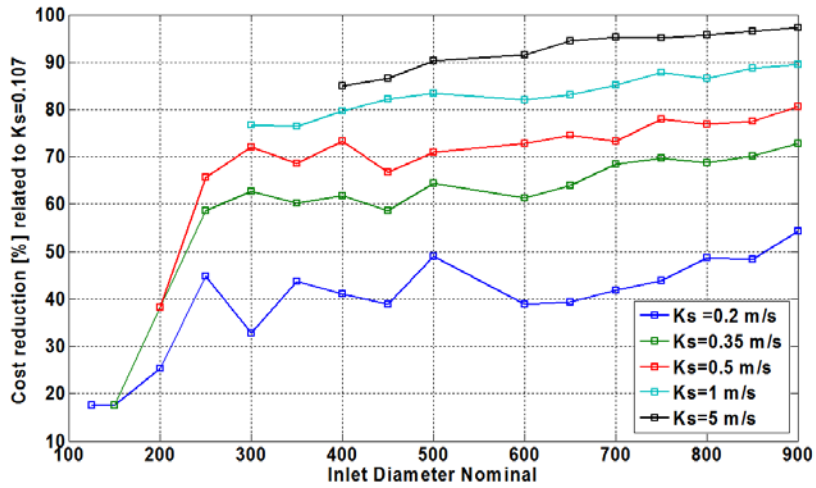


Figure 6.11 Effect of the gas load factor increase in the reduction of vessel and purchase costs respectively for hypothetical scrubbers at 20 bar³

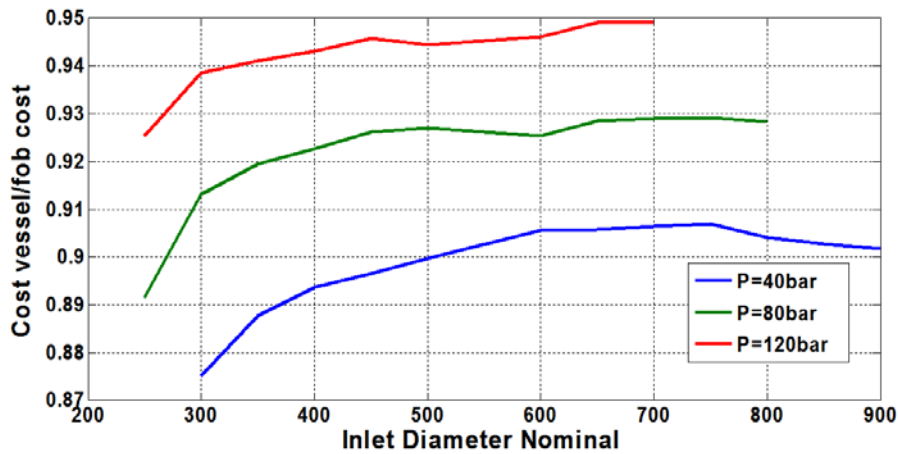


Figure 6.12 Ratio between cost of the vessel and total purchase cost for knitted mesh separators at 40, 80 and 120 bar respectively

³ It was assumed that the demisting pad for new technologies are five times more expensive than that used in traditional scrubbers

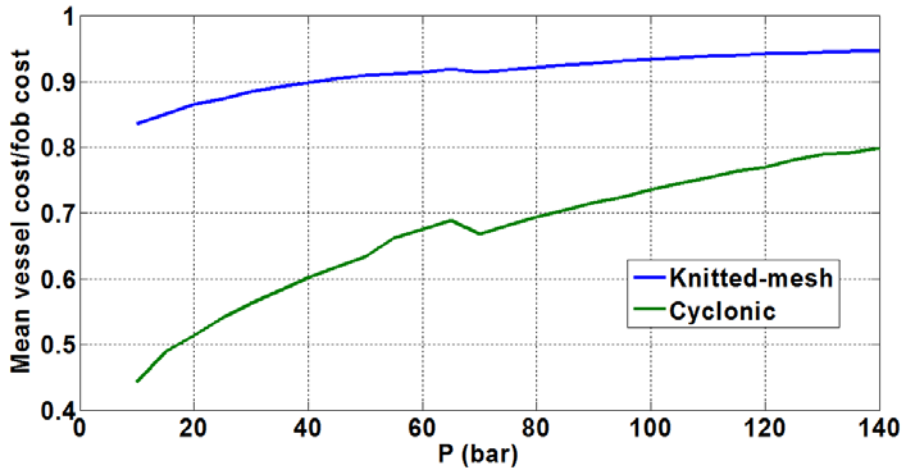


Figure 6.13 Mean ratio between vessel and total purchase (fob) costs for knitted-mesh and multi-cyclone scrubbers

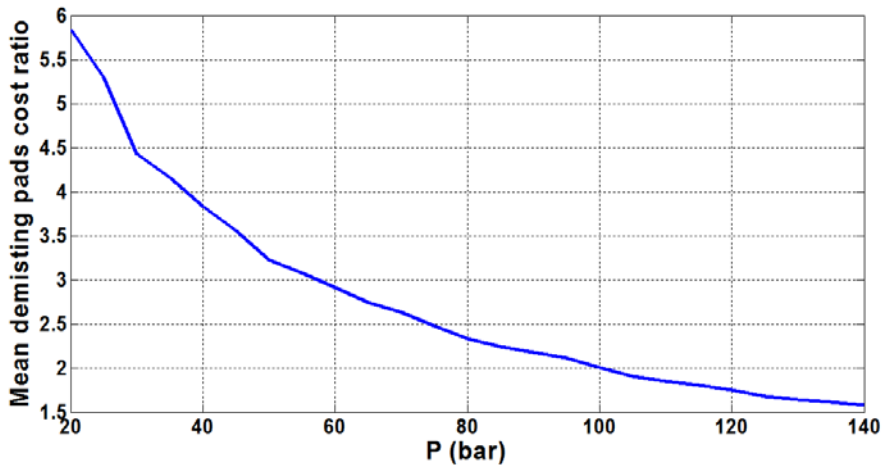


Figure 6.14 Ratio between demisting pads costs for multi-cyclone and knitted-mesh scrubbers at different pressures

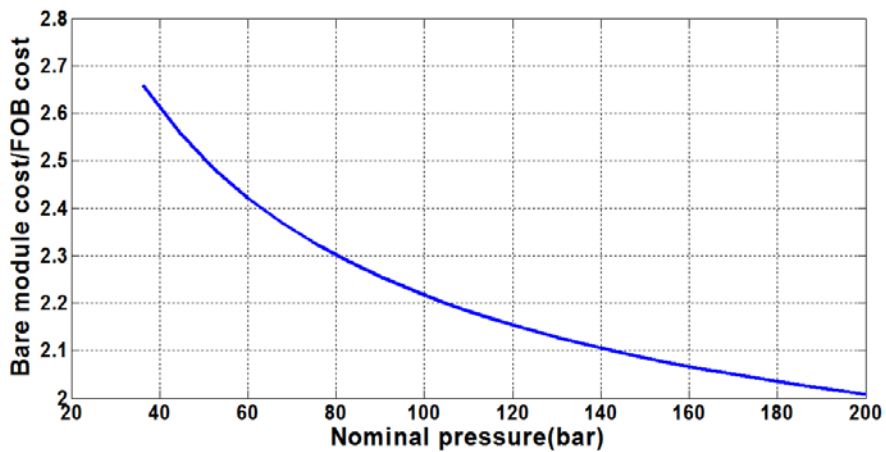


Figure 6.15 Variation of the ratio between bare module cost and purchase cost with regard to pressure for traditional scrubbers

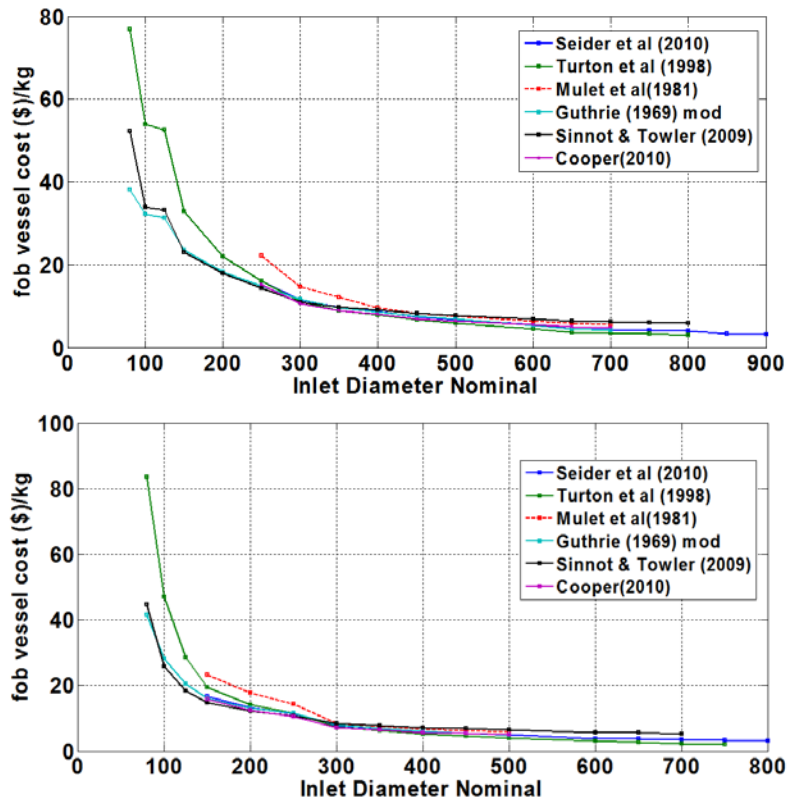


Figure 6.16 Purchase cost of the vessel per weight for knitted-mesh separators at 40, 80 bar respectively

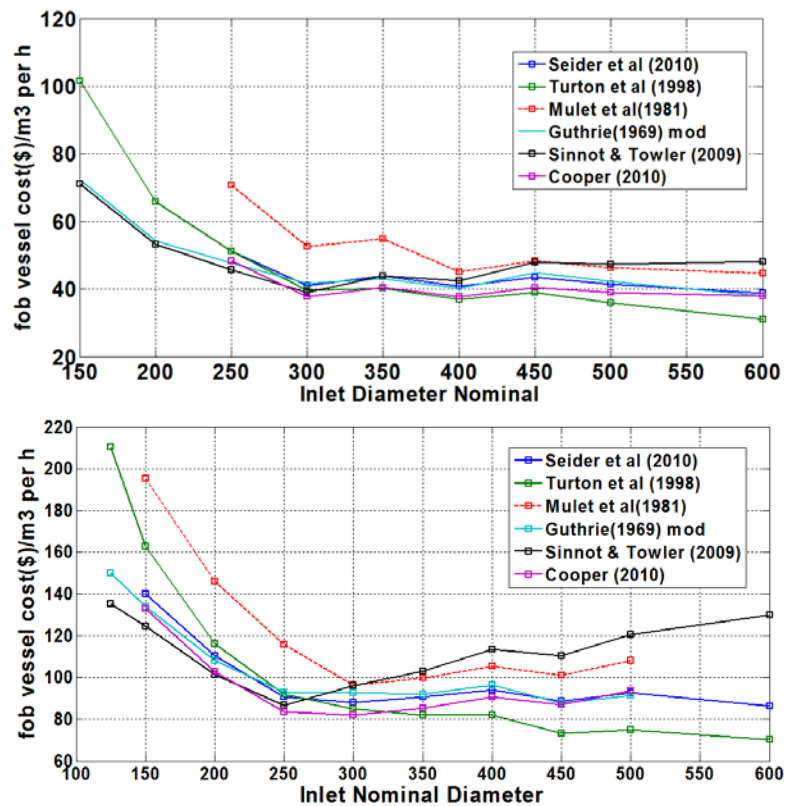


Figure 6.17 Purchase cost of the vessel per volumetric flow rate for knitted mesh separators at 40 and 80 bar respectively

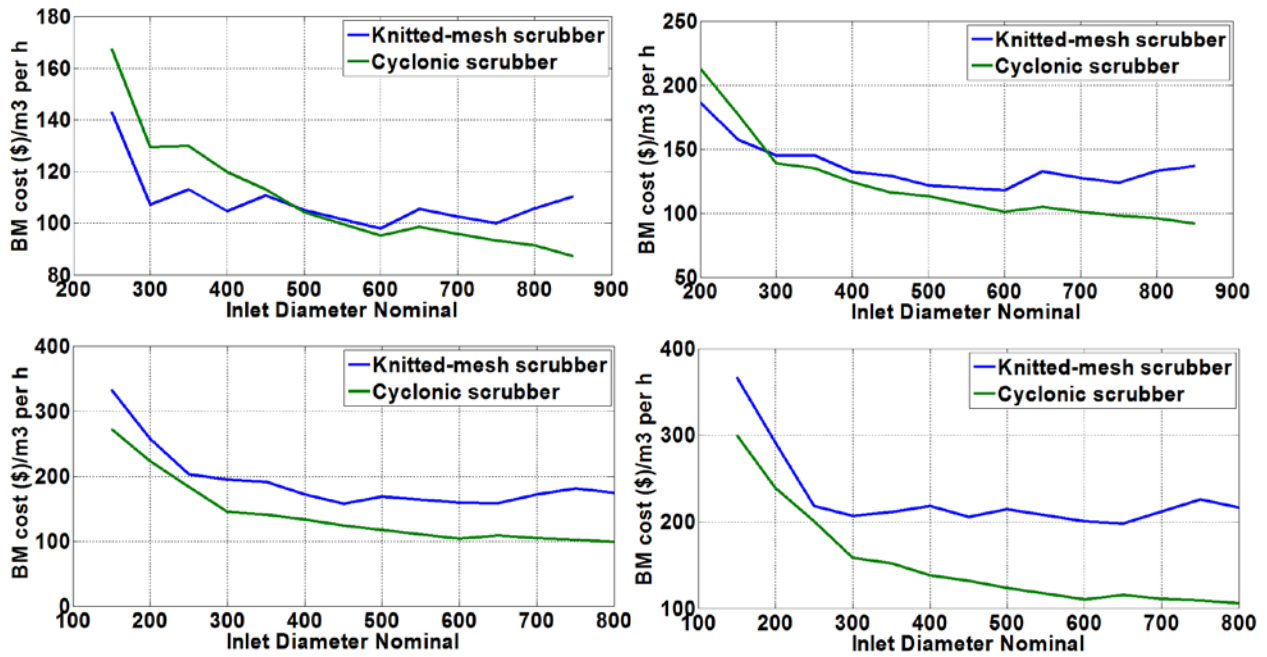


Figure 6.18 Bare module cost per flow rate (actual m^3 per hour) for knitted-mesh and multi-cyclone scrubbers at 40, 50, 70 and 80 bar respectively

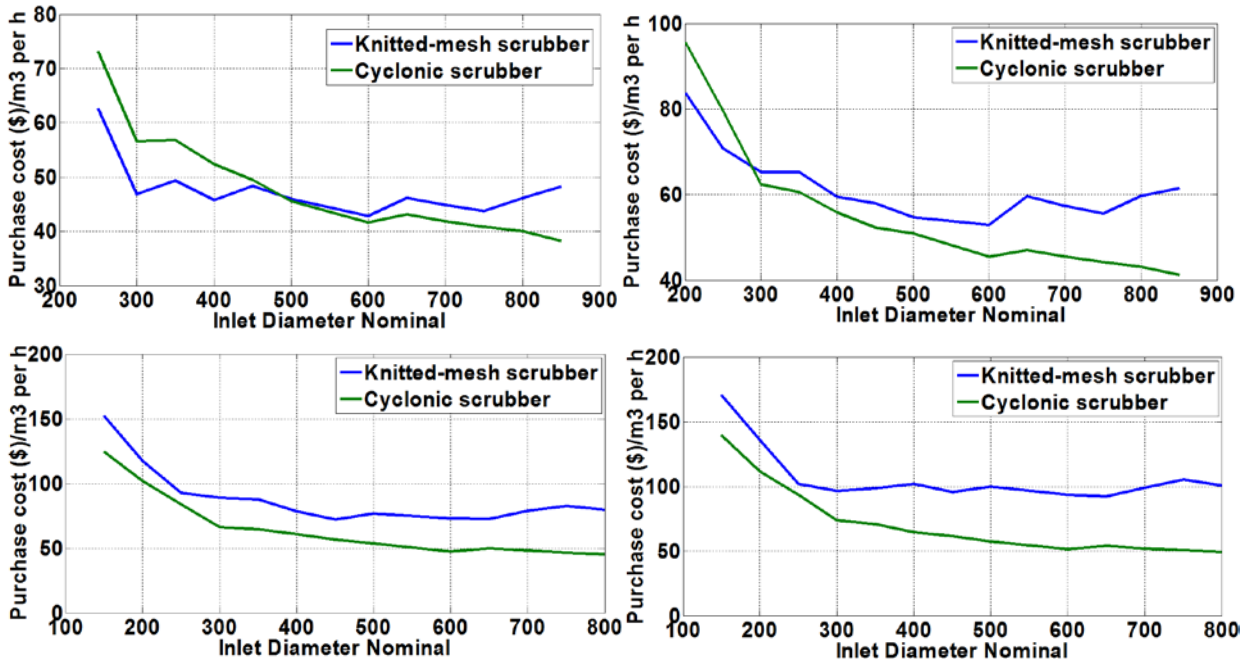


Figure 6.19 Purchase cost per flow rate (actual m^3 per hour) for knitted-mesh and multi-cyclone scrubbers at 40, 50, 70 and 80 bar respectively

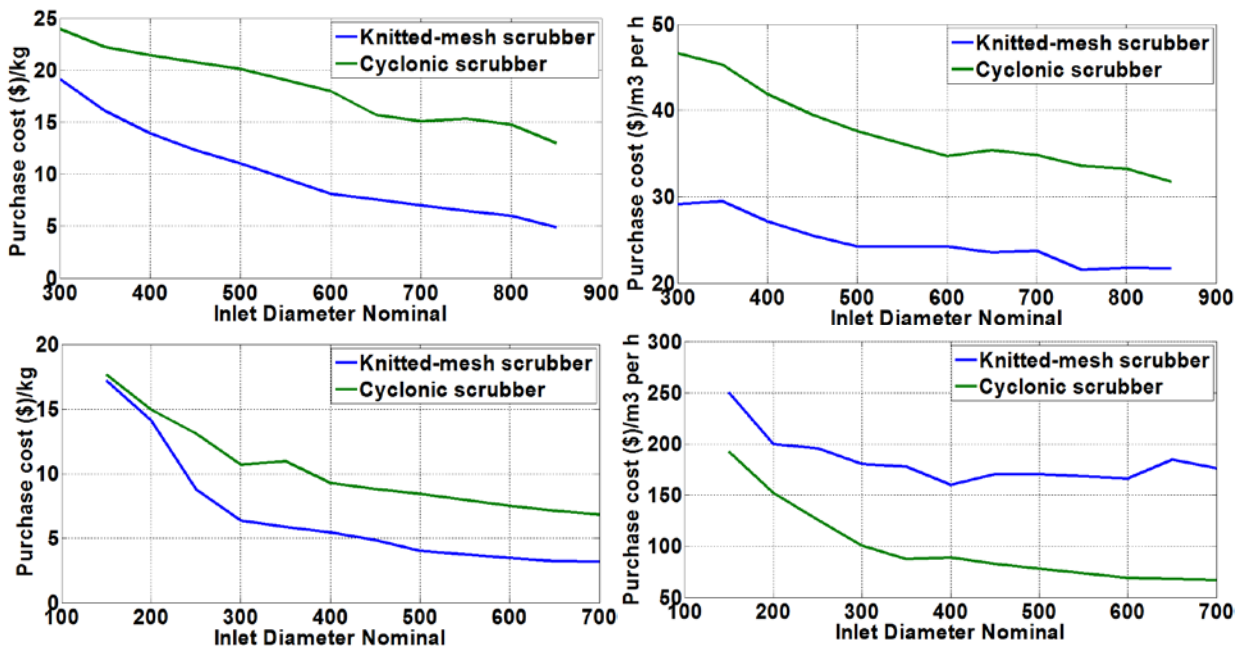


Figure 6.20 Comparison between the ratios of purchase cost per weight of separator and purchase cost per flow rate for knitted-mesh and multi-cyclone scrubbers at 20 and 120 bars respectively

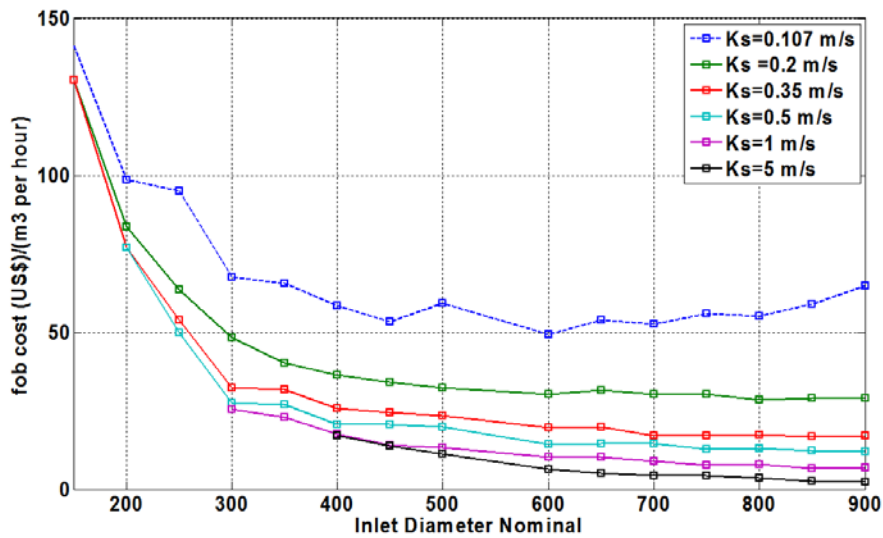


Figure 6.21 Effect of the gas load factor on the ratio of purchase cost per flow rate at 20 bars⁴

⁴ It was assumed that the demisting pad for new technologies are five times more expensive than that used in traditional scrubbers

6.3 Other parameters and considerations

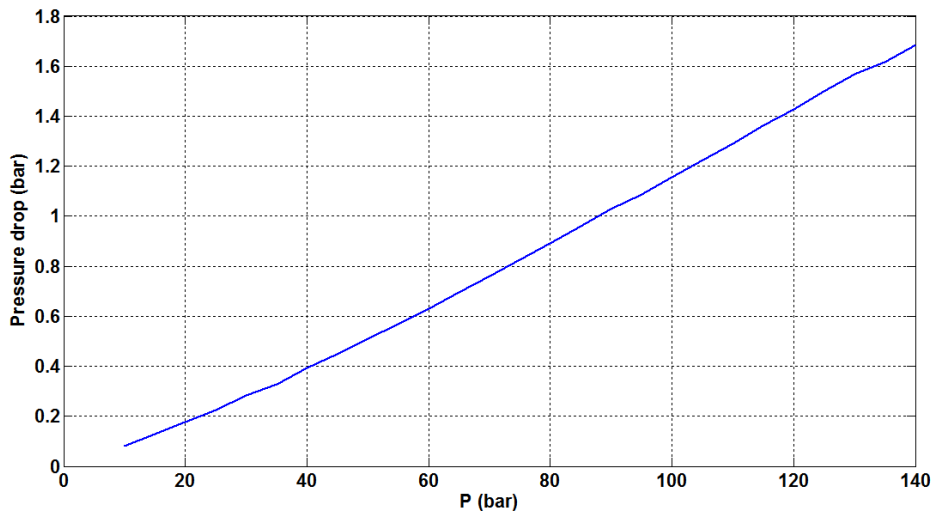


Figure 6.22 Average pressure drop across the cyclonic pad for multi-cyclone separators with cyclone inlet velocity of 20 m/s

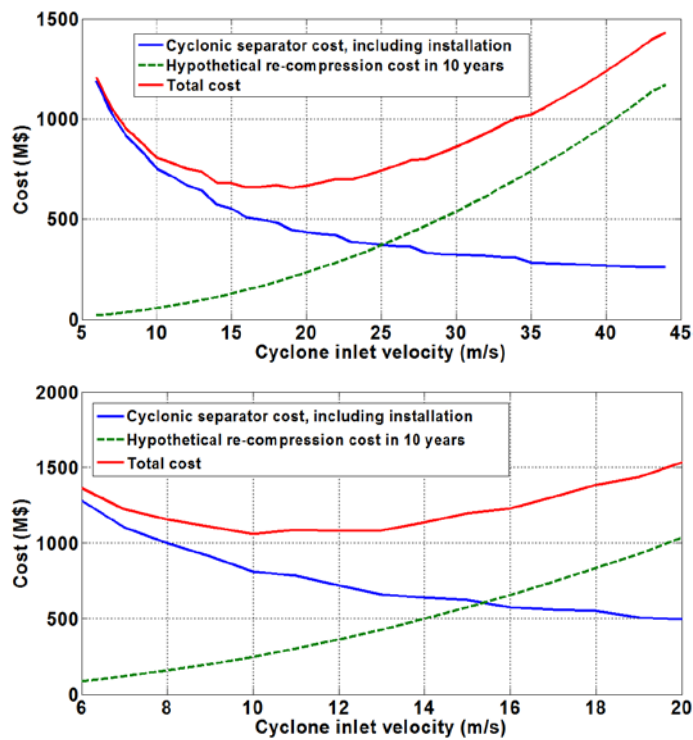


Figure 6.23 Trade-off between a multi-cyclone initial investment and pressure drop with DN 450 at 20 and 70 bar respectively

Table 6.5 Comparison among different cyclonic configurations at P=20 bar, DN 450 and cyclone diameter of 6'' (0.1524 m)⁵

Parameter	Cyclonic separator			Typical separator
	Cyclone inlet velocity (m/s)			
	10	16	20	
Vessel Diameter (m)	2.31	1.85	1.69	1.54
Vessel length (m)	3.23	3.14	3.11	3.85
Number of cyclones	142	89	71	--
Total weight (t)	15.1	9.2	7.8	7.7
Pressure drop (mbar)	45.9	122.2	194.7	1-2.5
Purchase cost (M\$), including chamber	252	171	146	95
Bare module cost (M\$)	627	426	362	236

Table 6.6 Comparison among different cyclonic configurations at P=70 bar, DN 450 mm and cyclone diameter of 6'' (0.1524 m)⁶

Parameter	Cyclonic separator		Typical separator
	Cyclone inlet velocity (m/s)		
	10	20	
Vessel Diameter (m)	2.31	1.69	2.00
Vessel length (m)	3.11	3.23	5.01
Number of cyclones	126	63	--
Total weight (t)	30.2	16.6	35.3
Pressure drop (mbar)	204.4	850.2	1-2.5
Purchase cost (M\$), including chamber	309	189	237
Bare module cost (M\$)	678	414	520

⁵ The velocities correspond to the units with lowest pressure drop, minimum cost according to the trade-off between pressure drop and initial investment, and lowest dimensions.

⁶ The velocities corresponding to the lowest pressure drop and trade-off are the same.

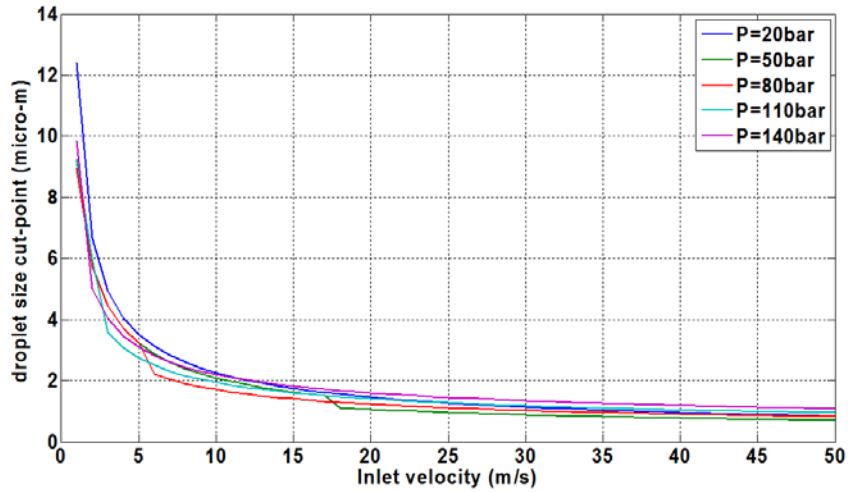


Figure 6.24 Variation of the cut-point droplet diameter (x_{50}) with cyclone inlet velocity

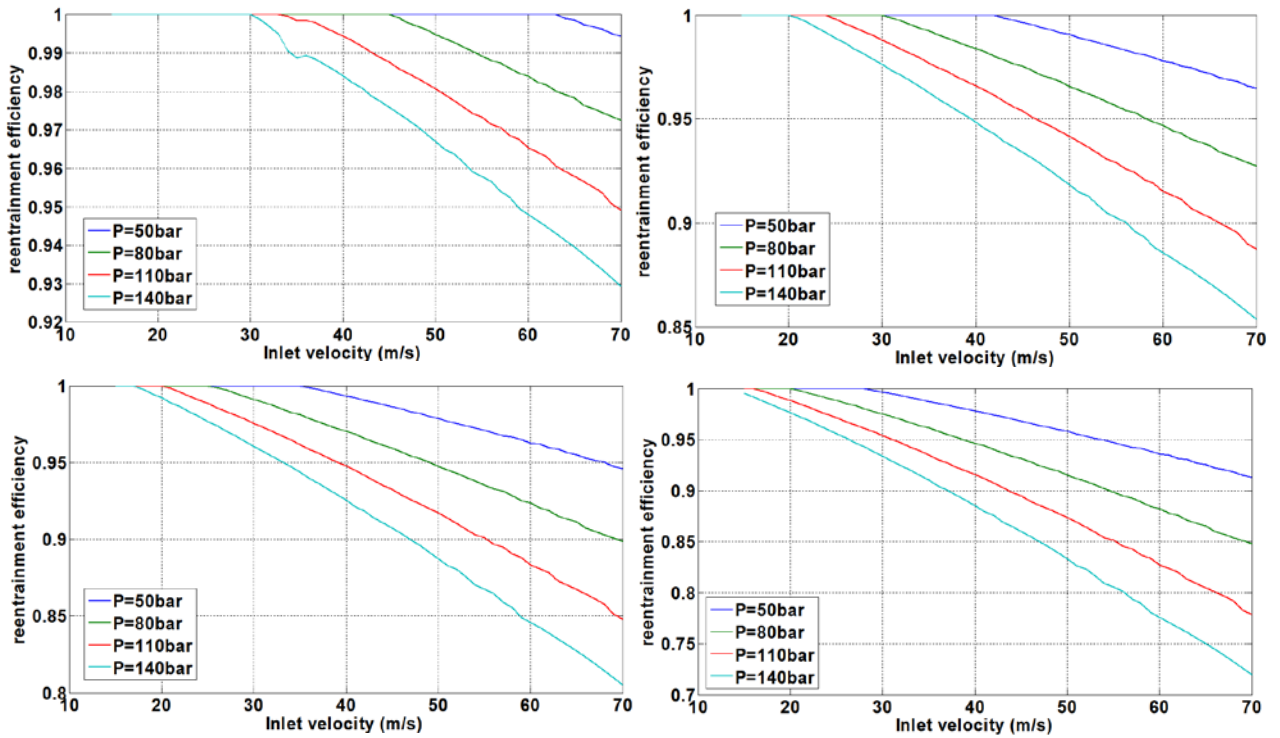


Figure 6.25 Effect of pressure on reentrainment for percentage of liquid on the gas stream of 0.02, 0.1, 0.2 and 0.5 respectively

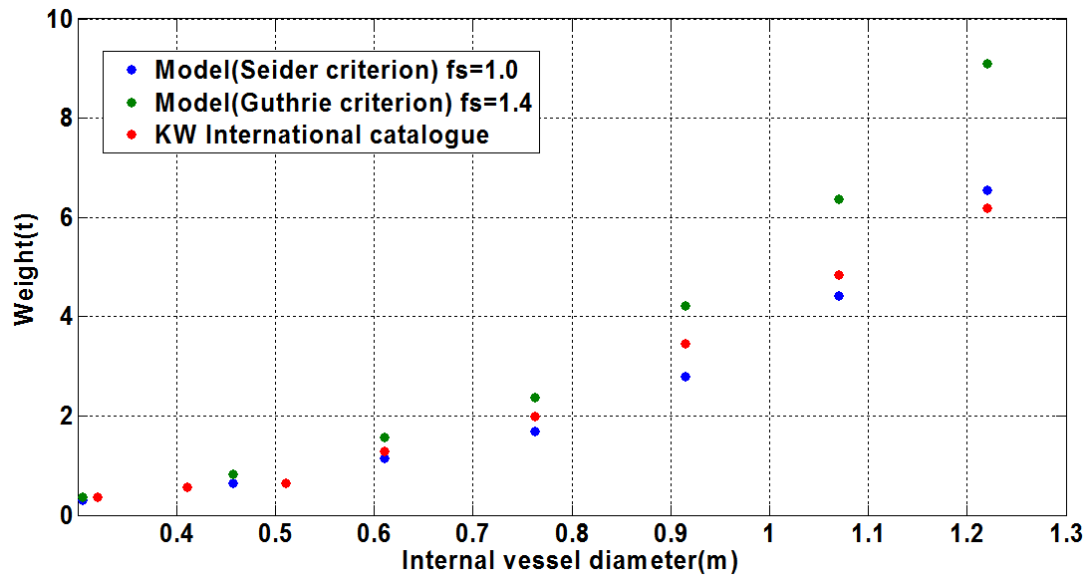


Figure 6.26 Validation of the vessel weight for knitted-mesh scrubbers against pressure vessels fabricated by KW International at 80 bars

7. DISCUSSION OF RESULTS

The gas load factor (K_s) is a critical factor on the selection of a gas scrubber. As this factor increases, the dimensions and weight of the gas liquid separator decreases correspondingly. In fact, the phenomena are presented on figures (6.1) and (6.3) for the selected technologies: knitted-mesh and centrifugal separators. Furthermore, figures (6.2), (6.5) and (6.7) illustrate it for hypothetical mist eliminators with different Souders-Brown factors. Consequently, the costs are reduced for more compact units as shown on figure (6.11). This factor is 0.107 m/s for traditional separators at low pressure, while for cyclonic scrubbers would be up 0.15 to 0.25 m/s for cyclonic scrubbers. In other state-of-the-art technologies, it has achieved 0.3-0.4 m/s. One of the main difficulties is determining the right value since it depends on different factors like pressure, drop size, superficial tension, among others. Therefore, authors recommend consult vendors to have a more accurate value.

For a particular case of knitted-mesh demisters, Fabian et al. (1993) suggested to adjust the factor by means of pressure; resulting in a decreasing tendency. Regarding to multi-cyclones, the crucial parameter on it is the maximum inlet velocity of each cyclone. When cyclone inlet velocity is fixed (20 m/s in this case), the gas load factor increases by means of pressure for a given as shown figure (6.8). The phenomena described above can be explained by means of mass flow rate, which goes up for a given nominal diameter. In the case of knitted-mesh scrubbers, the internal vessel diameter increases as pressure does according to the Souders-Brown equation. On the other hand, the number of cyclones in a centrifugal separator is more or less the same; for a given volumetric flow rate. As a result, the flow rate could be increased for the same demisting area until a recommended value. As shown the figure, the maximum value achieved is slightly superior to that recommended by NORSOK P-100. At low pressure, it would be achieved this value but the velocity and the relative pressure drop might be extremely high. In fact, we can infer from figure (6.22) that the pressure drop is about 1% of the working pressure.

As mentioned before, increasing the gas load factor favours the compactness and costs reduction of gas-scrubbers. In the case of multi-cyclones, this factor increases by means of pressure. In fact, figures (6.4), (6.6), (6.9), (6.11), (6.18), (6.19) and (6.20) show how changing pressure affects the relative competitive of these gas scrubbers. If the working pressure is low or moderate, the gas load factor is not good enough to guarantee a more compact and cheaper gas scrubber. At certain pressure, the tendency is reversed and multi-cyclone scrubbers become competitive despite its high pressure drop. At this point, the traditional demisting units become very bulky and heavy thus a more compact technology might be attractive; especially in offshore operations. However, the Souders-Brown factor is not enough to establish when alternative technology becomes attractive. In this way, additional parameters as cost per weight or cost per flow rate might be useful. Actually,

these parameters are shown for different references and pressures on figures (6.16) and (6.17).

On these figures, we can see a set of curves from different references such as Seider et al. (2010), Turton et al (1998) and so on. These references are related to different cost equations for vertical pressure vessels. As shown on figure (6.17), there are good match among the values provided from different equations. Nevertheless, on figure (6.18) we can see the difference in more detail since the scale of the 'Inlet Diameter Nominal' axis was adjusted for this purpose. Some equations tend overestimate costs while others underestimate them compared to the others, although the pattern of these equations changes throughout the nominal diameters studied. For instance, Turton et al (1998) tends to overestimate costs for small scrubbers while underestimates costs for medium and large equipment. The equations so-called Sinnott & Towler (2009) and Guthrie modified (1969) tends to match well for small equipment. Suddenly, the former tends to increase sharply while the latter almost levels off. This is motivated that the equation of Sinnott & Towler (2009) belongs to the Six-tenths rule category, which is applicable for small equipment close to the base dimensions. In this context, the equation so-called Seider et al (2010) has much higher range of applicability.

On these graphs, it is reflected how the costs per weight or flow rate are affected by increasing the size of equipment. As expected, the economy of scales takes place when the dimensions of equipment go up. For instance, small equipment has higher price per dimension than bigger equipment. Then, the price per dimension tends to decrease until certain point where the economy of scales is lost and the tendency is reversed. For both costs per weight of separator and per inlet flow rate, the tendency is decreasing when the dimensions are increased. However, the impact of pressure is different on these variables. With respect the cost per weight tends to decrease slightly with pressure, while the cost per flow rate increases as pressure does. As the results show, the cost of scrubbers increases by means of pressure for a given diameter nominal. Nevertheless, after multiplying the costs per weight and flow rate by the separator weight and flow rate respectively; the product is exactly the same.

Analysing in more detail these parameters, we can explain these phenomena. For example, costs per weight are used in the everyday life to compare products with similar features in supermarkets. In the hypothetical case that we have two presentations of butter: one has a price of 22 NOK per 250 grams while the other has 15 NOK per 150 grams. As first sight, the latter is more attractive since is relatively cheaper than the former. However, the first presentation is absolutely the cheapest one since its price per kilo is 88 NOK while the second is 100 NOK. In these particular cases, this parameter is very useful but it might be tricky in the selection of separator as shown figure (6.20). In this way, the cost per weight of a knitted-mesh scrubber will never overtake that for centrifugal separators. Looking back to the example of the two presentations of butters, we need the same quantity for cooking

regardless the presentation or brand. Therefore, the parameter is valid in this situation. On the other hand, it is advisable to consider the flow rate of gas stream to be treated for gas scrubbers. As a result, it seems that a cost per flow rate is more adequate for this particular case.

The cost per flow rate parameter was established to determine the limit, when the multi-cyclone technology might be taken into consideration. On figures (6.15) and (6.16), both alternatives are actually compared at different pressures. From the graphs corresponding to these figures, we can infer if pressure is higher than 70 or 80 bars; cyclonic separators might be competitive. In fact, Shell (2002) suggested a limit slightly higher between 90 and 100 bars. It has been explained the effect of pressure on the gas load factor value of centrifugal separators. Furthermore, pressure increase has an enormous impact on the dimensions and weight of typical separators because diameter, length and thickness are affected accordingly. Consequently, the cost of the gas scrubber vessel increases sharply. Figures (6.12) and (6.13) present actually the ratio between the vessel cost and the fob (free on board) cost or total purchase cost. On the latter, it is also shown the variation of the demisting pad for cyclonic separators with pressure.

As reflected on figures (6.13) and (6.14) the cyclonic demisting pad is more expensive than the traditional knitted-mesh. This relative comparison is applicable to other technologies since the wire-mesh pad tends to be the cheapest mist eliminator in the market. For this reason, it is required to achieved a reasonable gas load factor which allows counteract the effect of the cost of the demisting pad. However, figure (6.21) shows that technologies, which are able to achieve at least a load factor of 0.2 m/s, might be attractive even at 20 bars. In this hypothetical case, the ratio between the demisting pads of more compact technologies and the wire-mesh was established as five. In the particular case of cyclonic pads, this ratio tends to decrease as shown on figure (6.14). As mentioned before, the demisting area of traditional technologies increases as pressure does according to the Souders-Brown equation. On the other hand, the demisting pad area for centrifugal separators is more or less the same at different pressures. Regarding to the ratio of installed and purchase costs for both separators are more less the same for both gas scrubbers.

Regarding to the ratio between the bare module and purchase costs is reflected on figure (6.15) by means of nominal pressure. The bare module costs include purchase, installation and indirect costs as explained on chapter 4. As expected, it decreases as nominal pressure goes up. As mentioned before, the change of pressure or material of the equipment affects mainly the cost of piping while other costs associated to installation remain the same. On tables (6.3) and (6.4), we can establish this ratio by comparing the bare module cost and purchase cost. We can see on them the prices and dimensions of selected equipment at different nominal diameters and pressures. For the models proposed, the nominal pressure is estimated based on Seider et al (2004) criterion. However, it was adjusted according to

that proposed by Guthrie (1969) which advises to increase the working pressure by 50 percent. Therefore, the nominal pressure is about 50% more than the working pressure.

The main issue of cyclones is its high pressure drop as reflected graph (6.22). The pressure drop is a combined effect of gas density and cyclone inlet velocity. The velocity should be kept high to have good efficiency but avoiding re-entrainment. In other words, if the cyclone velocity is too low; it has not the capability to separate the liquid droplets efficiently. On the other hand, if the velocity is too high the liquid separated might be retaken by the gas stream. Additionally, as velocity increases the higher pressure drop is. For this reason, the literature recommends to operate in a range of 10 to 20 m/s of inlet velocity per each cyclone.

In fact, figure (6.24) provides an indirect way to determine the efficiency. On this graph, it is given the cut point of droplet size which means that the efficiency is 50% for this droplet size. As we can see, the cut point is reduced as the inlet velocity in each cyclone increases. In fact, according to this the efficiency tends to be very high when the inlet velocity is higher than 10 m/s. It was not shown the efficiency itself since the model provides almost 100% for all cases studied. Therefore, it is not possible to illustrate how the inlet velocity influences on the centrifugal scrubber. This very high efficiency values are possibly due to the mean droplet size is much higher than the cut point. In fact, many approximations were considered since there is lack of information about droplet distribution and mean droplet size. However, many authors argue that the efficiency of the traditional knitted-mesh separators for droplets with size higher than 10 μm .

At high pressure, the effect of reentrainment is worsened as mentioned before and the efficiency is affected in this way. This phenomenon has been proven on figure (6.25) where is shown the effect of pressure on reentrainment. For most simulations on the present work, it was used 0.02% of liquid in the gas stream. This figure is just below to the flooding point of knitted-mesh scrubbers at atmospheric pressure. However, as pressure increases the liquid capacity of the scrubber may increase. As we can see on these graphs, the velocity range is reduced as pressure goes up since the danger of reentrainment increases as well. For example, if the pressure is 50 bars we can have velocities up 30 m/s without reduction of efficiency according to the model. On the other hand, if the pressure is 140 bar a reduction of efficiency motivated for this phenomenon can be evidenced at 15 m/s. However, multi-cyclones can have a good performance up 20 m/s for different liquid percentages in the gas stream.

Nevertheless, the pressure drop is still very high for multi-cyclones with velocities of 20 m/s. Then, it was established a trade-off between the initial investment and the hypothetical recompression work required. The calculations are based on the efficiencies of the Brayton cycle for gas turbines and the price of electricity per kWh for industry in Norway. The initial investment includes installation costs and it is adjusted by the location factor for Western Europe, which allows having a more approximate result. Nevertheless, the velocity for minimum cost decreases by means of pressure, until the minimum velocity of 10 m/s. This velocity is not good enough to reduce the size of the separator compared to the traditional separator to justify the investment. The main reason of this is the large number of cyclones required to have a similar performance to the traditional separators. Consequently, it was used the maximum velocity of 20 m/s to compare the prospective cyclonic separator to the traditional one. The trade-off at different pressures is illustrated on figure (6.23) and tables (6.5) and (6.6).

Regarding to the validation of the models, it has been difficult since most information related is confidential; especially concerning to costs. In addition, some catalogues have incomplete information about working and nominal pressure, diameter nominal and other conditions. However, figure (6.26) presents a comparison between the weight per length for both criteria used in the knitted mesh model and dimensions provided by KW International. The criterion so-called Guthrie (1969) estimates the nominal pressure 50% than the working pressure. On the other hand, Seider et al. (2004) use a set of equations to estimate the nominal pressure. In this case, the nominal pressure is 10% than the working pressure. The factors (f_s) reflected on the graph are related to the adjustment made to the nominal pressure. This factor is used in the model to increment the nominal pressure, according to different conditions. In this way, if f_s is equal to 1.0 the calculation corresponds to the pure Seider criterion but if f_s is equal to 1.4 the nominal pressure corresponds to the Guthrie criterion. The factor adjusts mainly the thickness of the vessel but its internal diameter and length are more or less the same in most situations. For the particular design reflected on figure (6.26), the data provided by the vendor are between to that calculated by using both criteria. However, the values tend to be closer to the Seider criteria. In other cases, the nominal pressure selected might correspond to the Guthrie criteria; especially in offshore operations. Nevertheless, its selection does not influence on the decision making process since there is no a major impact on the costs expected.

8. CONCLUSIONS AND RECOMMENDATIONS

It was developed mathematical models for the traditional knitted-mesh and multi-cyclone scrubbers which might be taken as part of a decision making scheme. In fact, these models basically provide dimensions, weight, purchase and installed costs for the technologies selected; which allows compare both gas scrubbers or extrapolate them to others. Parameters like gas load factor and costs per flow rate might be used as a useful tool to compare the traditional technology to a potential substitute. The cost per separator weight resulted inappropriate as decision making parameter, because it does not establish clearly when a new technology is competitive or not.

The data compiled to construct the model for the knitted-mesh separator allowed sizing the vessel of both technologies selected. The vessel is designed following the same criteria for pressure vessels used in different chemical processes, despite of some particularities of them. After being calculated the vessel weight, it is possible to estimate its purchase and installed cost by using appropriate equations and factors. The cost of the vessel tends to be the major component of the total cost of the scrubber. Therefore, the knitted mesh model might be taken as starting point to evaluate new technologies from the technical and economical point of view.

Traditional gas scrubbers become very bulky and heavy, especially at high pressure. This conditional is specifically critical in offshore operations, where the plot area is restricted. Therefore, a much more compact technology would be very competitive. The compactness of this kind of equipment is closely related to the gas load factor. Therefore, it is intended to achieve a much higher value compared to that for traditional technology. In this way, gas scrubbers' costs and dimensions are reduced significantly. From the comparison among hypothetical technologies, it was established that technologies with gas load factors of 0.5 to 1 m/s could be very competitive even at moderate pressure. Beyond these figures, the difference in costs per flow rate between the new and traditional scrubbers tends to be more or less the same.

On the other hand, there would be restrictions in achieving the maximum gas load factor expected for a demisting devise. In the particular case of multi-cyclones, the main restriction is the cyclone inlet velocity. If this velocity is too high, it could be translated into a very high relative pressure drop and reentrainment. In fact, the former represents the main restriction at low pressure while the former at high pressure. Nevertheless, they might be very competitive at high pressure, especially is the working pressure is higher than 70 or 80 bars. At these pressures, the gas load or Souders-Brown factor is about 0.14 m/s with a cyclone inlet velocity of 20 m/s. The relative pressure drop is actually about 1% of the working pressure by using this velocity. Furthermore, the costs per flow rate related are lower than those for knitted mesh scrubbers; throughout all gas capacities studied by means of nominal diameter.

The present and other works related might be used to develop a systematic strategy in the selection of demisting units. If the gas load factor is known for a determined technology, it might be much easier to estimate the vessel dimensions and weight. In fact, its cost is often the higher component of the total cost of a gas scrubber. Furthermore, the costs per flow rate might be taken to estimate when a technology is economically feasible or not. Nevertheless, other factors should be incorporated in models with this purpose like pressure drop, the cost of the demisting pad itself, reentrainment and so on. It is required to research much more about the phenomena involved in the gas-liquid separator in cutting-edge technology. In fact, the phenomena related are usually very complex. However, their understanding would be necessary to establish the appropriate conditions for using a particular demisting devise.

Despite the difficulty of finding real costs in industry, it would be beneficial to incorporate them in future models to have more accurate values. In fact, the error could be at least 30 or 40 % according to the category of capital cost estimates. In addition, the results presented are based on costs of the US Gulf Coast area. The investment site factors would be used in this respect. According to the factor corresponding to Western Europe, the bare module costs presented might be at least 20% more for Norway. However, they are only applicable for the bare module costs and they consider Western Europe as a whole. As a result, the values provided for the models developed in the present work give a preliminary approximation. Nevertheless, they might be considered as starting point of further work where other parameters would be incorporated.

9. REFERENCES

Bolland, O. (2010): Thermal Power Generation. In *TEP4185 Industrial process and Energy Technology*. Trondheim: NTNU, Department of Energy and Process Engineering.

Branan, C. (2002): *Rules of Thumb for Chemical Engineers*, 3rd ed., Amsterdam; London: Gulf Professional.

Branan, C. (2005): *Rules of thumb for Chemical Engineers: a Manual of Quick, Accurate Solutions to Everyday Process Engineering Problems*, 4th ed., Burlington, USA; Oxford, Elsevier : GPP.

Cambridge University Press (2011): *Cambridge Dictionaries Online*. Retrieved 20th May, 2012, from <http://dictionary.cambridge.org/dictionary/british/>

Campbell, J. (2004): *Gas conditioning Processing*, Vol. 2, 8th ed., USA: John M. Campbell & Co. Books.

Chemical Engineering (2012): Economic Indicators, *Chemical Engineering*. New York: Access Intelligence LLC. 119: 51-52.

Coulson, J. M., Richardson, J. F., & Sinnott, R. K. (2005): Chemical Engineering Design. In *Coulson & Richardson's Chemical Engineering*, Vol. 6, 4th Ed., Amsterdam; London: Elsevier.

Couper, J. R., Penney, R., Fair, J., & Stanley, W. (2010): *Chemical Process Equipment: Selection and Design*. Amsterdam; Boston: Elsevier.

Cran, J. (1981): Charting Routes to Preliminary Cost Estimates, *Chemical Engineering*, 88(7): 64-79.

Ellenberger, J. P. (2010): *Piping and Pipeline Calculations Manual: Construction, Design, Fabrication, and Examination*. Amsterdam; Boston: Butterworth-Heinemann/Elsevier.

Fabian, P., Cusack, R., Hennessey, P., & Neuman, M. (1993): Demystifying the Selection of Mist Eliminators. *Chemical Engineering*, 100(11): 148-156.

Fredheim, A. (2010): Gas Processing. In *TEP 4185 Industrial Process and Energy Technology Compendium*, Trondheim, NTNU: Department of Energy and Process Engineering.

Gerunda, A. (1981): How to Size Liquid-Vapor Separators, *Chemical Engineering*, 88(9): 81-84.

Guthrie, K. M. (1969): Data and Techniques for Preliminary Capital Cost Estimating, *Chemical Engineering*, 76(6): 114-120.

Hoffmann, A. C., & Stein, L. E. (2008): *Gas Cyclones and Swirl Tubes: Principles, Design, and Operation*. Berlin; New York: Springer.

Karno, A. & Ajib, S. (2006): Effect of tube pitch on heat transfer in shell-and-tube heat exchangers - new simulation software, *Heat and Mass Transfer*, 42(4): 263-270.

Koch Glitsch (2007): *Mist Eliminators*. Retrieved May 18th, 2012 from www.koch-ottoyork.com

KW International (2012): *Oil & Gas Production Equipment: Gas-liquid Separators*. Retrieved June 20th, 2012 from <http://www.kwintl.com/separators.html>

Mecon Limited (2006): *Guidelines for Piping Design for Metallurgical Industries*. Retrieved February 25th, 2012 from <http://www.scribd.com/doc/50636931/15749975-Guidelines-for-Piping-Design-for-Metallurgical-Industries>

Mulet, A., Corripio, A. B., & Evans, L. B. (1981): "Estimate Costs of Pressure-Vessels via Correlations." *Chemical Engineering* 88(20): 145-152.

NORSOK (2001): *NORSOK Standard P-100*. Retrieved April 26th, 2012 from http://www.google.com/url?sa=t&rct=j&q=&esrc=s&frm=1&source=web&cd=1&ved=OCFAQFjAA&url=http%3A%2F%2Fwww.standard.no%2FPageFiles%2F1132%2FP-100.pdf&ei=EqjYT-rOO4aB4gT_6Ly6Aw&usg=AFQjCNGN3EnZR4r2atFYO-xYa6iMTPRxZw

NORSOK (2006): *NORSOK standard P-001*. Retrieved May 18th, 2012 from <http://www.standard.no/pagefiles/1134/p-001e5.pdf>

Oruch, T., DuPrè, C., Beckman, K., Grewal, G. & Christensen., K. (2009): ASME B31.3 Process Piping Guide, Revision 2. In *LANL Engineering Standards Manual PD342*. Retrieved March 15th, 2012 from http://www.google.no/url?sa=t&rct=j&q=&esrc=s&frm=1&source=web&cd=1&sqi=2&ved=0CGEQFjAA&url=http%3A%2F%2Fengstandards.lanl.gov%2Fesm%2Fpressure_safety%2Fprocess_piping_guide_R2.pdf&ei=SWS-T8KcC9HSsgaVnYjdDQ&usg=AFQjCNHcyQXLnKB897jl_xFQHKlc-7vnwg

Peerless (2012): Peerless Centrifugal Separators Retrieved June 2nd 2012, from www.peerlesseurope.com

Perry, R. H., D. W. Green, & Maloney, J. O. (1997): *Perry's Chemical Engineers' Handbook*. New York: McGraw-Hill.

Peters, M. S., Timmerhaus, K. D., & West, R. E. (2003): *Plant Design and Economics for Chemical Engineers*. New York: McGraw-Hill.

Solmon co., (2012): *Pipe Sizes and Dimensions*. Retrieved February 25th, 2012, from <http://www.maselmon.com/Content.aspx?ContentID=24>

Seider, W. D. (2010): *Product and Process Design Principles: Synthesis, Analysis, and Evaluation*, 3rd Ed., Hoboken: John Wiley & Sons.

Seider, W. D., J. D. Seader, & Lewin, D. R. (2004): *Product and Process Design Principles: synthesis, analysis, and evaluation*, 2nd Ed., New York: Wiley.

Shell (2002): *Gas/Liquid Separators: Type Selection and Design Rules: Design and Engineering Practice*. Retrieved May 31th, 2012 from <http://www.scribd.com/doc/50266640/23/CYCLONE-WITH-STRAIGHT-INLET-AND-SWIRLER-GASUNIE-CYCLONE>

Smith, R. (2005): *Chemical Process Design and Integration*. Chichester, England: Wiley.

Statistics Norway (2011): *Prices of Electric Energy, 4th quarter 2011*. Retrieved May 25th, 2012, from <http://www.ssb.no/en/elkraftpris/main.html>

Stewart, M. & Arnold, K. (2008): *Gas-liquid and Liquid-liquid Separators*. Amsterdam; Boston: Gulf Professional Publishers/Elsevier.

Sulzer (2010): *Gas/Liquid Separation Technology*. Retrieved February 27th, 2012 from www.sulzerchemtech.com

The Economist (2008, October 20th): Economies of Scale and Scope. *The Economist*. Retrieved May 20th, 2012 from <http://www.economist.com/node/12446567>

Tillerson, R. (2012): *ExxonMobil Projects Natural Gas Will Overtake Coal as Second Most Widely Used Source of Energy by 2025*. 25th World Gas Conference, June 4-8, Kuala Lumpur. Retrieved June 14th, 2012 from <http://www.greencarcongress.com/2012/06/xom-20120606.html>

Towler, G. P., & Sinnott, R. K. (2008): *Chemical Engineering Design: Principles, Practice and Economics of Plant and Process Design*. Amsterdam; Boston: Elsevier/Butterworth-Heinemann.

Turton R., Bailie R., Whiting, W., & Shaeiwitz, J. (1998): *Analysis, Synthesis, and Design of Chemical Processes*. USA: Prentice Hall.

Turton R., Bailie R., Whiting, W., & Shaeiwitz, J. (2003): *Analysis, Synthesis, and Design of Chemical Processes*. 2nd Ed., USA: Prentice Hall.

Turton R., Bailie R., Whiting, W., & Shaeiwitz, J. (2009): *Analysis, Synthesis, and Design of Chemical Processes*. 3rd Ed., USA: Prentice Hall.

Vågenes, K. (2011): *Properties of Natural Gas*. Retrieved April 30th, 2012 from <http://www.ipt.ntnu.no/~jsq/undervisning/naturgass/lysark/LysarkGudmundssonVagnesGasProperties2011.pdf>

Viguri, J. R. (2011): *Equipment Sizing and Costing: Chemical Process Design 7*. Retrieved May 26th, 2012 from <http://ocw.unican.es/enseñanzas-tecnicas/procesos-quimicos-de-fabricacion/materiales/>